A Geochemical And Petrological Study Of Volcanic Rocks In The Beardmore-Geraldton Archaean Greenstone Belt, Northwestern Ontario.

By

Kwong Yin Soo (B.Sc)

A Thesis Submitted To The Department Of Geological Sciences In Partial Fulfillment Of The Requirements For The Degree Of Master Of Science

July 1988

Brock University

St. Catharines, Ontario

TABLE OF CONTENTS

TITLE---------- 1

TABLE OF CONTENTS---------- 2

LIST OF FIGURES---------- 5

LIST OF PLATES---------- 7

LIST OF TABLES---------- 8

ABSTRACT---------- 9

ACKNOWLEDGEMENTS---------- 11

CHAPTER 1: INTRODUCTION---------- 12
1.1 Introduction---------- 12
1.2 Scope of study---------- 12
1.3 Previous work---------- 13
1.4 Fieldwork ---------- 13

CHAPTER 2: GEOLOGY OF BEARDMORE-GERALDTON BELT(BGB)---------- 16
2.1 General Geology ---------- 16
2.2 Local Geology---------- 18
2.3 Sedimentary rocks ---------- 19
2.4 Volcanic rocks---------- 20
2.5 Intrusive rocks---------- 22
2.6 Lithological contacts---------- 23

CHAPTER 3: PETROGRAPHY AND METAMORPHISM---------- 24
3.1 Introduction---------- 24
3.2 Description of Minerals---------- 24
3.21 Amphibole---------- 24
3.22 Epidote---------- 25
3.23 Plagioclase feldspar---------- 29
3.24 Chlorite ---------- 29
3.25 Quartz---------- 31
3.26 Sphene---------- 31
3.27 Carbonate---------- 31
3.28 Opaque ---------- 31
3.29 Mica ---------- 32
3.3 Textures---------- 32
3.4 Determination of Metamorphic Condition ---------- 35
3.5 Epidotisation and Carbonitisation ---------- 39
3.6 Metamorphism in Shear Zones ---------- 41

CHAPTER 4: GEOCHEMISTRY OF BGB VOLCANIC ROCKS ---------- 43
4.1 Introduction---------- 43
4.2 Analytical Methods---------- 43
4.3 Geochemical Results (Major and Trace)---------- 44
4.31 Ni and Cr---------- 44
4.32 Ca---------- 44
4.33 Al---------- 56
4.34 Sr---------- 56
4.35 Na---------- 57
4.36 K---------- 57
4.37 Co---------- 58
4.38 Sc---------- 58
4.39 Cu---------- 58
4.40 V---------- 59
4.41 Ti, Y, Zr---------- 59
4.42 P---------- 60
4.43 Mn and Zn ---------- 61
4.4 Summary---------- 61
4.5 Geochemical Classification ---------- 62
4.6 Rare Earth Elements: Introduction---------- 65
4.7 Geochemical Results (Rare Earth Elements)---------- 65
4.8 Effects of Alteration on Elements ---------- 75
4.9 Molecular Proportion Ratio Diagrams---------- 76
4.10 Factor Analysis---------- 81
4.11 CO_2 vs HFS Diagrams---------- 84

CHAPTER 5: TECTONIC SETTING FOR THE BGB Basalts ---------- 87
5.1 Introduction---------- 87
5.2 Discriminant Diagrams and the BGB Volcanic Rocks---------- 88
5.3 Spidergrams---------- 90
5.4 Geochemical Comparison with Ancient and Recent Ophiolite------- 96
5.5 Discussion ---------- 97

CHAPTER 6: OVERALL TECTONIC HISTORY---------- 100
6.1 Rare Earth Data ---------- 100
6.2 Discrimination Using Structural and Stratigraphy---------- 101
6.3 Is BGB Representative of an Ophiolite? ---------- 102

CHAPTER 7: PETROGENETIC MODELLING ---------- 106
7.1 Basics of Partial Melting ---------- 106
7.2 Source Composition ---------- 108
7.3 Tholeiitic Basalts (Group I) ---------- 109
7.4 Crystal Fractionation ---------- 111
7.5 Calc-Alkaline Basalts (Group II) ---------- 114

CHAPTER 8 SUMMARY---------- 118
8.1 The Developmental History of BGB---------- 118
8.2 Further Work---------- 118
8.3 Closing Remarks ---------- 119

REFERENCES---------- 120

APPENDIX I (Geochemical Analyses) ---------- 141
APPENDIX II (Sample Localities) ---------- 147

LIST OF FIGURES

Figure 1.1 Location and Access ---------- 15

Figure 2.1 General geology ---------- 17

Figure 4.1 Ni vs. Mg#---------- 47

Figure 4.2 Cr vs. Mg#---------- 47

Figure 4.3 CaO vs. Mg#---------- 48

Figure 4.4 Al_2O_3 vs. Mg#---------- 48

Figure 4.5 Sr vs. Mg#---------- 49

Figure 4.6 Na_2O vs Mg#---------- 49

Figure 4.7 K_2O vs. Mg#---------- 50

Figure 4.8 Co vs. Mg#---------- 50

Figure 4.9 Sc vs. Mg#---------- 51

Figure 4.10 Cu vs. Mg#---------- 51

Figure 4.11 V vs. Mg#---------- 52

Figure 4.12 TiO_2 vs. Mg#---------- 52

Figure 4.13 Y vs. Mg#---------- 53

Figure 4.14 Zr vs. Mg#---------- 53

Figure 4.15 P_2O_5 vs. Mg#---------- 54

Figure 4.16 MnO vs. Mg#---------- 54

Figure 4.17 Zn vs. Mg#---------- 55

Figure 4.18 AFM Diagram---------- 63

Figure 4.19 P_2O_5 vs. Zr ---------- 64

Figure 4.20 REE Results for PW105, PW107, PW109B---------- 67

Figure 4.21 REE Results for PE104A, PE104, S202, BLX ---------- 68

Figure 4.22 REE Results for OX115, OX113, OX101---------- 69

Figure 4.23 REE Results for GG, KPP---------- 70

Figure 4.24 REE Results for BM104, WD113---------- 74

Figure 4.25 K_2O/Al_2O_3 vs. Fe_2O_3/Al_2O_3---------- 78

Figure 4.26 Sr/Al_2O_3 vs. Fe_2O_3/Al_2O_3 ---------- 78

Figure 4.27 Ca/Al_2O_3 vs. Fe_2O_3/Al_2O_3---------- 79
Figure 4.28 Sc/Al_2O_3 vs. Fe_2O_3/Al_2O_3 ---------- 79
Figure 4.29 Y/Al_2O_3 vs. Fe_2O_3/Al_2O_3---------- 80
Figure 4.30 V/Al_2O_3 vs. Fe_2O_3/Al_2O_3---------- 80
Figure 4.31 P_2O_5 vs. CO_2 ---------- 85
Figure 4.32 Zr vs. CO_2---------- 85
Figure 4.33 TiO_2 vs. CO_2---------- 86
Figure 4.34 Y vs. CO_2---------- 86
Figure 5.1 Ti/100-Zr-Y Diagram ---------- 89
Figure 5.2 TiO_2-K_2O-P_2O_5 Diagram---------- 91
Figure 5.3 Ti/100-Zr-Sr/2 Diagram---------- 92
Figure 5.4 Samples Normalised to MORB Diagram---------- 94
Figure 5.5 Samples Normalised to IAT Diagram---------- 94
Figure 5.6 Samples Normalised to MBB Diagram---------- 95
Figure 5.7 TiO_2-($Fe_2O_3^t$/MgO) Diagram---------- 95
Figure 6.1 Schematic Diagram of Tectonic Setting---------- 105
Figure 7.1 Petrogenetic Modelling for tholeiitic basalts---------- 110
Figure 7.2 Crystal Fractionation Modelling for within suite rocks---- 112
Figure 7.3 Petrogenetic Modelling for calc-alkaline basalts---------- 116

LIST OF PLATES

Plate 2.1 Amygdules from Undeformed Flow---------- 21

Plate 2.2 Undeformed Pillowed Flow---------- 21

Plate 3.1 Bimodal Grain Sizes of Amphibole---------- 26

Plate 3.2 Actinolitic Hornblende---------- 26

Plate 3.3 Poikiloblastic Hornblende and Biotite---------- 27

Plate 3.4 Amphibole from lower Amphibolite Facies---------- 27

Plate 3.5 Epidote in Veinlets---------- 28

Plate 3.6 Relict Textures---------- 28

Plate 3.7 Deformed Amygdules infilled with Chlorite---------- 30

Plate 3.8 Opaque and Ferromagnesian Mineral Association--------- 30

Plate 3.9 Preferred Oriented Amphibole---------- 33

Plate 3.10 Undeformed Secondary Amphibole---------- 33

LIST OF TABLES

Table 1	Precision of Geochemical Analysis----------	45
Table 2a and 2b	Varimax Rotated Factor Analysis----------	83
Table 3	Summary of Discriminant Results----------	98
Table 4	Least Square Mixing----------	113

ABSTRACT

Three repetitive sequences of northward younging, east striking, linear, volcano-sedimentary units are found in the late Archaean Beardmore-Geraldton greenstone belt, situated within the Wabigoon subprovince of the Superior Province of northwestern Ontario. The volcanic components are characterised by basaltic flows that are pillowed at the top and underlain by variably deformed massive flows which may in part be intrusive. Petrographic examination of the volcanic units indicates regional metamorphism up to greenschist facies (T=325° C - 450° C, P=2kbars) overprinted by a lower amphibolite facies thermal event (T=575° C, P=2kbars) confined to the south-eastern portion of the belt.

Chemical element results suggest olivine, plagioclase and pyroxene are the main fractionating mineral phases. Mobility studies on the various chemical elements indicate that K, Ca, Na and Sr are relatively mobile, while P, Zr, Ti, Fe^t (total iron = Fe_2O_3) and Mg are relatively immobile. Discriminant diagrams employing immobile element suggests that the majority of the samples are of oceanic affinity with a minor proportion displaying an island arc affinity.

Such a transitional tectonic setting is also reflected in REE data where two groups of volcanic samples are recognised. Oceanic tholeiites are LREE depleted with [La/Sm] N = 0.65 and a relatively flat HREE profile with [Sm/Yb] N = 1.2. Island arc type basalts (calc-alkaline) are LREE enriched, with a [La/Sm] N = 1.6, and a relatively higher fractionated HREE profile with [Sm/Yb] N = 1.9.

Petrogenetic modelling performed on oceanic tholeiites suggests derivation from a depleted spinel lherzolite source which undergoes 20% partial melting. Island arc type basalts can be derived by 10% partial melting of a hypothetical amphibolitised oceanic tholeiite source.

The majority of the volcanic rocks in the Beardmore-Geraldton Belt are interpreted to represent fragments of oceanic crust trapped at a consuming plate margin. Subsequent post accretionary intrusion of gabbroic rocks (sensu lato) with calc-alkaline affinity is considered to result in the apparent hybrid tectonic setting recognized for the BGB.

ACKNOWLEDGEMENTS

I would like to thank Dr. Howard Williams for giving me the opportunity to work on this project and for providing me with the necessary fundings to carry out this work (NSERC A8513 and OGRF 242). It has been a pleasure to work with him in the field; the knowledge and insight gained during the field season has been invaluable. Many thanks to Greg Finn for his patient and helpful discussion. Most rewarding to have you as one of my supervisors. Discussion with Dr. Jolly with regards to Archaean volcanics has been both intriguing and enlightening. I think we are still mystified by what did actually happen during the Archaean. A time machine (perhaps?) would facilitate in solving some of these enigmas. I guess every one has his own individual preference with respect to what did actually happened in the Archaean. I would like to acknowledge the help of other members of the faculty, including Drs. Cheel, Brand and Kennedy. Candy Kramer assisted with the final touches of the thin sections and Peter Brown and Peter Barclay help is much appreciated. My appreciation to the past graduate students, especially Brian Reilly, Shane Buck, Ed Lorek and Brad Cummings, for creating an environment which is conducive to graduate studies. My gratitude to Jerry Celetti for being there and for introducing me to the mathematical world of chaos. Geochemical analyses were carried out at the labroratories of the Ontario Geological Survey and were funded by the Canada-Ontario Mineral Development Agreement. Last but not least, my thanks to all those researchers out there who have contributed generously and unselfishly to our understanding of the world of sciences around us.

CHAPTER 1

1.1 INTRODUCTION

Geologists have been intrigued by the origin of Archaean greenstone belts and associated lithologies compelling them to propose numerous hypotheses for the origin of these ancient rocks. Beginning with Wegener's (1912) theory of continental plate displacement and its subsequent rejuvenation in the early 1970's, two schools of thought were established, fixist versus mobilist, concerning the origin and evolution of early crustal material. The former group invoke that structures found in granite-greenstone belts are essentially produced by vertical movement resulting mainly through diapirism while the latter group attributes all structural features found in granite-greenstone belts, to horizontal plate movements. Up to the present day there exist no general consensus as to how the early crustal materials were formed. The central problem of Archaean geology lies not only within field geology and accessibility to these areas but also in the tectonics, geochronology and geochemical relationships between the greenstone belts and their adjacent granitic terranes. Often these fields do not correlate well with one another, that is, they are not internally consistent. Therefore to understand the origin and the evolution of the Archaean rocks, these differences have to be reconciled.

1.2 SCOPE OF STUDY

One of the main themes of this study is to examine the geochemical composition (major, trace and rare earth elements) of the volcanic rocks in the Beardmore-Geraldton Archaean greenstone belt. Geochemical characterisations are subsequently employed to determine the possible palaeotectonic setting for the volcanic rocks in the study area. The results are then compared with proposed palaeotectonic settings, derived from

independent structural and sedimentological studies carried out by other workers. This treatment can be viewed as an attempt to determine whether the palaeotectonic setting derived in this study using geochemical data is compatible with other studies. Other objectives of this study include i) the documentation of the prevailing metamorphic grade (based on petrographic criteria) recorded for the volcanic rocks and ii) a petrogenetic study of the volcanic rocks with emphasis on the identification of possible source material.

1.3 PREVIOUS WORK

Early work on the Beardmore-Geraldton Belt was carried out by the Ontario Department of Mines in separate studies by Bruce and Laird (1937); consisting of lithostratigraphic mapping of the area. These studies were undertaken to provide the geological framework for gold mining operations in the area. Subsequent detailed work was carried out by Horwood and Pye (1951) and Pye (1951), consisting of a compilation of both surficial and sub-surficial geological data. Other intensive work was performed by various mining companies prior to the outbreak of war in 1939. Resurgence of geological activity, encouraged by the higher gold prices, began in the late 1970's and continues to the present day. Recent work in the Beardmore-Geraldton Belt (BGB) consists of detailed mapping (Mackasey, 1975; 1976), sedimentological (Devaney and Fralick, 1985; Devaney, 1987) and structural studies (Kehlenbeck, 1983; 1986; Buck and Williams, 1984; Williams 1986; Stott, 1984a and b; Anglin and Franklin, 1985; Carter, 1983; Buck, 1986 and Reilly, 1988). Work on iron formations was carried out by Fralick and Barrett (1983).

1.4 FIELDWORK

Figure 1.1 illustrates the location of and access to the study area. Fifteen north-south traverses were run across the volcanic belts using

pace and compass method. Representative samples, along each traverse together with local sampling sites, were collected for thin-sections and geochemical analysis. Access to each traverse was provided along the logging roads of Domtar Incorporated, while densely vegetated abandoned-trails and canoe were used to reach the least accessible localities. The varying degree of access across each volcanic belt resulted in a sampling bias favouring the southern belt (Figure 3.1). In addition, the exposure in each traverse is quite variable, with the majority of them having less than 5% exposure.

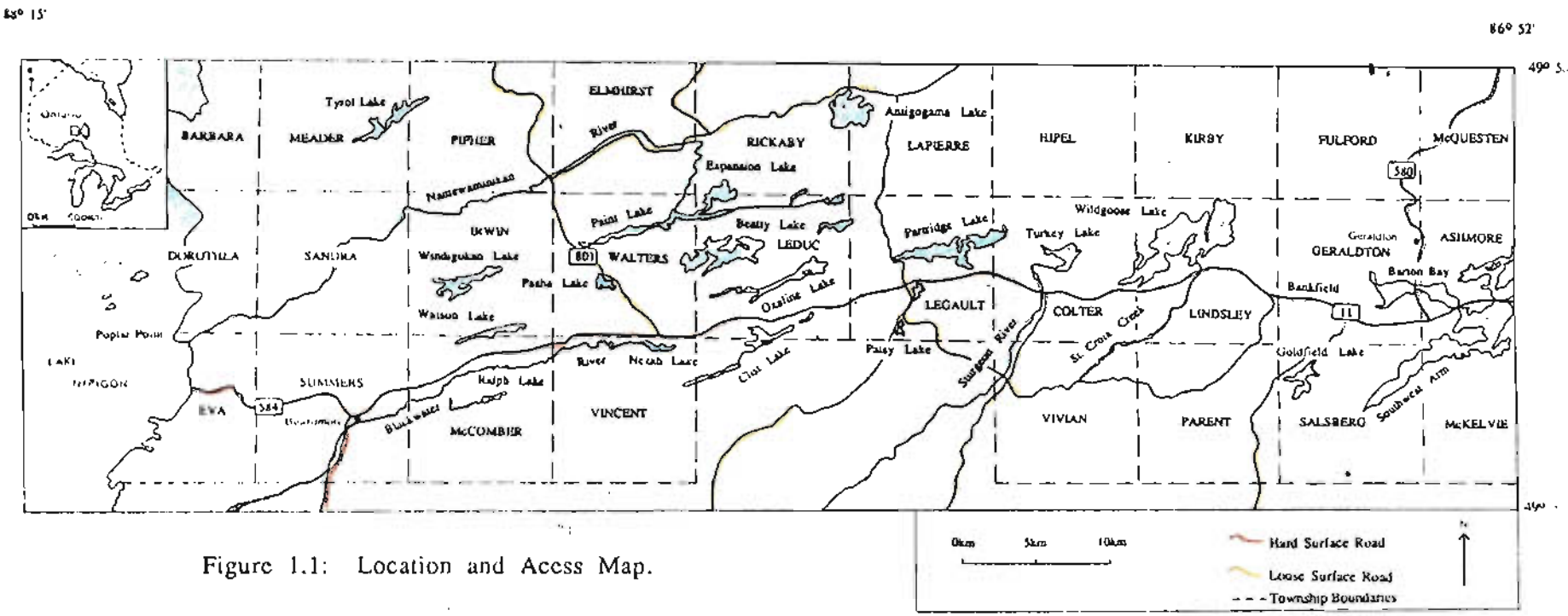

Figure 1.1: Location and Access Map.

CHAPTER 2

GEOLOGY OF BEARDMORE-GERALDTON BELT (BGB)

2.1 GENERAL GEOLOGY

The Beardmore-Geraldton Belt is located in northwestern Ontario, approximately 100 km north of Lake Superior. Situated within the Wabigoon subprovince of the Superior Province, Figure 2.1, its northern boundary is marked by the Paint Lake Deformation Zone (PLDZ) and to the south by the northern boundary of the Quetico subprovince. The belt trends approximately west-east, from the eastern shore of Lake Nipigon to Geraldton, a distance of approximately 100 km, with a maximum width of 25 km.

To the north of the BGB, the Onaman-Tashota Terrane (OTT) is characterised by a typical granite-greenstone terrane. Thurston (1980) and Amukun (1980) have interpreted the OTT to be an island arc based on the prevaling rock types observed. Volcanism and plutonism in the Wabigoon subprovince was suggested to have occurred around 2.75 Ga to 2.69 Ga, followed by major deformation, metamorphism and plutonism at 2.7 Ga to 2.66 Ga (Card, 1986).

To the south of the Beardmore-Geraldton Belt, the Quetico subprovince is characterised by a monotonous sequence of variably deformed and metamorphosed feldspathic, graded and massive greywackes. Individual beds seen in this terrane exhibit preserved primary sedimentary structures such as fluid escape features and grain size grading, indicating regional younging to the north (Pye 1965; Williams 1987; Carter 1983).

Based on observed lithological changes, progressing from the Quetico subprovince to the OTT and the relative positioning of the BGB, early workers suggest that the BGB represents a zone of lithologic transition from a sediment-dominated terrane in the south, to an idealized granite-

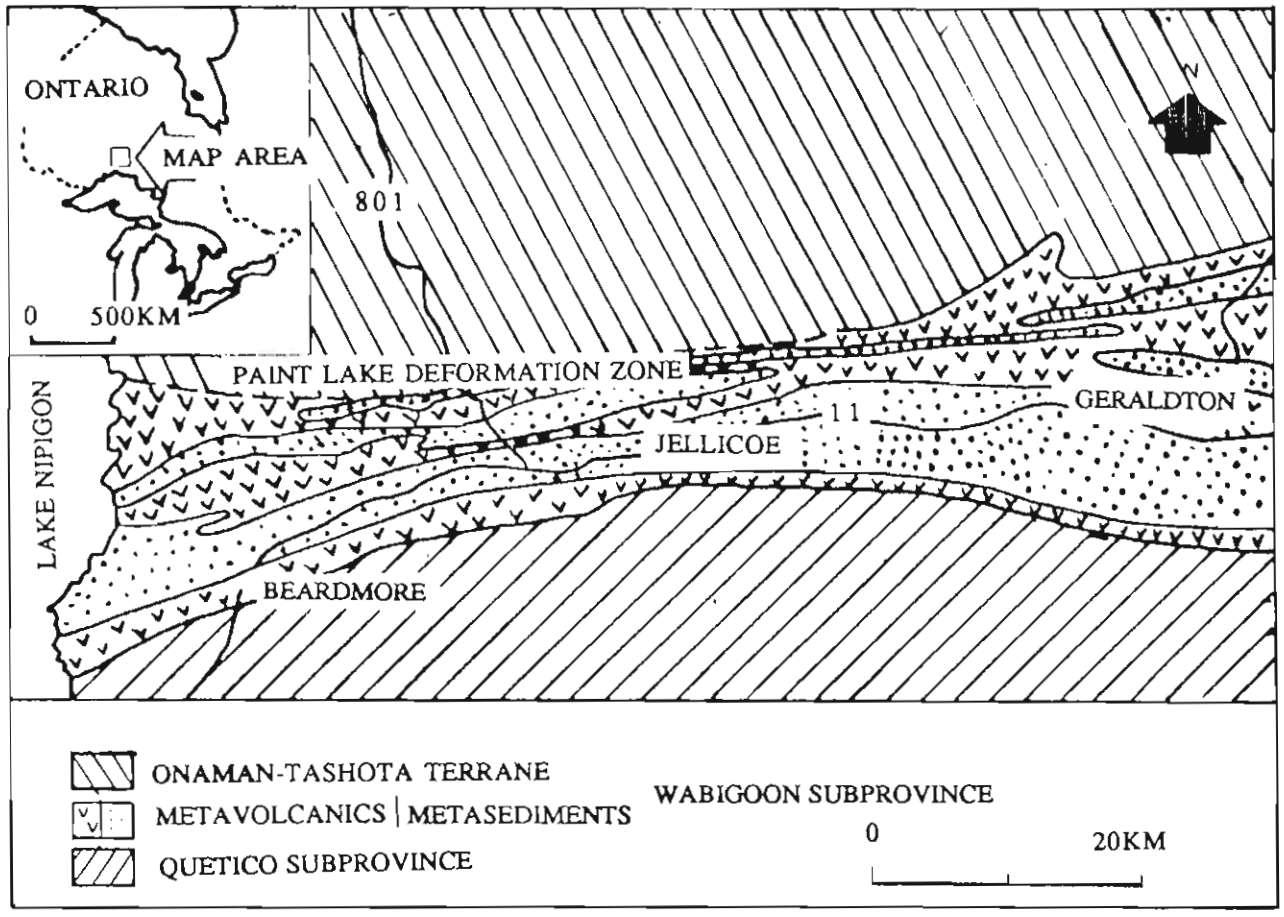

Figure 2.1: A simplified geological map of Beardmore-Geraldton Belt, modified from Stott (1984a,b). Inset shows the study area with respect to its location in the province of Ontario.

greenstone terrane in the north (Langford, 1929; Bruce, 1937; Laird, 1937; Ayres, 1969). Recent studies carried out by Langford and Morin (1976) and Williams (1986; 1987) have shown that the development of the Superior Province can be explained by a series of merging island arcs.

Williams (1986) considered the BGB to represent a complex zone of tectonically imbricated slices formed at the leading edge of an overriding plate system. The presence of this hypothesized complex zone is evidenced by i) repetition of volcanic and sedimentary belts; ii) minor isoclinal folding; iii) dip slip overthrust shearing as indicated by steeply dipping foliation and plunging stretching lineation and iv) inhomogeneous ductile dextral shearing along the contacts of contrasting lithologies (Williams 1986). Comparable structural and lithological features have been reported for the Southern Uplands of Scotland (McKerrow and Leggett, 1977), on Signy Island, off the Antarctic Peninsula (Storey and Menneilly, 1985) and the Shimanto accretionary complex (Needham and Mackenzie, 1988).

2.2 LOCAL GEOLOGY

The BGB is characterised by alternating belts of east-west trending, nearly vertical dipping, metasedimentary and metavolcanic rocks. Unlike other greenstone belts in the Superior Province, the BGB depicts an apparent lack of felsic plutonic activity.

The metasedimentary rocks have been subdivided into northern, central and southern belts (Mackasey, 1975; Devaney, 1987). The intervening metavolcanic rocks are subdivided into 3 belts in a similar manner. Metasedimentary and metavolcanic rocks will be addressed as sedimentary and volcanic rocks, respectively, for the balance of this work.

2.3 SEDIMENTARY BELTS

The northern sedimentary belt (NSB) is characterised by poorly sorted, polymictic orthoconglomerate with predominantly felsic volcanic clasts (Mackasey, 1975; 1976). The NSB is massive to crudely bedded, with minor feldspathic sandstone lenses. Pebble and cobble bands define a crude bedding with north facing younging directions (Devaney and Fralick, 1985). A similar lithologic belt to the west of Lake Nipigon has also been documented by Tanton (1935), Pye (1968) and Mackasey (1975; 1976).

Devaney (1987) has divided the central sedimentary belt (CSB) into three components, each of which exhibits a progressive increase in grain size and consistent younging directions to the north. The southern component of this belt is characterised by mudstone, sandstone and minor iron stone. The middle component is sandstone rich, with conglomeratic beds, pebble bands and minor mudstone. The northern component is similar to the NSB. Minor south facing younging directions have been documented in this central belt (Kehlenbeck, 1983; Anglin and Franklin 1985; Williams, 1986). Williams (1986) considered this reversal of facing directions to be confined to major lithological boundaries.

The southern sedimentary belt (SSB), is characterised by a monotonous sequence of feldspathic-greywackes with minor iron-stone and thin conglomeratic beds. Individual beds fine northwards, while the whole sequence coarsens and youngs to the north (Mackasey, 1975; 1976; Devaney and Fralick 1985; Williams, 1986).

Deformation within the sedimentary belts is generally inhomogeneous, confined to lithologic boundaries and to the less competent lithologies. In the SSB, undeformed greywacke can be observed in contact with a more deformed, equivalent lithology. Detailed sturctural analysis of the sedimentary belts has been carried out by Anglin and Franklin (1985) and Williams (1986; 1987). The sediments record evidence of greenschist facies metamorphism (Mackasey, 1975). Devaney and Fralick (1985)

interpret the sedimentary belts to represent a laterally continuous, prograding clastic wedge, with the northern and southern sedimentary belts representing proximal to distal deposits, respectively.

2.4 VOLCANIC BELTS

Three distinct volcanic belts are recognised in the BGB. Pillowed flows, usually observed at the top of each volcanic belt, are underlain predominantly by massive flows with minor amounts of variolitic, porphyritic and brecciated flows (Mackasey, 1975; 1976). In the field, the flows are dark-green to greenish black in colour, with a medium to fine grain size. The pillowed and massive flows possess varying amounts of vesicles and amygdules. Amygdules are filled with varying proportions of quartz, epidote, carbonate and/or chlorite. In least deformed flows, spherical amygdules (generally less than 1 cm) are preserved (Plate 2.1), with ellipsoidal shapes present in the deformed flows (Plate 3.7).

Undeformed pillow lavas in the three volcanic belts are generally less than 1 m by 0.4 m in size. Larger pillows were observed in the vicinity of Poplar Point (Figure 1.1). Each pillow is defined by an approximately 1 cm thick, dark green, aphanitic selvage. Individual pillows exhibit a gradual increase in grain size from selvage to core. Pillowed flows located in the northern and central volcanic belts are relatively undeformed, such as those seen near Windigokan Lake, (Plate 2.2) and in the vicinity of Poplar Point. Well defined pillow cusps, with constant selvage thicknesses, indicate a north facing direction. At Poplar Point, pillows are surrounded by inter-flow breccias with subrounded to angular volcanic fragments embedded in a dark green matrix. These breccias have been interpreted to be of flow top origin (Mackasey, 1975). In contrast to the northern and central volcanic belts, the pillow flows in the southern volcanic belt are usually elongated, with the long axis of the pillow parallel or subparallel to the regional foliation. In Ralph Creek

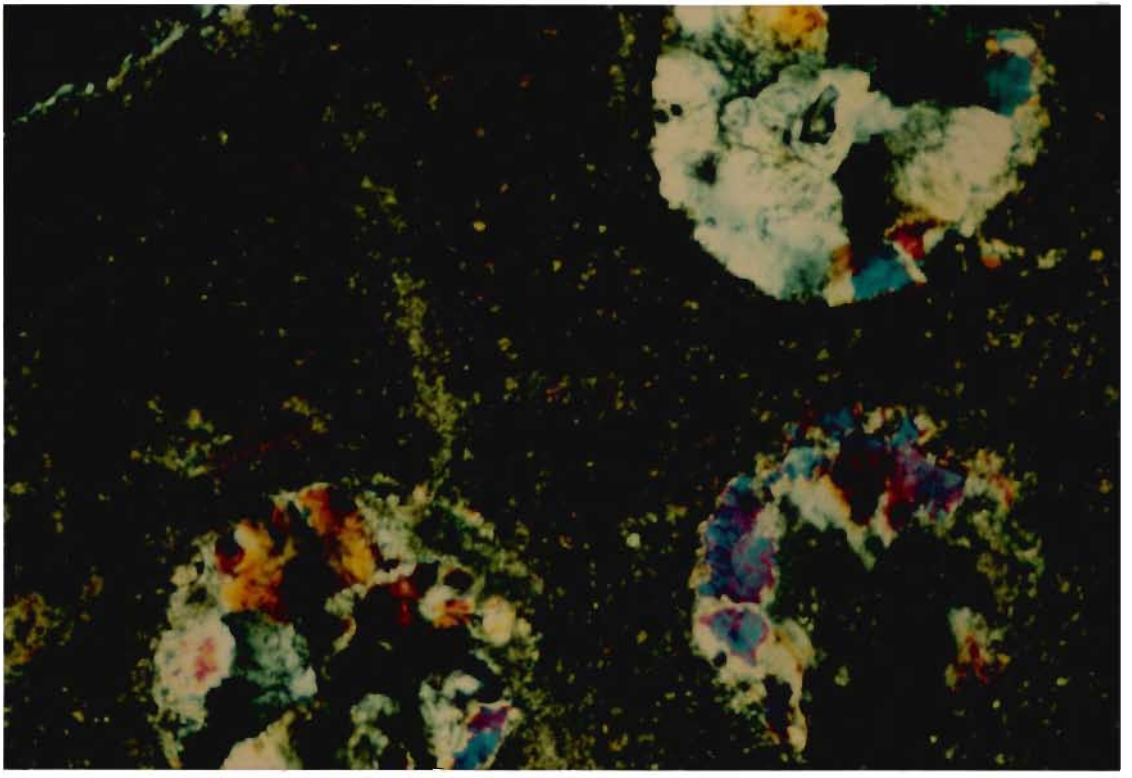

Plate 2.1: Spherical amygdules infilled with quartz and calcite. Sample obtained from an undeformed pillowed flow in the central volcanic belt. (Cross polars; X25)

Plate 2.2: Outrop of undeformed pillowed flow with uniform selvage thickness around individual pillow.

traverse, (Figure 3.1), varioles within the flow are elongated parallel with the regional foliation. These variolitic flows can be traced for a distance of 10 km along strike in the southern volcanic belt. Variolitic flows are considered to result from liquid immisibility (Gelinas et al., 1976).

Individual massive flows below the pillow sequence are difficult to delineate due to varying degrees of alteration and deformation as manifested by the presence of both penetrative and non-penetrative deformation. Undeformed, coarse grained gabbroic flows are characterised by their knobby weathering appearance in the field. Petrographic examination (Chapter 3) reveals that these flows have been metamorphosed to greenschist facies. It should be pointed out that some of the coarse-grained flows are indistinguishable from later gabbroic intrusions due to the nature of the outcrop and the lack of contact metamorphic aureoles. Thin layers of volcaniclastic material and iron stone were found interbedded with the volcanic flows.

Deformation features including both ductile and brittle deformation are seen in the volcanic rocks. This is manifested by the presence of s, c, and c' fabrics, minor asymmetric folds, kink bands, steeply plunging mineral lineation and slickenside surfaces in these volcanic belts. Details on the deformational features of the volcanic rocks can be found in Williams (1986; 1987), Buck (1986) and Reilly (1988).

2.5 INTRUSIVE ROCKS

Mafic intrusive rocks have been documented within the volcanic and sedimentary rocks by Mackasey (1975;1976) and Carter (1983). On a regional scale, the mafic intrusives exhibit a SE-NW linear pattern, with the distribution controlled by a fracture system (Mackasey, 1976). Carter (1983) has documented a suite of NE trending, massive, medium to coarse-grained, gabbroic intrusives. The latter suite exhibits minor evidence of foliation along their contacts with the volcanic flows. In the

vicinity of Oxaline Lake the volcanic and sedimentary rocks are intruded by dioritic intrusives (Mackasey 1975; 1976).

Quartz-feldspar porphyry dykes, less than a metre wide, common throughout the study area, have been documented to possess a northeasterly trend (Carter, 1983). They are greyish pink in colour, with variable amounts of oligoclase feldspar and quartz phenocrysts in a sericitized matrix of fine-grained quartz and feldspar. In the field, they are foliated to non-foliated. The exact ages of most of these intrusives are unknown. Late Archaean and early Proterozoic diabase dikes are massive, fine to medium grained, generally north trending, and weather to a reddish brown colour (Mackasey 1975; 1976, Carter, 1983).

2.6 LITHOLOGICAL CONTACTS

The contacts between the sedimentary and volcanic belts are demarcated by faults and shear zones. Displacements, with a dominantly dextral sense are recognised by reorientation and displacement of quartz veins across lithological boundaries and sigmoidal en echelon veins (Williams 1986;1987; Buck 1986; Reilly 1988).

CHAPTER 3

PETROGRAPHY AND METAMORPHISM

3.1 INTRODUCTION

A total of 250 thin sections of volcanic rocks, were examined to determine the prevailing metamorphic conditions within the study area. Unlike the pelitic rocks, where a specific P-T condition can be approximated to a narrow range by the occurrence of a particular index mineral or mineral assemblage, metamorphosed volcanic rocks require compositional changes of the coexisting minerals to determine the P-T conditions to which they were subjected. This is especially true for the transition from greenschist and amphibolite facies due to the absence of 'new and distinct' minerals which characterise this transition. This transition is characterised by the compositional changes in plagioclase, as recorded by an increase in anorthite component, and the concomitant change in the colours of the amphibole.

Wiseman (1934) documented the change in colour of the amphibole from light green (actinolite) in the greenschist facies to blue green hornblende in the epidote-amphibolite facies and eventually to green hornblende in the lower amphibolite facies. Liou et al. (1974) attributed the colour change to result from an increase in Al, Ti, Na and Fe/Mg and a decrease in Si and Ca contents in the amphibole. The increase in An content of the plagioclase is attributed to the decreased Ca content of amphibole, combined with the Ca released during the breakdown of epidote and sphene at higher temperature and pressure.

3.2 DESCRIPTION OF MINERALS

3.21 Amphibole

Amphibole found in the volcanic rocks can be divided into 4 types based upon their individual optical properties:

1) Actinolite: Exhibits a fibrous form, is weakly pleochroic with a pale green colour, and may define a preferred oriented growth. A distinct bimodality, with respect to grain size within individual thin sections was observed (Plate 3.1).

2) Actinolitic-hornblende: Crystal forms range from xenoblastic to idioblastic and exhibit a combination of pale green and blue-green colours reflecting the coexistence of actinolite and hornblende. Hornblende often occurs as rims encircling actinolite crystals and/or as a parallel growth with actinolite (Plate 3.2). The contacts between these two amphiboles range normally from sharp to gradational in nature. These amphiboles occur either as oriented or unoriented grains.

3) Hornblende: Crystal forms range from subidioblastic to idioblastic, to poikiloblastic grains with quartz, epidote, mica, carbonate and plagioclase inclusions (Plate 3.3). Hornblende is usually strongly pleochroic, from blue-green to green. Pleochroic brown hornblende was also observed, however it occurs only rarely in the eastern portion of the southern belt (Plate 3.4).

4) Cummingtonite: This form of amphibole is differentiated from the above amphiboles by a biaxial positive optic sign and a neutral colour. Cummingtonite is generally observed in the southern volcanic belt. Miyashiro (1978), suggests that the existence of cummingtonite indicates metamorphism at lower amphibolite facies.

3.22 Epidote

Epidote occurs as granular to columnar aggregates. It is an essential constituent of the matrix material in the volcanic rocks, with amphibole being the porphyroblasts. In thin section, epidote is found either as scattered granular masses or localised along veinlets (Plate 3.5). Epidote is ubiquitous up to the lower amphibolite facies. Some are seen to

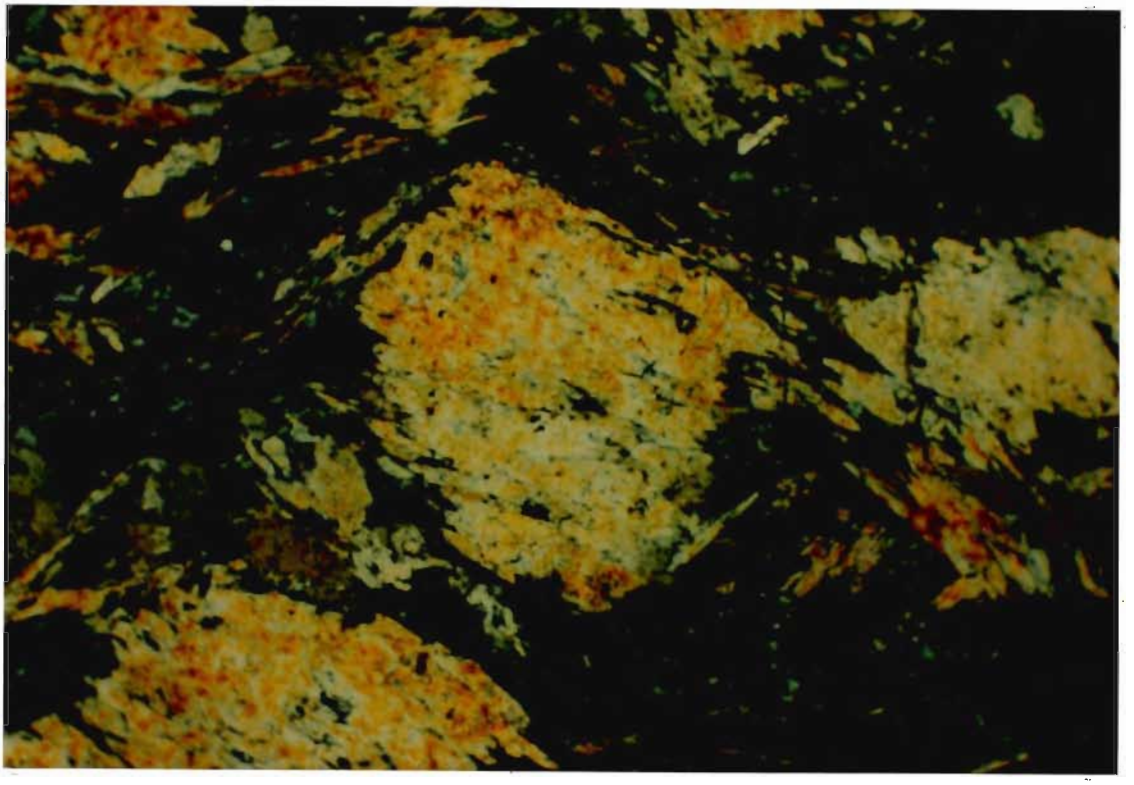

Plate 3.1: Occurrence of bimodal grain sizes of actinolite; a common feature in most thin sections of greenschist facies. (Cross polars; X40)

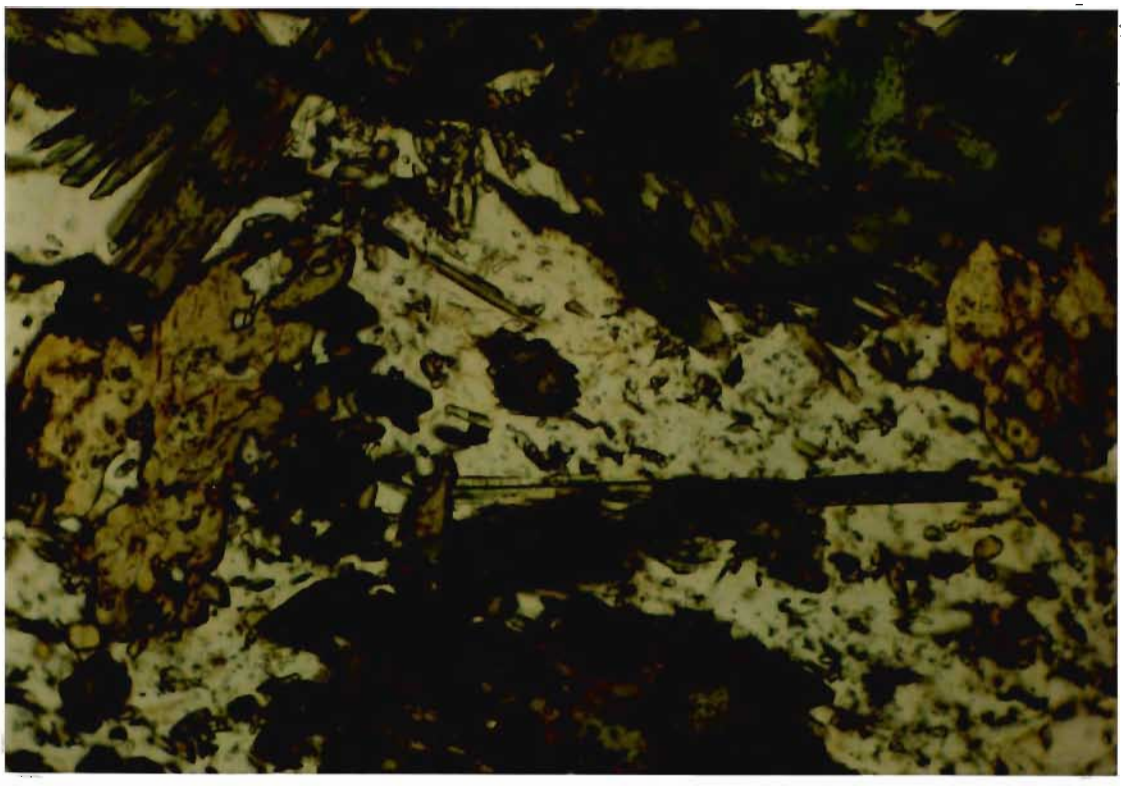

Plate 3.2: Actinolitic hornblende with actinolite rimmed by and paralled by blue green hornblende. (X40; plane light)

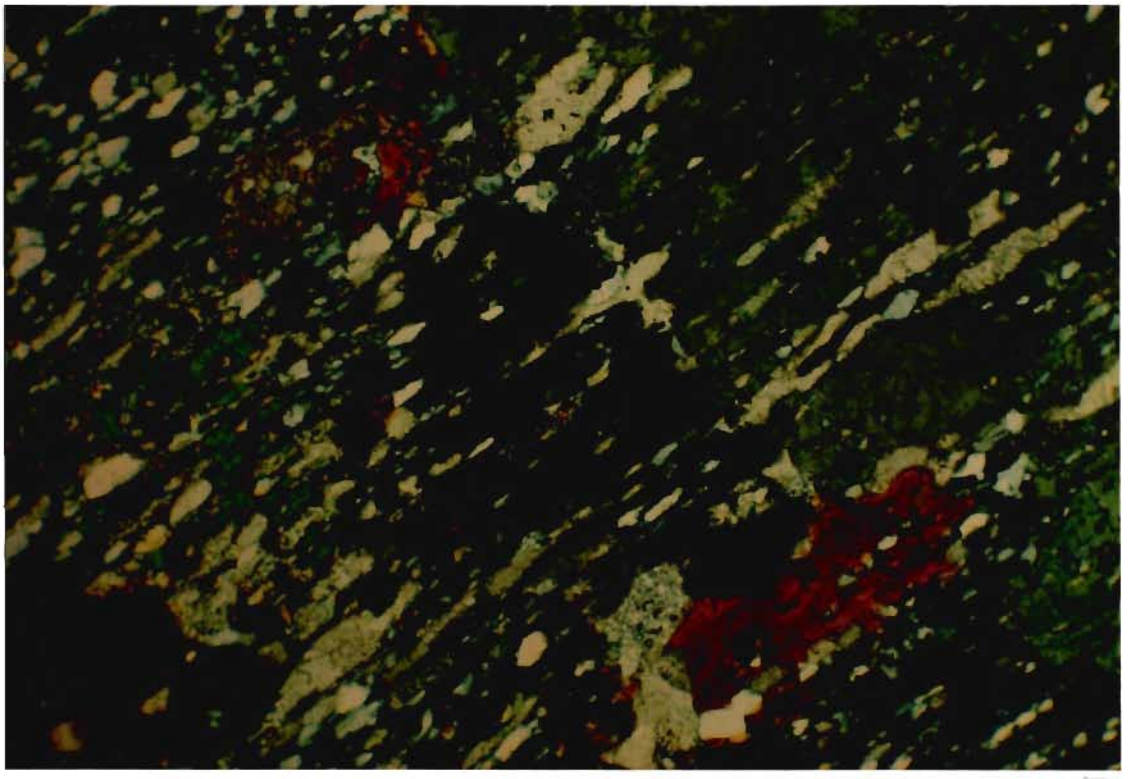

Plate 3.3: Poikiloblastic hornblende and biotite, with inclusions of carbonate, quartz and epidote. (X40; cross polars)

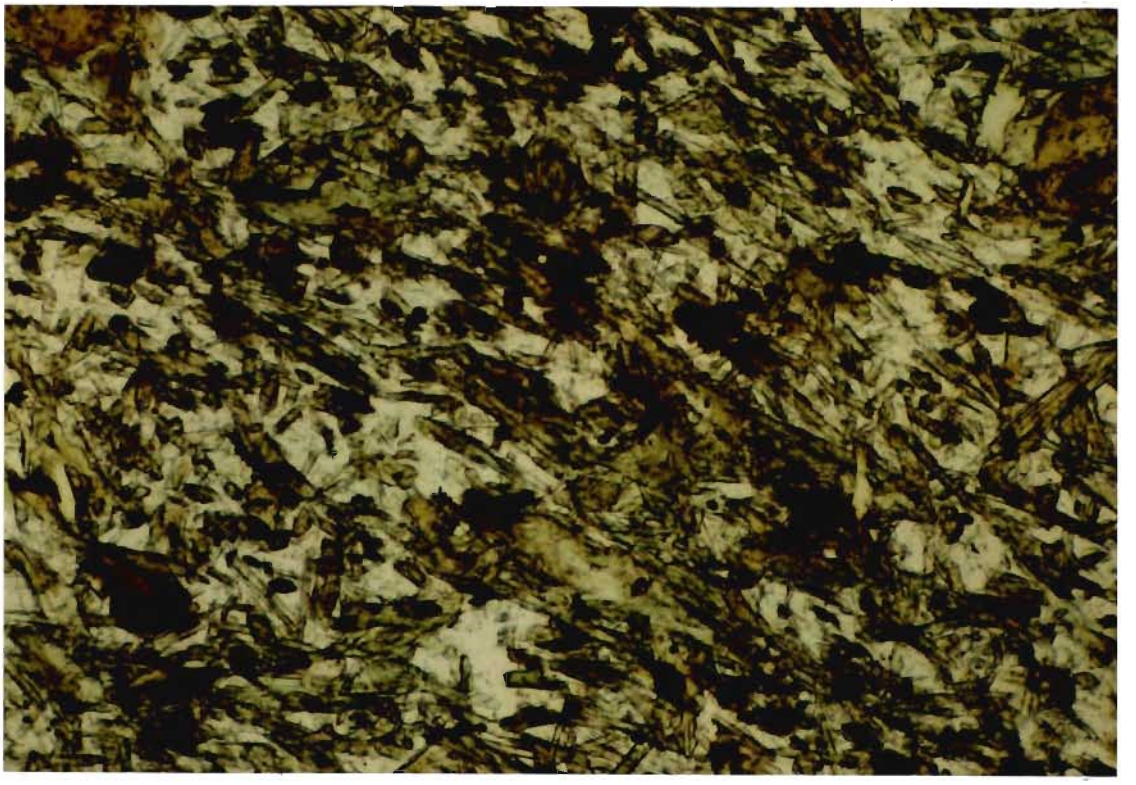

Plate: 3.4 High grade amphiboles: Brown hornblende observed in volcanics of lower amphibolite facies. (X 25; plane light)

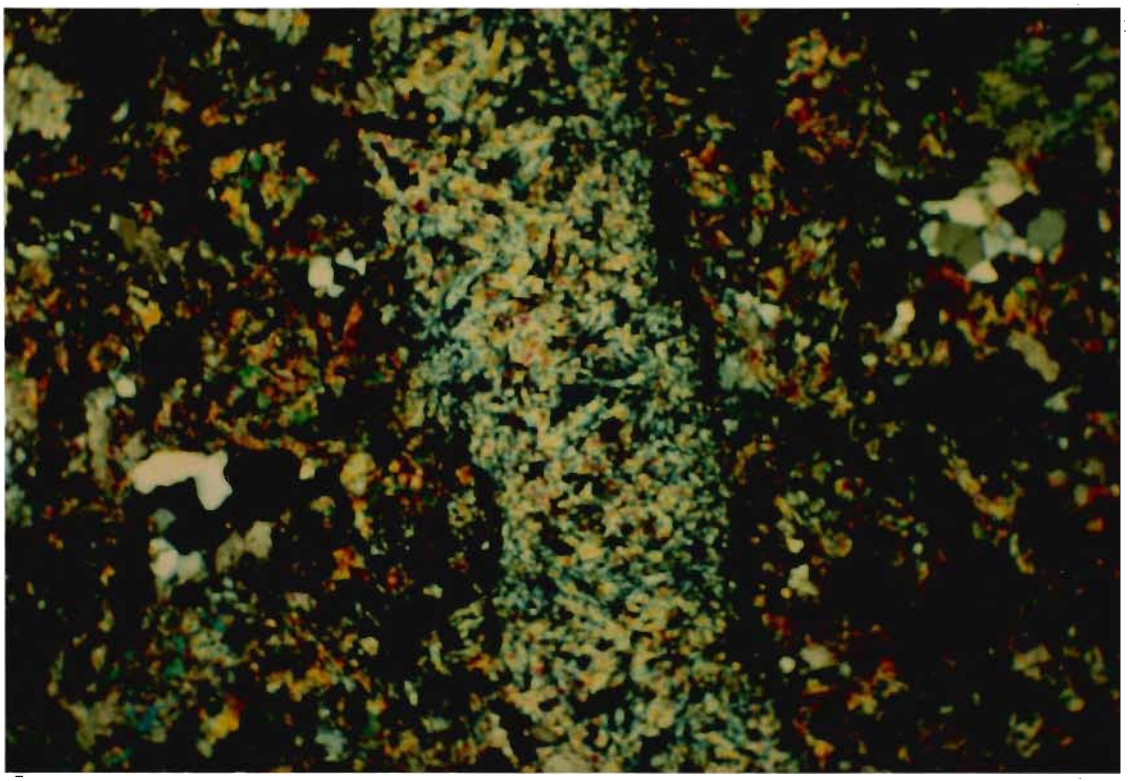

Plate 3.5: Epidote in veinlets (X40; cross polars)

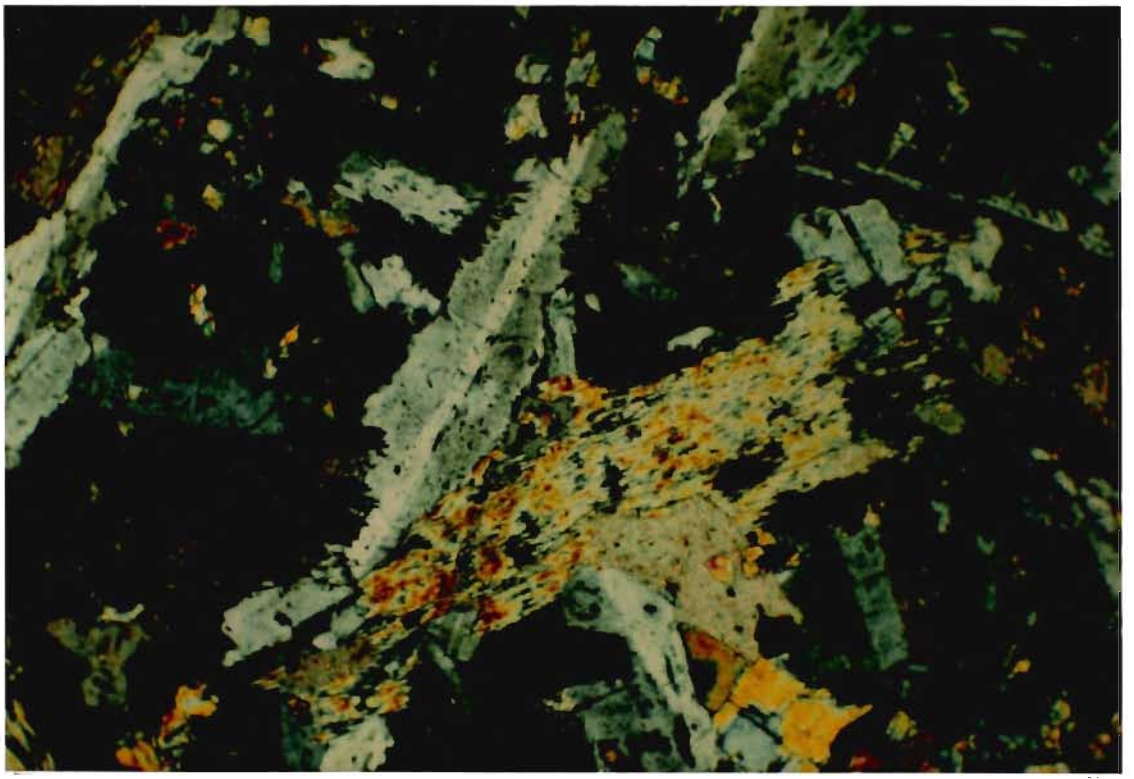

Plate 3.6: Relict blasto-ophitic texture with corroded, albitized plagioclase laths, and pyroxene being replaced by actinolite. (X40; cross polars)

pseudomorph original feldspar crystals. The relative abundance of epidote is seen to decrease with increasing metamorphic grade.

3.23 Plagioclase feldspar

Both primary and secondary plagioclase feldspar is present in the volcanic rocks. The former being in the labradorite composition range while the latter ranges from albite to andesine. Both groups of feldspar occur as either idioblastic, subidioblastic or xenoblastic forms. During the initial stage of albitization, the labradorite lath (0.3 mm to 0.4 mm) is often corroded (Plate 3.6). In addition to albitization, the labradorite also undergoes sericitization, saussuritization and replacement by carbonate. Albite produced from alteration of labradorite is clear, untwinned and unzoned, with some exhibiting a cloudy appearance due to incomplete replacement of the primary mineral. Albitization also entails the removal of the anorthite molecule which is involved in the formation of epidote. The presence of epidote aggregates in conjunction with minor sericite is used to identify the saussuritization process. Sericite is recognised by the appearance of a phyllosilicate mineral similar to muscovite and is suggested by Ehlers and Blatt (1982) to be a result of alteration in the presence of potassium ions. The An content of the plagioclase, at higher grade, changes to a range between oligoclase to andesine. This change will be discussed in section 3.4.

3.24 Chlorite

This mineral occurs in acicular or patch-like forms. Chlorite is a common constituent of the matrix assemblage. Interconnected veinlets of chlorite are common in deformed metavolcanic rocks of the greenschist facies. The abundance is seen to decrease with increasing metamorphic grade. Chlorite also occurs as an amygdule filling (Plate 3.7) and in veins as a monomineralic assemblage.

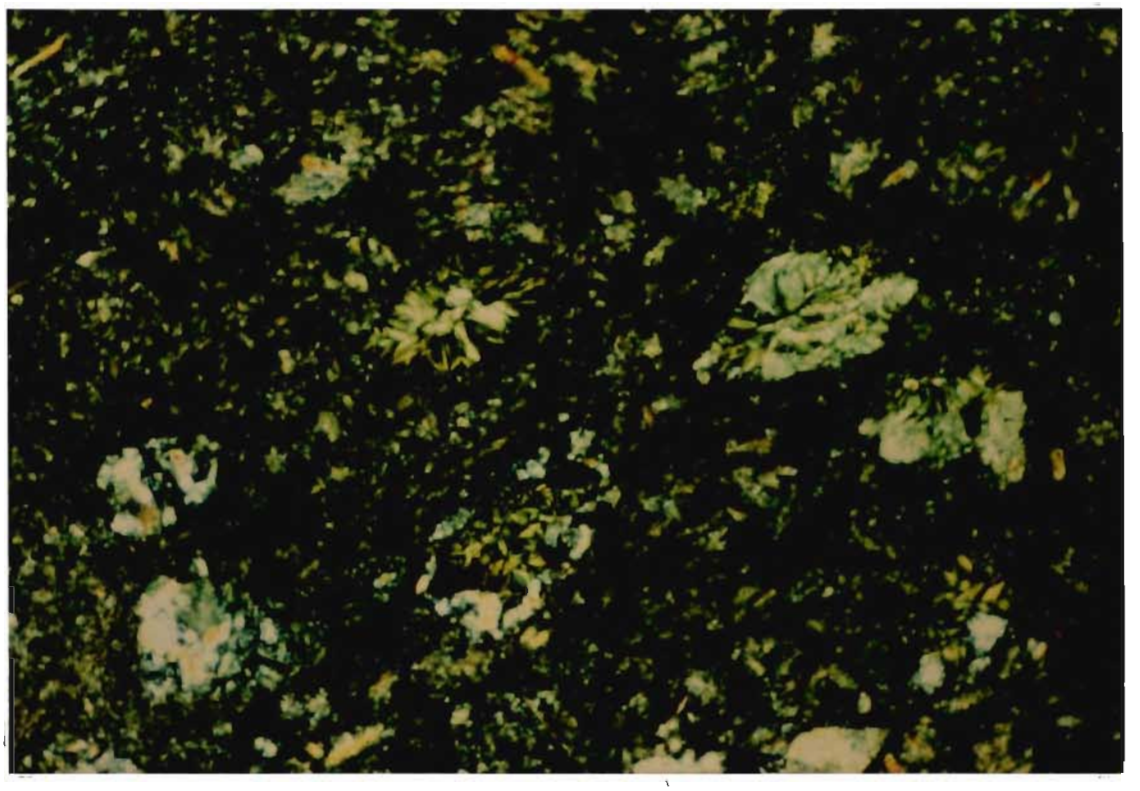

Plate 3.7: Ellipsoid amygdules infilled with chlorite (X25; cross polars)

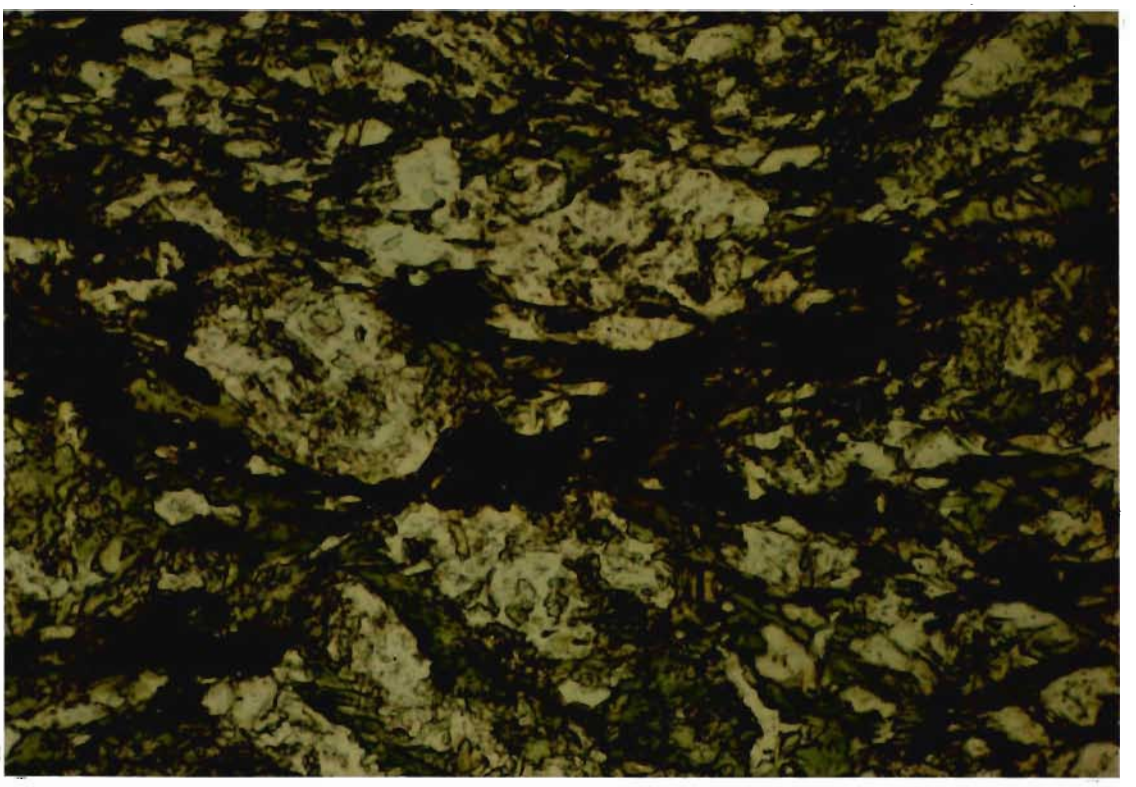

Plate 3.8: Opaque in close proximity to amphibole and chlorite. (X100; plane light)

3.25 Quartz

This mineral is usually xenoblastic, and rarely lensoidal in form with relative proportions varying from sample to sample. Undulose extinction is commonly seen in thin section. Quartz is found in veins, amygdules and matrix.

3.26 Sphene

Most of the sphene identified is subidioblastic to xenoblastic. When in xenoblastic forms, they occur as slivers, with a preferred orientation paralleling the amphibole.

3.27 Carbonate

Carbonate is generally xenoblastic in form. The two most common forms of occurrence are either as patches or as lenses defining a preferred orientation. They also occur in veins, cavities, amygdules and are seen replacing plagioclase. Carbonate is widely distributed, especially in the greenschist facies rocks. The relative abundance of carbonate is more pronounced in the western portion of the study area (Figure 3.1).

3.28 Opaque

Opaques range from subidioblastic to xenoblastic forms. They are mainly magnetite, however, pyrite and pyrrhotite are present in sulphide rich samples. Magnetite can be recognised by a metallic lustre in reflected light, while pyrite and pyrrhotite can be identified by brassy yellow and bronze metallic lustre respectively. Magnetite also occurs in elongated forms paralleling the amphibole and most often, they are in close proximity to chlorite or amphibole (Plate 3.8). Some opaques are rimmed by reddish brown hematite, indicating possible signs of alteration.

3.29 Mica

This mineral is xenoblastic to idioblastic in appearance, with the former being common. The principal mica commonly seen in the volcanic rocks is muscovite. Biotite is rarely found in the regional greenschist assemblage but it is observed in the transition and lower amphibolite facies (Figure 3.1). The presence of biotite may be related to dewatering of the adjacent sediments or to hydrothermal activity associated with higher metamorphic grade. These hypotheses can be tested using oxygen isotopes, where meteoric waters are considered to be characterised by a lower $d^{18}O$ value than water derived from magmatic activity (Henderson, 1984). Biotite occurs as poikiloblastic forms (Plate 3.3) at higher metamorphic grade.

3.3 TEXTURES

In the volcanic rocks, most of the primary textures of the protolith have been effaced by metamorphism and deformation. As a result, it is difficult to distinguish a completely altered basalt from a totally altered diabase or gabbro since the metamorphic assemblages are essentially identical. The identification of a specific lithology can only be made if primary emplacement features, such as pillow outline, are preserved. In the following sections, the textures described refer to volcanic rocks in general, unless otherwise stated.

The metamorphic textures seen in the volcanic rocks of the BGB are divided broadly into those which correspond to regional and thermal metamorphic events.

The textures resulting from regional metamorphism are essentially dictated by the orientation of the dominant mineral, amphibole. Preferred oriented texture is characterised by the alignment of 'platy' minerals, such as amphibole (Plate 3.9) and mica, and is manifested in the form of foliation observed in the outcrop. This texture has been

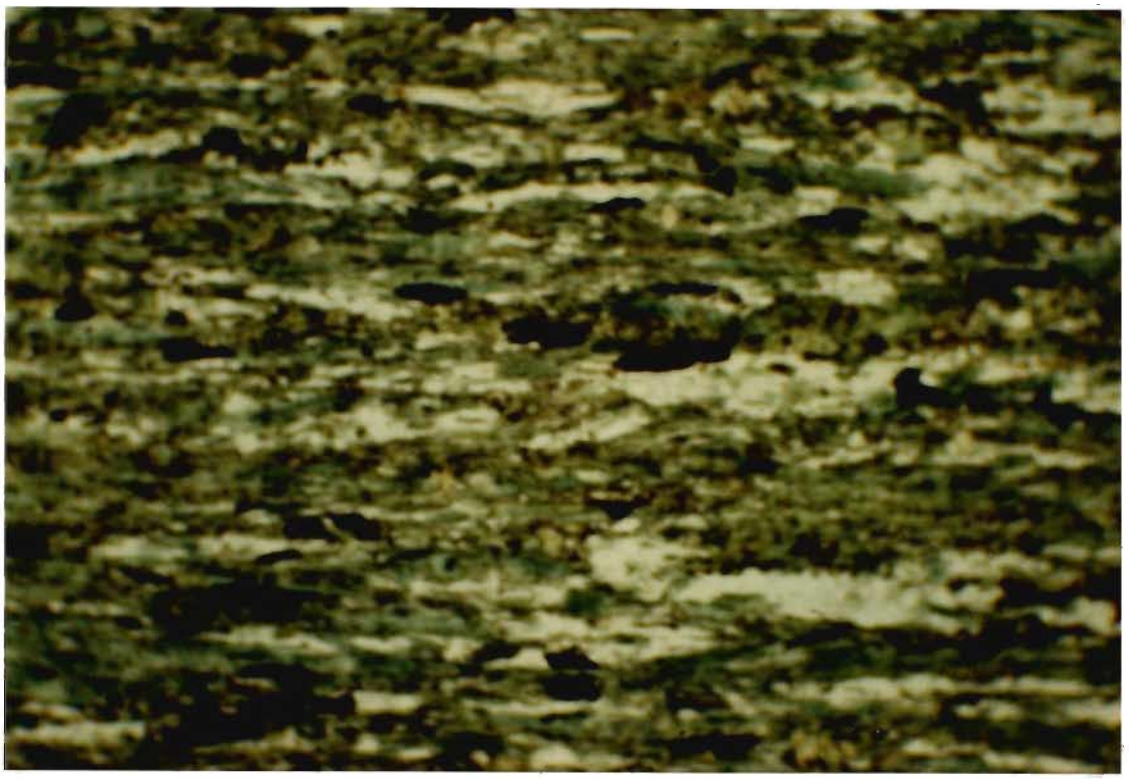

Plate 3.9: Amphibole showing preferred orientation in deformed rocks. (X 25; plane light). This is manifested as foliation in the outcrop.

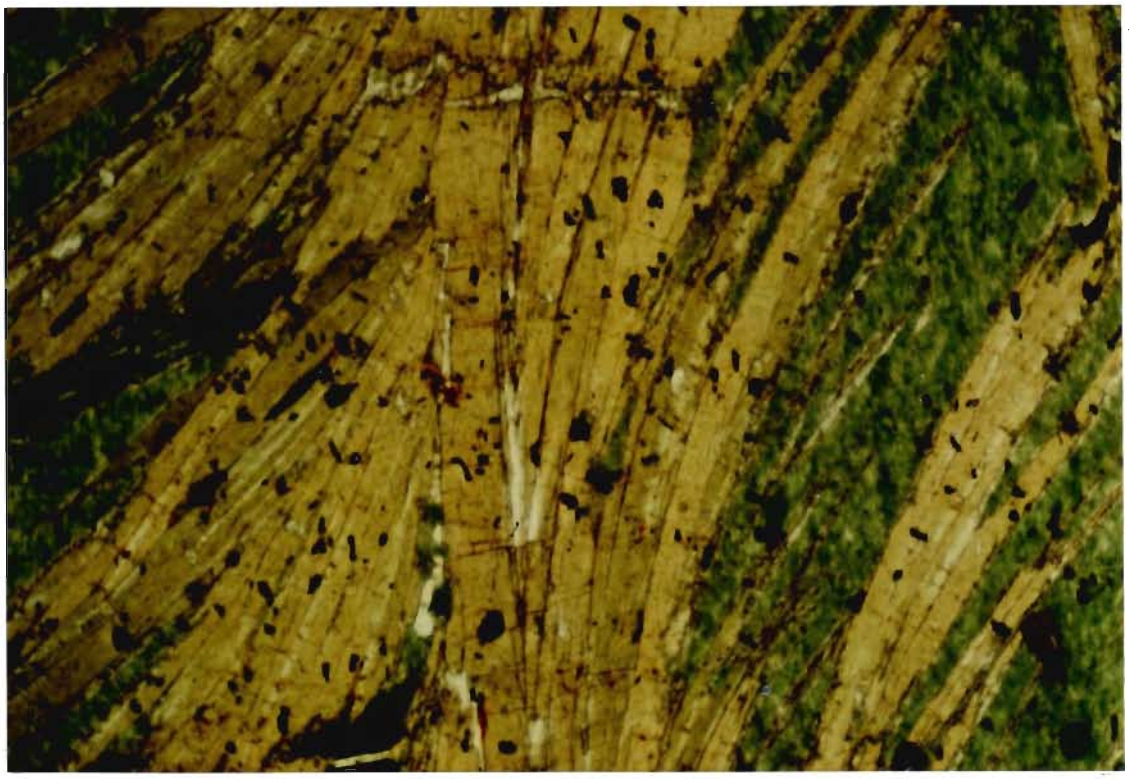

Plate 3.10: 'Feathery', secondary, undeformed, blue green amphibole obtained from a mafic lens within a quartz vein in a shear zone. (X100; plane light).

suggested by Hobbs et al. (1976) to result from several possible mechanisms including rotation of pre-existing grains or growth of grains in preferred orientation under the influence of regional stress.

The texture resulting from the thermal overprinting is recognised by the presence of a decussate texture and the random orientation of idioblastic grains. In the latter, randomly oriented poikiloblasts of biotite and blue-green hornblende are found in a matrix consisting of quartz, chlorite, epidote and plagioclase. The matrix minerals also occur as inclusions in the poikiloblasts (Plate 3.3), suggesting that some of these inclusions were there first and may have been involved in the production of hornblende and biotite. Both the former and latter features are produced under the influence of a low directed stress.

In addition to these features, the textures resulting from thermal overprinting are also observed to mimic the pre-existing regional texture. This texture is exemplified by the preferential growth of recrystallised minerals such as hornblende on the pre-existing fabric defined by actinolite. This texture differs from that of the regionally produced preferred oriented texture in that it is characterised by more idioblastic and less strained or contorted crystals while the latter is typified by xenoblastic (fibrous) crystals that have been subjected to strain.

Relict texture such as blasto-ophitic texture (Spry, 1983), are observed in localities which are designated as flow center (Plate 3.6). These localities are most likely sheltered from deformation and hence were subjected to limited fluid mobility (Etheridge et al., 1983). Brodie and Rutter (1985), have pointed out that the reduction in grain size through deformation will facilitate the reaction kinetics by enlarging the grain's surface area available for metamorphic reaction(s). In thin section, secondary ferromagnesian minerals such as chlorite and actinolite are seen to epitaxially replace the pyroxene minerals, while

the primary plagioclase (labradorite) undergoes albitization, saussuritisation, sericitization and replacement by carbonate.

3.4 DETERMINATION OF METAMORPHIC CONDITIONS

In this section, an attempt is made to determine the prevailing metamorphic conditions the volcanic rocks have undergone, especially with respect to the three different facies observed in the BGB. This derivation of the metamorphic conditions is based solely on comparing of observed mineral assemblage recorded in the facies concerned with those derived experimentally under specific P-T conditions.

The volcanic rocks of the BGB are characterised by a regional greenschist facies mineral assemblage. In the eastern portion of the southern volcanic belt, this assemblage is overprinted by a late stage thermal metamorphic event that is characterised by the presence of a transition and lower amphibolite facies, Figure 3.1. A typical greenschist facies is recognised by the mineral assemblage albite - chlorite - actinolite - epidote - sphene - quartz +/- micas whereas the lower amphibolite facies is characterised by the assemblage blue-green to green hornblende - plagioclase (An 10 to 40) - epidote and quartz. In contrast, the transition facies typically contains over-lapping mineral assemblages found in both the greenschist and lower amphibolite facies. The amphibole in the transition facies is termed 'actinolitic-hornblende'.

The regional metamorphism, documented by the greenschist facies mineral assemblages suggest an upper temperature and pressure limit of approximately 450°C at P= 2 kbar (Liou et al., 1974), while the absence of pumpellyite in these rocks implies a lower limit of about 325°C at P=2 kbar (Schiffman and Liou, 1980) .

Attempts have been made to refine the pressure regime of this regional metamorphic event in the study area using the metamorphic assemblage recorded in the adjacent sedimentary rocks. Due to the

broadness of the P-T stability field of this assemblage, that is, biotite - muscovite - chlorite - amphibole (Robinson, 1986); the refinement of the pressure regime was not possible. It should be pointed out that the variation in the Al^{vi} concentration of the amphibole can be used to define the pressure regime of the regional metamorphism (Raase 1974).

Hypothetical metamorphic reaction(s) that characterise the greenschist facies are as follow:

3-1] $5Ca(Mg,Fe)Si_2O_6 + 3CO_2 + H_2O$ ---------->

AUGITE + CARBON DIOXIDE + WATER

$Ca_2(Mg,Fe)_5Si_8O_{22}(OH)_2 + 3CaCO_3 + 2SiO_2$

ACTINOLITE + CARBONATE + QUARTZ

3-2] $4(NaAlSi_3O_8 - CaAl_2Si_2O_8) + H_2O$ ---------->

LABRADORITE + WATER

$4NaAlSi_3O_8 + 2Ca_2Al_3Si_3O_{12}(OH) + 2SiO_2 + Al_2O_3$

ALBITE + EPIDOTE + QUARTZ + CORUNDUM

3-3] $Ca_2(Mg,Fe)_5Si_8O_{22}(OH)_2 + 2CO_2 + 3H_2O + Al_2O_3$ ---->

ACTINOLITE + CARBON DIOXIDE + WATER + CORUNDUM

$(Mg,Fe)_5Al_2Si_3O_{10}(OH)_8 + 2CaCO_3 + 5SiO_2$

CHLORITE + CARBONATE + SILICA

The thermal metamorphism is characterised by the transformation of greenschist facies actinolite, into actinolitic-hornblende in the transition facies and eventually to hornblende in the lower amphibolite facies. In conjuction with this, the plagioclase becomes enriched in the anorthite component. Other features suggesting a late increase in grade include a depletion in relative abundances of chlorite and epidote and an increase in the relative abundances of magnetite towards the higher

grade rocks. These observation concur with a series of possible reactions proposed by Cooper (1972), Graham (1974) and Kuniyoshi and Liou (1976) for the transition facies. The reactions are as follows:

3-4] $NaAlSi_3O_8 + Ca_2(Mg,Fe)_5Si_8O_{22}(OH)_2 \rightarrow$

ALBITE + ACTINOLITE

$NaCa_2(Mg,Fe)_5AlSi_7O_{22}(OH)_2 + 4SiO_2$.

EDENITE + QUARTZ

3-5] $Ca_2(Mg,Fe)_5Si_8O_{22}(OH)_2 + 14(Mg,Fe)_5Al_2Si_3O_{10}(OH)_8 +$

ACTINOLITE + CHLORITE

$24Ca_2Al_3Si_3O_{12}(OH) + 28SiO_2 \rightarrow$

EPIDOTE + QUARTZ

$25Ca_2(Mg,Fe)_3Al_4Si_6O_{22}(OH)_2 + 44H_2O$

TSCHERMAKITE + WATER

3-6] $3(Mg,Fe)_{10}Al_4Si_6O_{20}(OH)_{16} + 12Ca_2Al_3Si_3O_{12}(OH) +$

CHLORITE + EPIDOTE

$14SiO_2 \rightarrow$

QUARTZ

$10Ca_2(Mg,Fe)_3Al_4Si_6O_{22}(OH)_2 + 4CaAl_2Si_2O_8 + 20H_2O$

TSCHERMAKITE + ANORTHITE + WATER

In the above reactions, the transformation of actinolite to hornblende is attributed to (1) edenite substitution: $(Na,K)Al^{iv} = Si$ and (2) tschermakite substitution: $(Al,Fe^{3+})Al^{iv} = (Mg,Fe)Si^{iv}$ (Graham 1974; Miyashiro 1978). A combination of these two substitutions yields the pargasite end member.

The determination of P-T conditions for the thermal metamorphism can be made through the use of the chlorite-out reaction curve. Fawcett and Yoder (1966) have shown that chlorite coexisting with quartz begins to breakdown at temperature above 565°C at 2kb P_{H2O}. Liou et al. (1974) suggest that the total disappearance of chlorite occurs at approximately 575°C at 2kb P_{fluid}. As mentioned earlier, chlorite was absent in some of the lower amphibolite samples. This therefore suggests that the temperature of 575°C has been reached in some of the localities containing the thermal assemblages.

Liou et al. (1974) proposed the following reaction:

3-7] albite + epidote + chlorite + quartz <===>

oligoclase + tschermakite + magnetite + water

to describe the transition from greenschist to lower amphibolite facies over a temperature range of 470°C to 550°C at 2kb. This reaction is in accord to the observation made through the petrographic analysis of this study. Furthermore, xenoblastic magnetite was seen in close proximity to chlorite and blue-green hornblende (Plate 3.8), supporting the inference that chlorite is involved in the production of magnetite and the transformation of lower grade amphibole to higher grade amphibole.

According to Cooper (1972), the coexistence of magnetite with blue-green hornblende commonly suggests that the bulk rock oxidation is high. Apted and Liou (1983) , found that the stability of chlorite is reduced as f_{O_2} increases, which is also in agreement with Cooper (1972). Based on the chlorite stability field, the upper temperature limit reached by the thermal metamorphic event is taken as 575°C. This temperature corresponds with an f_{O_2} of 10^{-17} to 10^{-25} bars, based on the stability relations of Fe oxides and native iron (Miyashiro, 1978). The high oxidation state seen here encourages the conversion of Fe^{2+} to Fe^{3+} in minerals such as chlorite and epidote. The Fe^{3+} is then available for the tschermakite substitution that takes place in the transition facies.

To confirm the P-T conditions (575°C and 2kb) documented for the thermal metamorphic event of the volcanic rocks, the intercalated sedimentary rocks were also examined. An assemblage containing biotite, chlorite and blue green amphibole was observed in these sedimentary rocks. The existence of this assemblage, especially the presence of blue green amphibole, lends further support for the P-T conditions invoked for the thermal metamorphic event. It therefore appears that the P-T inference for the thermal metamorphic event is reasonable.

The cause of the thermal event is not readily apparent in the field as intrusive bodies were not observed in the vicinity of the study area. The nearest, large intrusive body which could produce the observed aureole is located approximately 10 km, to the south of the most eastern traverse of the southern volcanic belt (Figure 3.1). The observed increase in metamorphic grade in the southern volcanic belt may be attributed either to the presence of an intrusion beneath the present surface or to differential rate of uplift. The southern volcanic belt may be a reflection of a greater rate of uplift and exhumation than those seen in the northern and central belt. Further data is required to test these hypotheses.

3.5 EPIDOTISATION AND CARBONATISATION

Figure 3.1 presents a summary of areas possessing high carbonate content with concomitant absence of actinolite and areas of high epidote content. The latter phenomenon (epidotisation) could be explained by redistribution of Ca to areas of pronounced deformation, such as intersecting joints, similar to those proposed by Smith (1968). In outcrops where epidote is considered to be prominent, anastomosing shear features were observed. Turner and Verhoogen (1960) pointed out that in low grade metamorphism of basic igneous rocks, the removal of CaO

and Al_2O_3 in aqueous solution from one locality and introducing it to adjacent rocks to form epidote is not uncommon.

In contrast to areas of high epidotization, areas where actinolite is completely absent were also observed (Figure 3.1). Such occurrences could be explained by the whole rock chemistry or by the physio-chemical conditions existing at that particular locality during alteration (Deer et al., 1982; Turner and Verhoogen, 1960). For instance, a possible reaction, proposed by Turner and Verhoogen (1960), that could have been involved in this phenomenon could be:

3-8] chlorite + carbonate + quartz <===>

actinolite + water + carbon dioxide .

An increase in P_{H_2O} and P_{CO_2} would drive the reaction to the left resulting in the breakdown of actinolite. Miyashiro (1978) has suggested that an increase in P_{H_2O} and P_{CO_2} would result in the increase in the temperature of formation of actinolite. Hence, P_{H_2O} , P_{CO_2} and temperature are interacting factors which govern the stability of actinolite.

A feature that is closely affiliated with the absence of actinolite is the existence of high carbonate content in localities where actinolite is absent (Figure 3.1). This can be explained with reference to equation (3-8). An increase in P_{CO_2} would drive the reaction to the left and hence produce chlorite, quartz and carbonate. The Ca needed for the production of carbonate is furnished by the actinolite. It should be noted that epidote is also a Ca bearing mineral, and it too will eventually react to produce more carbonate (Miyashiro, 1978). Other elements such as Al, Fe and Si would be taken in by the mineral chlorite. The origin of this high P_{CO_2} environment appears to be associated with the numerous faults that are located in this portion of the study area (Figure 3.1). According to Anglin and Franklin (1985), schisty rocks found adjacent to fault zones are usually characterised by a high degree of carbonatisation. The pervasive

carbonatisation seen in the vicinity of the Beardmore area may also be due to the intrusion of pegmatites to the south of the study area, where CO_2 may have been introduced into the study area (Zayachkivsky, 1985). The above explanation appear to suggests that the P_{CO_2} condition throughout the thesis area are variable.

3.6 METAMORPHISM IN SHEAR ZONES

Shear zones are common features in the BGB, especially along boundaries of contrasting lithologies. Most of the shear zones observed in the study area are located either within the volcanic rocks or along lithologic breaks between volcanic and sedimentary rocks. Shear zones vary in width from a few centimetres to a metre or more and are characterised by strong linear and planar fabrics resulting from lateral ductile deformation. Thin sections of shear zone lithologies are characterised by a mylonitic fabric and the development of a retrograde assemblage such as chlorite - quartz - muscovite, suggesting hydrous conditions of formation. Samples 109b to 110 from the Patsy Lake West traverse (Figure 3.1) represent samples collected across a shear zone. From these samples, it was observed that as the shear zone is approached, the lithologies are retrogressed from transition facies to greenschist facies, with chlorite and quartz as the predominant constituents. This transformation can be documented by the following reaction as proposed by Beach (1980):

3-9] $6Na_{1/2}Ca_2(Mg,Fe)_{4\ 1/2}Al_{1/2}Si_7Al\ O_{22}(OH)_2 + CaAl_2Si_2O_8 +$

HORNBLENDE + ANORTHITE+

$NaAlSi_3O_8 + 3(Mg,Fe)^{2+} + 24H^+ + 6H_2O$--->

ALBITE + HYDROTHERMAL FLUID

$3(Mg,Fe)_{10}Al_2Si_6Al_2O_{20}(OH)_{16} + 4Na^+ + 13Ca^{2+} + 29SiO_2$

CHLORITE + QUARTZ

Sample 109c (Figure 3.1), was collected from a lens, embayed by quartz, within the shear zone. This sample is characterised by undeformed blue green hornblende (Plate 3.10), which is indicative of lower amphibolite facies metamorphism. The existence of this blue green hornblende is interpreted to result from metasomatism. Introduction of Na, amongst other elements, from the shear zone fluid has transformed the pre-existing actinolitic hornblende to blue green hornblende enriched in Na, as suggested by Liou et al. (1974). The Na needed for this transformation could have been derived from the retrogressive reaction as shown in reaction 3-9. From the above, it appears that the shearing took place fairly late in the metamorphic history, after the thermal metamorphism. This inference is supported by the retrogression of the thermally produced transition and lower amphibolite facies into a lower greenschist facies resulting from the shearing .

CHAPTER 4

GEOCHEMISTRY OF BEARDMORE-GERALDTON VOLCANIC ROCKS

4.1 INTRODUCTION

Elemental abundances in fresh, unaltered volcanic rocks is quite variable and this variation is attributed to a number of factors, some of which include the source composition, the degree of partial melting and the subsequent crystal fractionation within the ascending magma prior to extrusion. Once solidified, these fresh, unaltered volcanic rocks are further subjected to weathering, metamorphism and other secondary processes. Such secondary processes have the effect of redistributing the primary elemental abundances in these volcanic rocks and thereby further complicating their chemistry. Precautionary measures should therefore be taken before making inferences regarding the evolutionary history of the magmas. In this chapter, elemental abundances and their variations in the volcanic rocks are evaluated qualitatively. Mobility of various elements is also examined.

4.2 ANALYTICAL METHODS

From a suite of more than 250 samples collected, 55 of the least visibly altered representative samples were selected for chemical analysis. These samples were then analysed for the following elements:- SiO_2, MgO, $Fe_2O_3^t$ (total iron), Al_2O_3, CaO, Na_2O, K_2O, TiO_2, MnO, P_2O_5, CO_2, S, LOI, Sr, Y, Zr by XRF and LECO-Method. Co, Cr, Cu, Ni, Zn by AA Flame and V and Sc by ICP (Inductive Coupled Plasma) at the Ontario Geological Survey. From this sample set, 14 samples were further analysed for rare earth elements using ICP/MS (mass spectrometer). The accuracy of the individual methods for the various elements are given in Table 1.

4.3 GEOCHEMICAL RESULTS (Major and Trace Elements)

Geochemical results are presented graphically using Harker type variation diagrams with Mg# ($MgO/MgO+Fe_2O_3t$) as the abscissa. Such plots enable the direct comparison of analyses plotted together and provide a qualitative means for deriving the behaviour of specific elements or oxides with respect to primary magmatic processes. The interpretation of such plots, to identify correlations between element distribution and primary fractionation processes must be carried out with caution due to the effect of secondary processes on element distribution. The mobility of elements during secondary processes will be examined in the next section.

The Mg number ($MgO/MgO+Fe_2O_3t$) has been employed as the abscissa on Figure 4.1 to 4.17, as it represents a qualitative fractionation index, which decreases with the continued evolution of the melt. The trends and scatters shown in Figure 4.1 to 4.17 for each element are explained as follows:-

4.31 Nickel (Ni) and Chromium (Cr)

The behaviour of Ni and Cr, partitioned into olivine and pyroxene respectively, is considered to be similar as they both decrease in abundance as the melt becomes more evolved (Figure 4.1 and 4.2). The trends observed for the BGB data are poorly defined due to the large scattering of the data. However, such scattering is considered to be original as comparable results are observed in fresh, unaltered basalts (Keays and Scott 1976, Melson and Thompson 1971; Humphris and Thompson 1978).

4.32 Calcium (Ca)

The behaviour of the element Ca is shown in Figure 4.3 as CaO. Ca is partitioned into a number of rock forming minerals such as the pyroxene,

Table 1: Accuracy of Geochemical Analysis.

Methods:	XRF/LECO		AA/ICP		ICP/MS
SiO_2	+/- 2.0%	Co	+/- 5ppm	La	+/-0.05ppm
Al_2O_3	0.4%	Cr	20 ppm	Ce	0.05ppm
$Fe_2O_3^t$	0.6%	Cu	4ppm	Pr	0.05ppm
MgO	0.3%	Ni	6ppm	Nd	0.18ppm
Na_2O	0.5%	Zn	10ppm	Sm	0.15ppm
K_2O	0.1%	Sr	5ppm	Eu	0.07ppm
CaO	0.15%	Y	10ppm	Gd	0.14ppm
P_2O_5	0.15%	Zr	10ppm	Tb	0.03ppm
TiO_2	0.16%	V	10ppm	Dy	0.13ppm
MnO	0.01%	Sc	15ppm	Ho	0.03ppm
CO_2	0.4%			Er	0.10ppm
				Tm	0.03ppm
				Yb	0.11ppm
				Lu	0.04ppm

FIGURE 4.1 to 4.17 : Variation diagrams of volcanic rocks from the BGB in which all elements are plotted against Mg#(MgO/MgO+Fe_2O_3). CaO, Al_2O_3, Na_2O, K_2O, TiO_2, P_2O_5, MnO are in weight per cent. Ni, Cr, Sr, Co, Sc, Cu, V, Y, Zr and Zn are in parts per million.

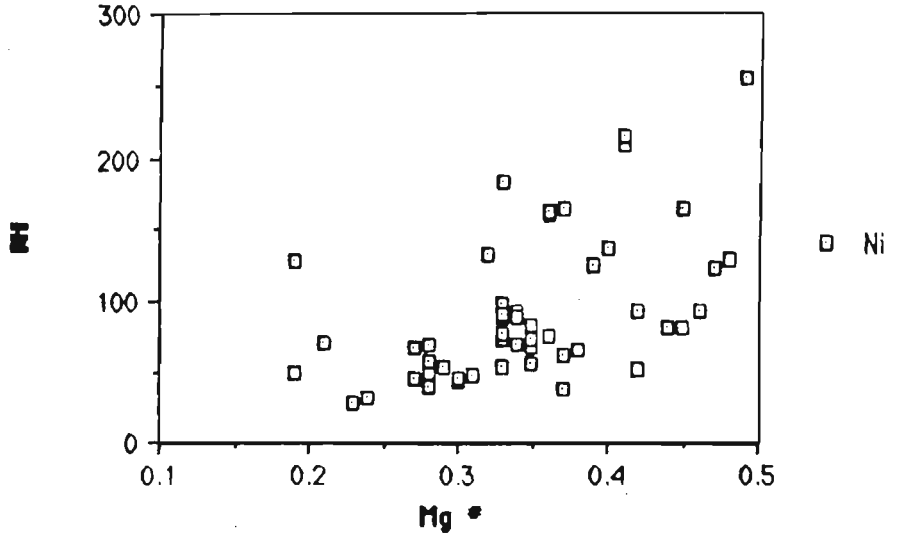

Figure 4.1

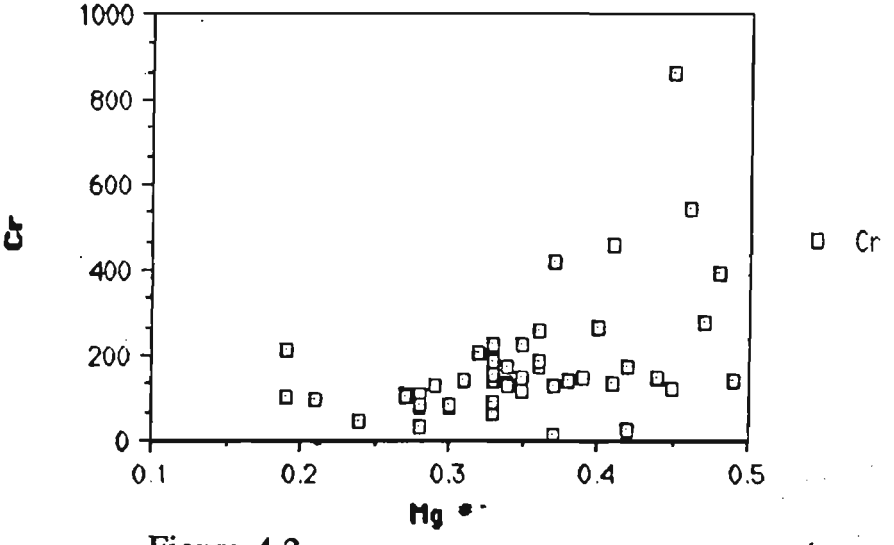

Figure 4.2

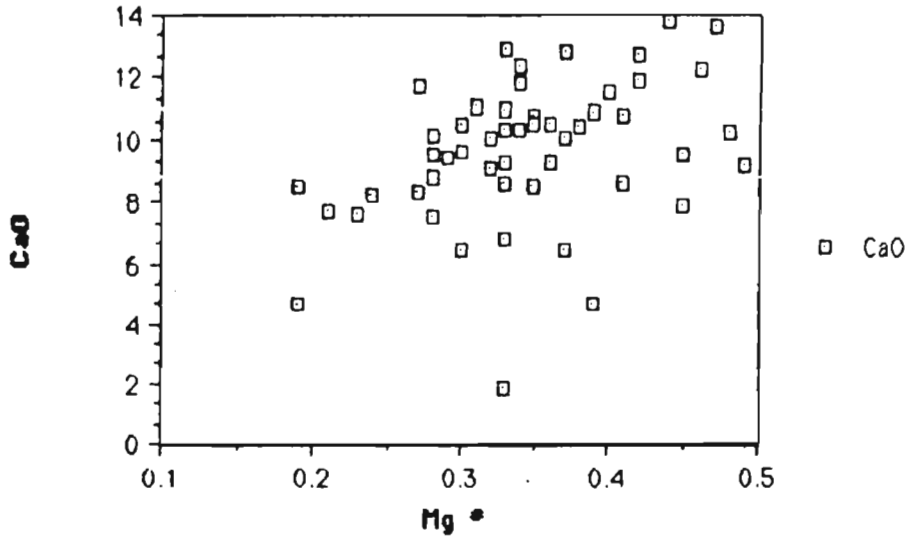

Figure 4.3

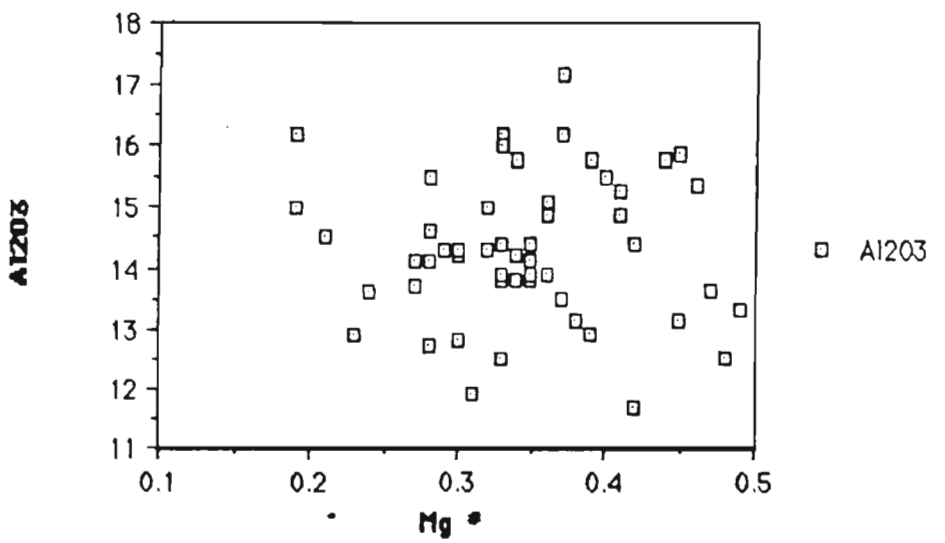

Figure 4.4

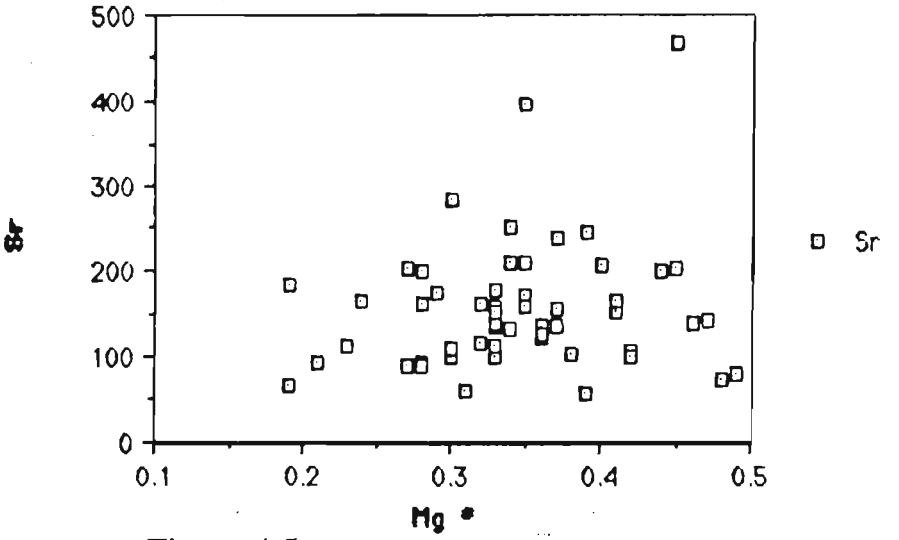

Figure 4.5

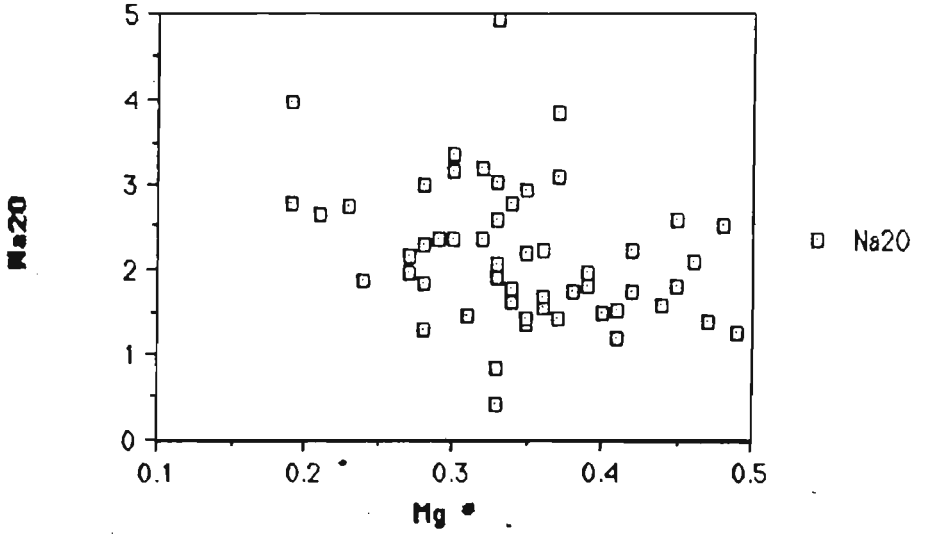

Figure 4.6

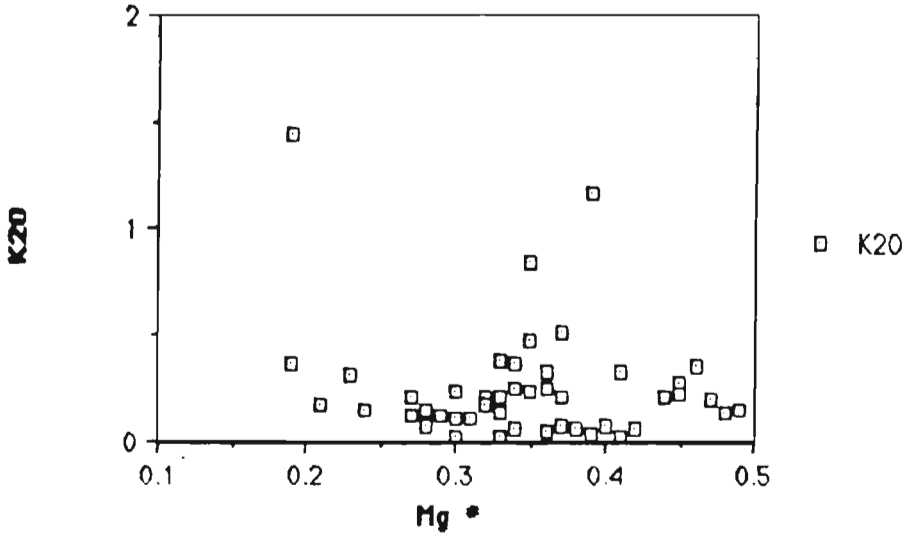

Figure 4.7

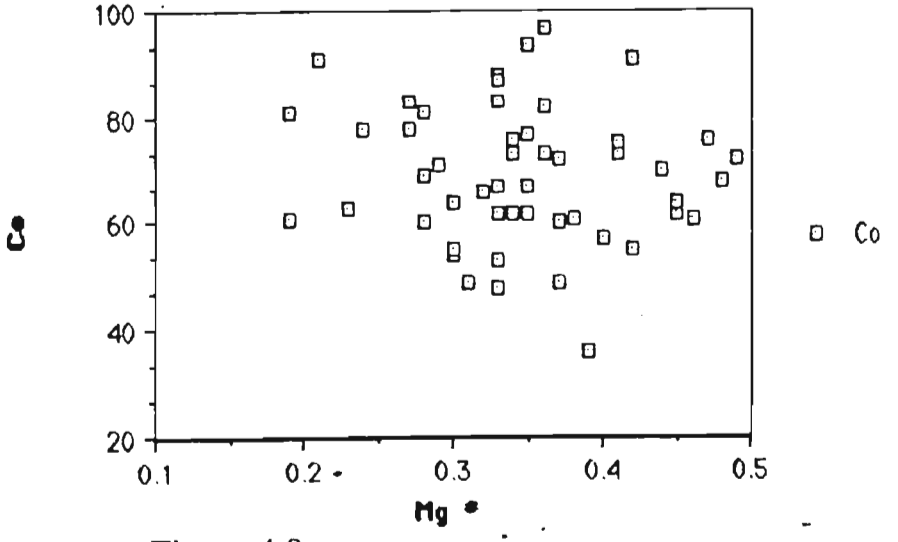

Figure 4.8

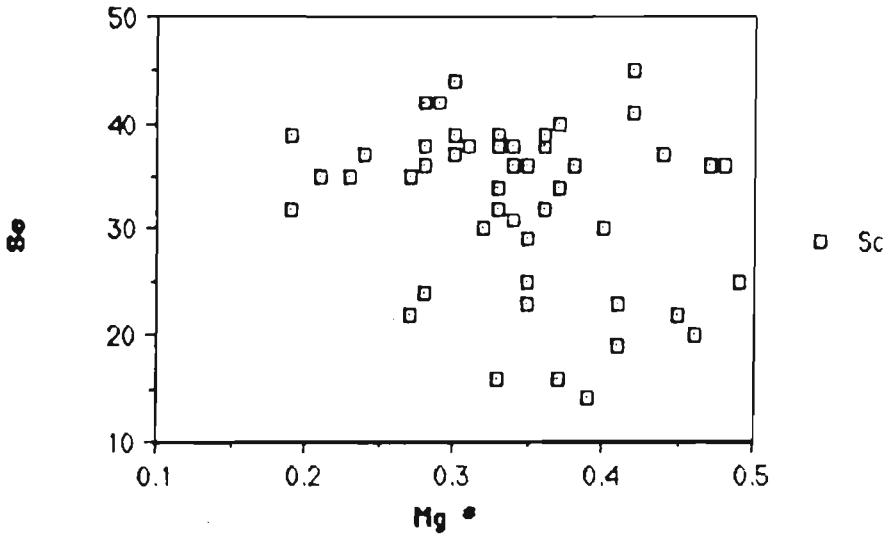

Figure 4.9

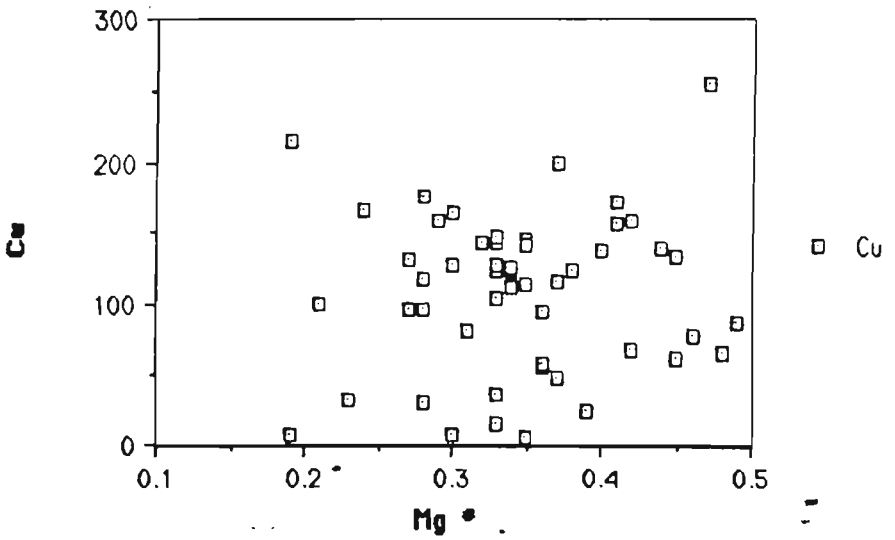

Figure 4.10

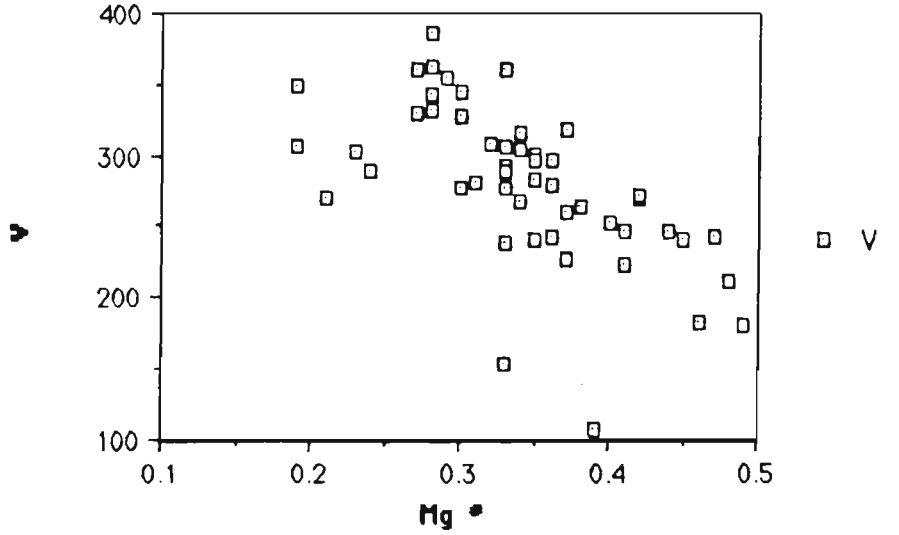

Figure 4.11

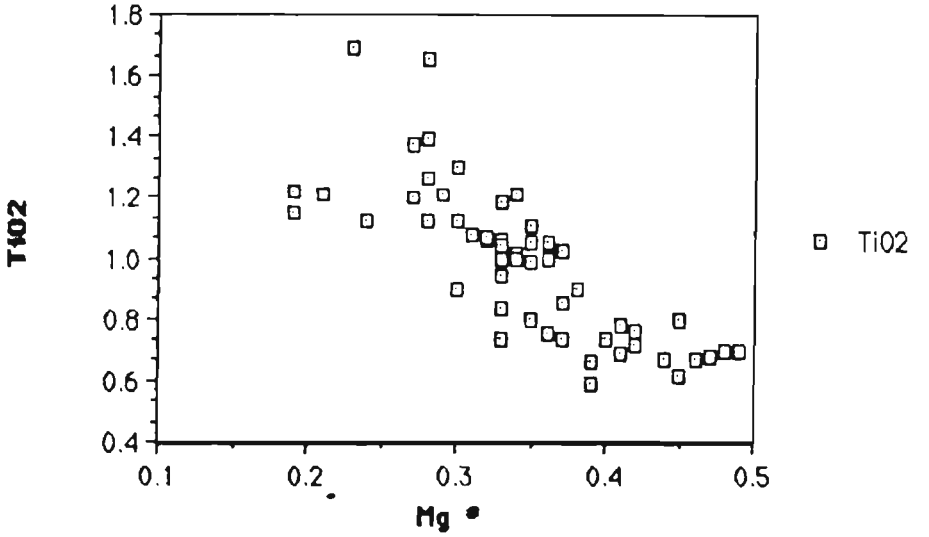

Figure 4.12

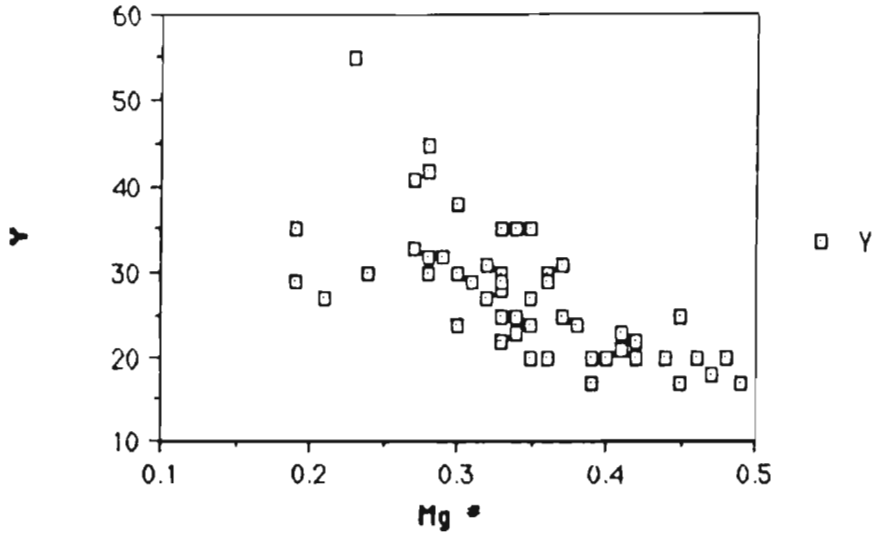

Figure 4.13

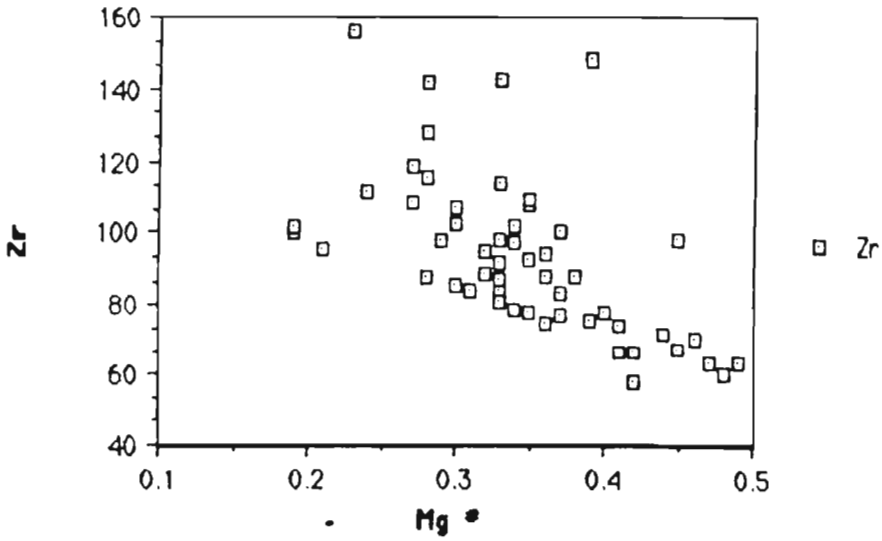

Figure 4.14

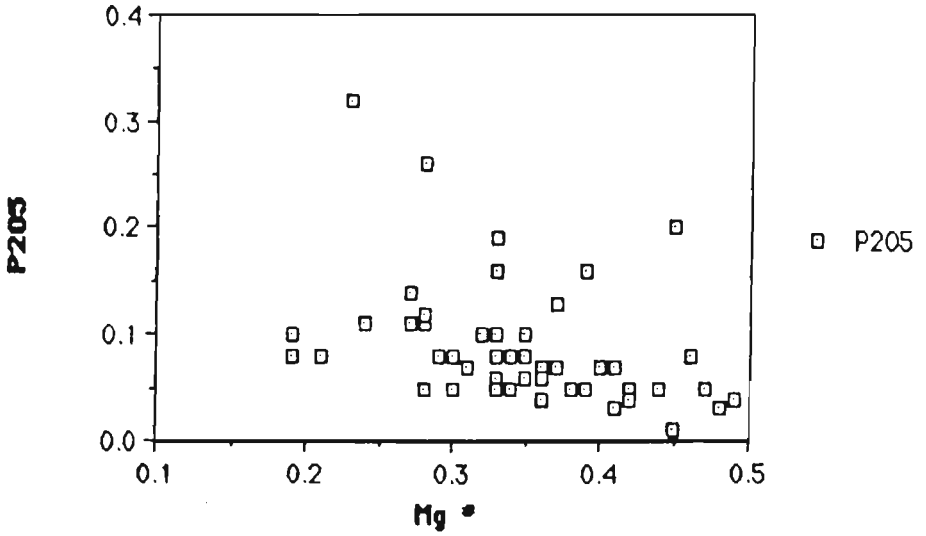

Figure 4.15

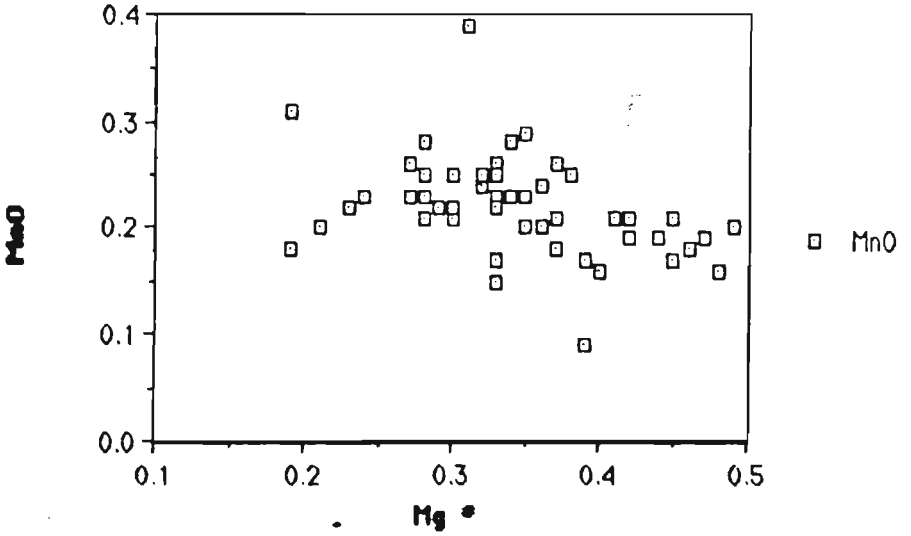

Figure 4.16

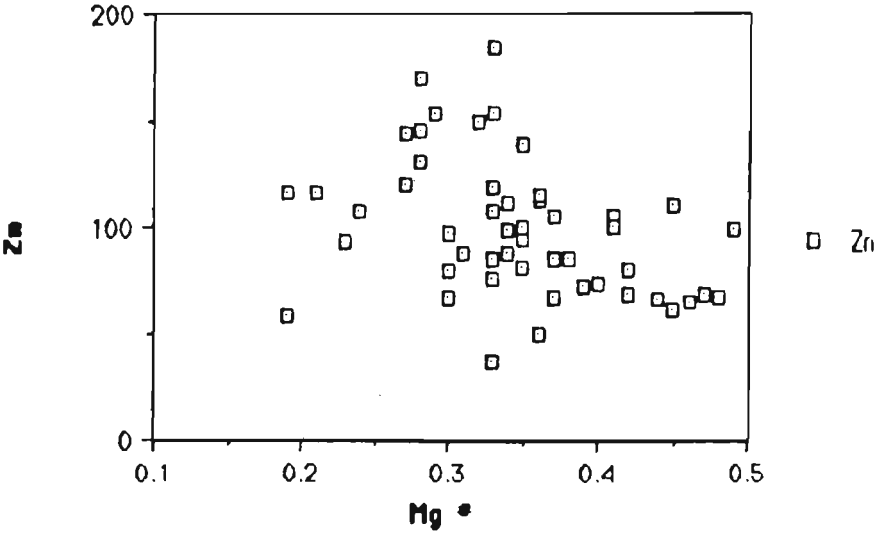

Figure 4.17

amphibole and plagioclase. However, the majority of Ca in a basaltic melt is incorporated into Ca-rich plagioclase and clinopyroxene. Figure 4.3 depicts considerable scattering of the data. This scattering is to be expected, especially when secondary processes have occurred. Ca leaching is common during chloritization of ferromagnesian minerals such as pyroxene, where Ca is replaced by iron and magnesium and during albitization, where Ca is replaced by sodium (CaAl=NaSi). Mobility of Ca is also evidenced by the varying concentration of epidote and carbonate mineral abundances from one sample site to another. All of the fore-mentioned secondary processes are documented earlier in the Chapter 3.

4.33 Aluminium (Al)

In modern, unaltered tholeiitic rocks aluminium concentrations, reported as Al_2O_3, can vary from as much as 12 wt. % to 19 wt. % (Jakes and Gill, 1970; Jakes and White, 1972; Sun and Nesbitt, 1977; Basaltic Volcanism Study Project, 1981). The relative immobility of aluminium during secondary alteration has been widely documented in Archaean volcanics (Vallance, 1974; Jolly and Smith 1972; and Jolly, 1980). The variation observed in Figure 4.4 is considered to be primary and the large scattering is probably due to the varying primary mineralogy, such as plagioclase feldspar. The data shown here are also comparable to other Archaean tholeiitic rock suites of similar Mg number as shown by the Basaltic Volcanism Study project (1981).

4.34 Strontium (Sr)

Strontium is mostly partitioned into albitic plagioclase during the late stages of fractionation where albitic plagioclase replaces Ca-rich plagioclase. It is also partitioned into apatite and augite in minor amounts. In more evolved tholeiitic basalts (Mg # < .5), strontium concentrations generally decrease with decreasing Mg number (Wood, 1978), however,

such is not the case here (Figure 4.5). The lack of a well defined trend is most likely to be attributed to mobility of Sr during alteration processes. Sr has been documented to be mobile during zeolitization (Wood, 1978) and epidotization (Smith and Smith 1976, and Humphris and Thompson 1978). Presumably alteration processes that are responsible for Ca mobilisation may be responsible for the behaviour of Sr since they have similar physical attributes.

4.35 Sodium (Na)

Sodium in the melt is usually fractionated into plagioclase during the late stages of a melt differentiation. Therefore, sodium increases during the early stages of the melt evolution until Na-rich plagioclase or amphibole starts to fractionate. In addition, sodium is also introduced during regional metamorphism by a variety of sources such as hydrothermally introduced fluids or through seawater interaction (Jolly 1980; Beach, 1980) giving rise to processes such as albitization. Figure 4.6 shows an apparent absence of primary magmatic trend. This is likely due to processes such as albitization, where Na is introduced during Ca leaching of the calcic plagioclase. This inference is supported by the petrographic analysis documented in Chapter 3.

4.36 Potassium (K)

Potassium is considered to be an incompatible element since most major rock forming minerals possess a low partition coefficient (Kd) value for potassium. The Kd value is an expression of the extent to which an element is partitioned into a fractionating mineral phase (Henderson 1984). The extremely large ionic radius of K is responsible for its exclusion from fractionating phases, except in more siliceous melts where alkali feldspar and mica are removed. As a result, K would be expected to accumulate as the melt evolved. In addition to this primary characteristic,

K is also introduced during regional metamorphism via hydorthermal fluids. Figure 4.7 illustrates the absence of the expected trend. Most of the basalts contain a low content of K and this is considered to be primary, since seven of the data points are from samples containing relict mineralogy. Samples with high K content are considered to result from a higher grade of metamorphism. Comparable results were also shown by Pharaoh and Pearce (1984). The mean K value for the greenschist facies rocks is 0.16% while that for the lower amphibolite facies is 0.30%. This interpretation is also supported by the formation of biotite in lower amphibolite facies rocks. As mentioned in Chapter 3, the source of K could be derived from subsurficial intrusion or dewatering of adjacent sediments. Such hypothesis might be tested by isotopic work.

4.37 Cobalt (Co)

The behaviour of cobalt (Co) is similar to that for Fe^{2+}. However, its behaviour during alteration is not extensively studied. The Co vs. Mg# plot (Figure 4.8) depicts a large scattering of data. This scattering may be due to secondary effects if one assumes a systematic incorporation of Co into ferromagnesian minerals with progressive fractionation, similar to that of ferrous iron.

4.38 Scandium (Sc)

Scandium is a lithophile element with a radius similar to ferrous iron but with a higher charge. Little is known regarding its behaviour during alteration, therefore scattering effect seen in Figure 4.9 could either be a primary or a secondary feature.

4.39 Copper (Cu)

The element copper (Cu) is generally concentrated into the sulphide phases of the melt as a minor constituent rather than substituting into the

silicate rock-forming minerals (Craig and Vaughan 1981). This element has been documented to be leached from metamorphosed basaltic rocks by Reid et al. (1987). The scatter observed in Figure 4.10 is likely to be due to alteration processes such as sulphidisation that had occurred after consolidation and emplacement of the magma. In the field, zones of sulphidisation are common.

4.40 Vanadium (V)

Vanadium is preferentially incorporated into magnetite over ilmenite and chromite over pyroxene, in order of decreasing Kd values. Figure 4.11 illustrates an increasing concentration of V with increasing melt differentiation. This suggests that the fore-mentioned opaque oxide phases are not precipitating out. The fractionation of oxides is controlled strongly by the partial pressure of oxygen, where a high partial pressure of oxygen would generally favour the precipitation of oxide phases.

4.41 Titanium (Ti), Yttrium (Y), and Zirconium (Zr)

Figure 4.12, 4.13 and 4.14 depict the behaviour of the elements Ti, Y, and Zr in BGB samples. All these elements illustrate relative enrichment as crystal fractionation continues or as the melt becomes progressively more evolved. This enrichment is attributed to the low Kd values for these elements in the fractionating phases.

Ti is partitioned into ilmenite, magnetite, hornblende, and clinopyroxene in decreasing Kd values. However, Figure 4.12 suggests that these oxides are not fractionating out in the melt. Magnetite starts to fractionate out when the oxygen fugacity is high ($fO_2 > 10^{-11}$). This implies that the oxygen fugacity of the melt involved in the genesis of the BGB basalts is not likely to be high. This inference is consistent with the observed increase in total iron and vanadium in Figure 4.11, where the behaviour of these two elements are also strongly dependent on the

precipitation of oxide phases. Support for this inference is also shown by the negative europium anomaly seen in the rare earth results which will be described in a forthcoming section.

The element Y is partitioned into garnet, hornblende and clinopyroxene in decreasing Kd values. The increase in Y in the residual fraction of the melt further attests to the fact that Y behaves as an incompatible element during melt differentiation. Sun and Nesbitt (1978) suggested that the abundance of this element is controlled by the source and the degree of partial melting since it is poorly fractionated out by the main fractionating phases. The minor scatter seen in Figure 4.13 may well be attributed to the source heterogeneity.

Zirconium is incorporated to a small extent into pyroxene, phlogopite, garnet and hornblende, but it is largely partitioned into the mineral zircon. Figure 4.14 depicts the relative coherency of the Zr distribution with respect to decreasing Mg number. This suggests that the mineral zircon is not a fractionating phase since Zr continues to accumulate in the melt fraction as the melt evolves. The behaviour of this element is predominantly due to its large ionic radius or oxidation states which precludes its incorporation to any significant amount into the rock forming phases. Another feature observed in this plot is that there is some scattering of Zr in the plot. This scatter could be due to minor mobility of this element which will be elaborated in a later section.

4.42 Phosphorus (P)

Phosphorus expressed in Figure 4.15 as P_2O_5 is strongly incorporated into apatite since it is an essential structural constituent in this mineral [$(Ca_5(PO_4)_3(OH,F,Cl)]$. Apatite is also considered a important minor phase because many trace elements are strongly partitioned into it (Henderson, 1984). Crystallisation of apatite usually commences when P2O5 in the liquid exceeds 1.0 wt. % (Anderson and Greenland, 1969). However, most

of the samples in the study area generally contain less than 0.1 wt. % of P2O5 and it tends to be concentrated into the residual fraction suggesting that apatite is not a major phase participating in the melt evolution, Figure 4.15.

4.43 Manganese (Mn) and Zinc (Zn)

These two elements are partitioned into olivine, iron-titanium oxide phases and in pyroxenes. Wood (1978) documented that the element Mn usually replaces ferrous iron in the fractionating phases and that iron rich pyroxene and olivine phenocrysts tend to contain higher Mn than Mg rich pyroxene and olivine. This led him to suggest that crystallisation of iron rich pyroxene and olivine and iron-titanium oxide phases is responsible for the ultimate depletion of Mn in the residual melt. As for the element Zn, Mason and Moore (1982) suggested that magnetite and ilmenite are more effective in incorporating Zn than silicate mineral and that minor amounts of Zn are incorporated into sulphide minerals. Figure 4.16 illustrates that Mn shows a weak constant increase in relative abundance as the melt evolves. The behaviour of Mn is consistent with the behaviour seen in iron. Figure 4.17 depicts a similar trend observed in the Mn plot, except that it has lesser coherency. The lack in coherency could be due to secondary processes such as sulphidisation where Zn may be redistributed.

4.4 SUMMARY

From the observed behaviour of the various elements, it can be concluded qualitatively that some of the more evolved basaltic rocks seen in the study area could have resulted from fractional crystallisation of less evolved rocks. This will be examined quantitatively in the section on the petrogenesis of the BGB basalts. The major mineral phases fractionating out, as derived from the chemical characteristics of the elements, appear to be olivine and clinopyroxene, as shown by the depletion of Mg, Ni, and Cr

with increasing melt differentiation. The possible mobility of the elements Ca, Na, and Sr, however, has masked the results of plagioclase fractionating out from the melt. The increase in total iron with increasing melt differentiation, is in accordance with the tholeiitic nature of the melt (Miyashiro, 1973). This increase in total iron accompanied by titanium and vanadium further suggests that iron-titanium oxide phases are not fractionating out in the melt. This would also imply that the geological environment from which the basalts were derived is likely to have a low oxygen fugacity. The pyroxene and olivine fractionating out in the early stages of the fractionation process are probably iron poor as well. Beside this, the low Mg number seen in most of the basalts in the study area attest to the evolved nature of the BGB basalts and that they could not have resulted directly from the melting of the mantle material since direct melting would give rise to a much higher Mg number of .80 (Sun and Nesbitt, 1978).

It should pointed out that the variation trend documented above are from three different volcanic belts. The trend shown on these plots (e.g. Figure 4.11 and Figure 4.12) may in fact represent three overlapping trends, i.e. one for each belt, suggesting the belts have similar liquid line-of descent paths. Information on the characteristics of each individual belt is not readily apparent due to the agglomeration of the data. This latter treatment is necessitated by the fact that outcrops in each volcanic belt are widely scattered, discontinuous and deformed, i.e. sheared.

4.5 GEOCHEMICAL CLASSIFICATION

Geochemical classification of the BGB samples were carried out using Irvine and Baragar's classification (1971), Figure 4.18. This division is further confirmed by classification employing immobile elements of Floyd and Winchester (1975), Figure 4.19. Both Figure 4.18 and 4.19 indicate that the BGB volcanics are tholeiitic.

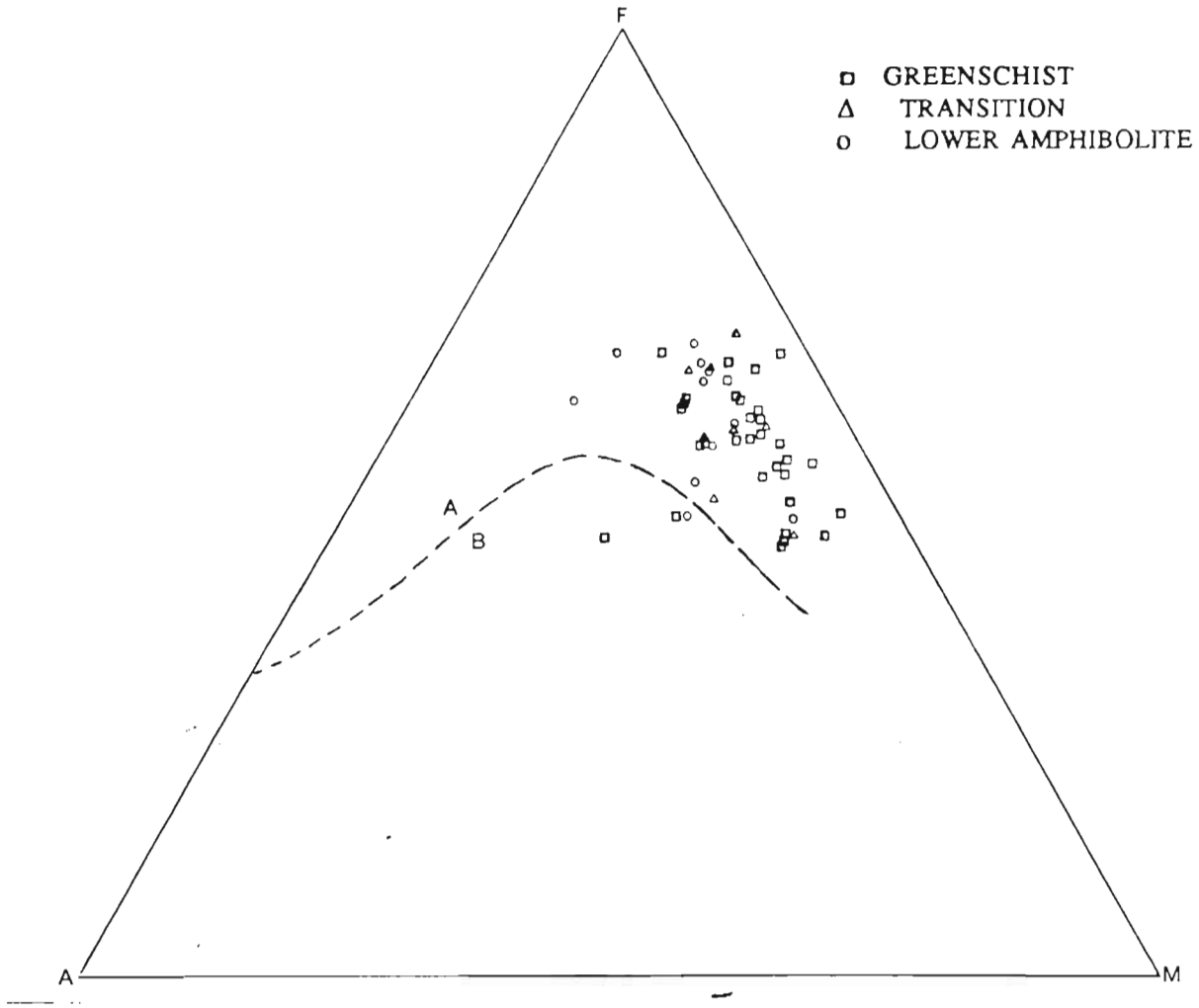

Figure 4.18: AFM plot of volcanic rocks of the BGB. A = Na_2O+K_2O, F = $Fe_2O_3^t$, and M = MgO, with all oxides in weight percent. Field A represents tholeiitic field while field B represents calc-alkaline field (after Irvine and Baragar 1971).

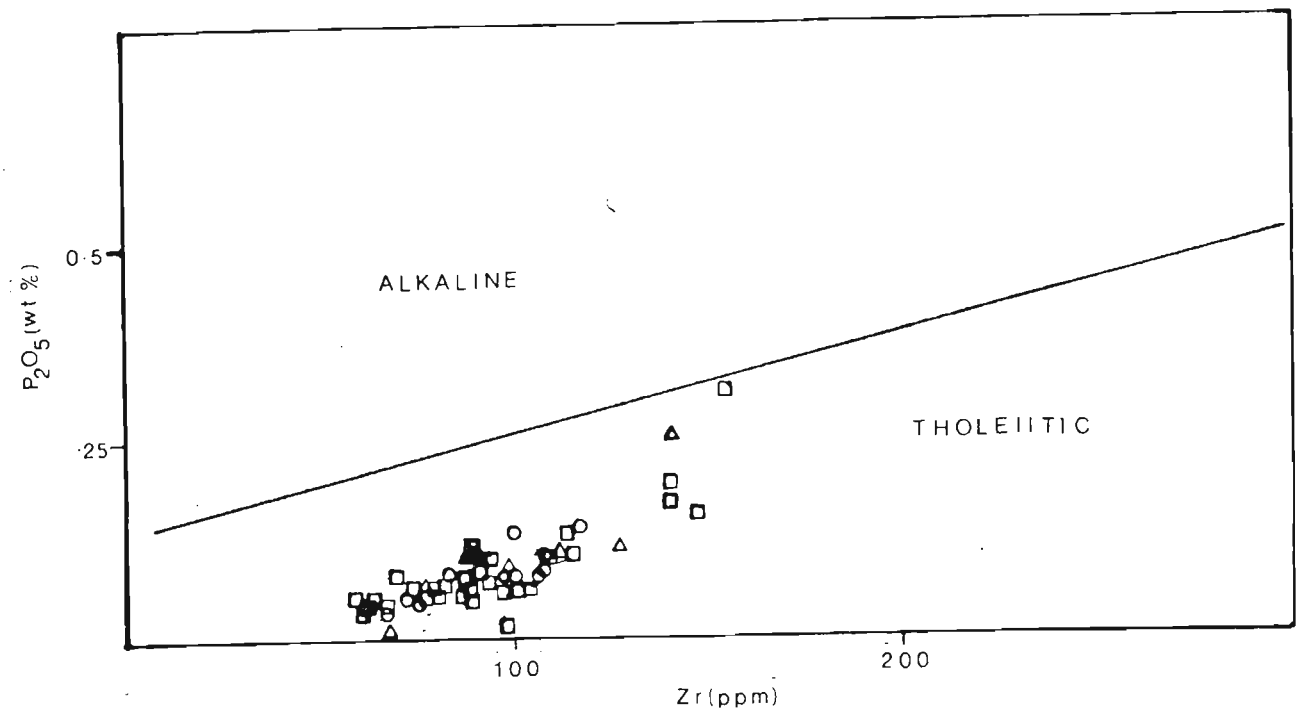

Figure 4.19: P_2O_5 (wt.%) - Zr (ppm) variation diagram for volcanic rocks of the BGB. Fields of alkaline and tholeiitic basalts are from Floyd and Winchester (1975). Symbols as in Figure 4.18.

4.6 RARE-EARTH ELEMENTS: INTRODUCTION

Rare Earth Elements (REE), like the major and trace elements are not immune to the effects of post emplacement alteration. The mobility of the REE is governed by several factors, among which include: i) the REE concentration in the primary and accessory minerals in the parent, since these minerals provide the initial sites for REE concentration and dictates their distribution; ii) their stability during weathering and alteration, stability being dependant on the order of crystallisation; iii) the nature of the fluids; fluids rich in F^-, Cl^- and CO_2 have been documented by Alderton et al. (1980) to have the capability to mobilise REE; iv) the ability of the secondary minerals to accommodate the REE released during alteration/weathering; v) the fluid/rock ratio; vi) the duration of and exposure to alteration/weathering; and vii) the stability of REE complexes. However, REE have been found to be immobile under most greenschist metamorphic conditions (Humphris and Thompson, 1978; Ludden and Thompson, 1979). This observation is further supported by experimental work which shows that REE are immobile under condition of low fluid/rock ratio and under pressure conditions not exceeding 15 kb (Mysen, 1979).

4.7 GEOCHEMICAL RESULTS (Rare Earth Elements)

Chondrite-normalised REE profiles for the 14 analysed samples are shown in Figure 4.20-4.24. The regularity and coherency of the REE profiles for samples from different belts, exhibiting varying metamorphic grades, including some which preserve relict igneous textures, suggest that the REE have remained immobile. Based on the profiles, the samples are divided into two groups according to the nature of the light rare earth element (LREE) segment of their profiles. Group I, the tholeiitic group, to which the majority of the samples belong, are characterised by a depleted

FIGURE 4.20 to 4.23: Chondrite normalised rare-earth patterns for Group I tholeiitic basalts of BGB. Normalising values for the rare earth element (REE) are given in the appendix.

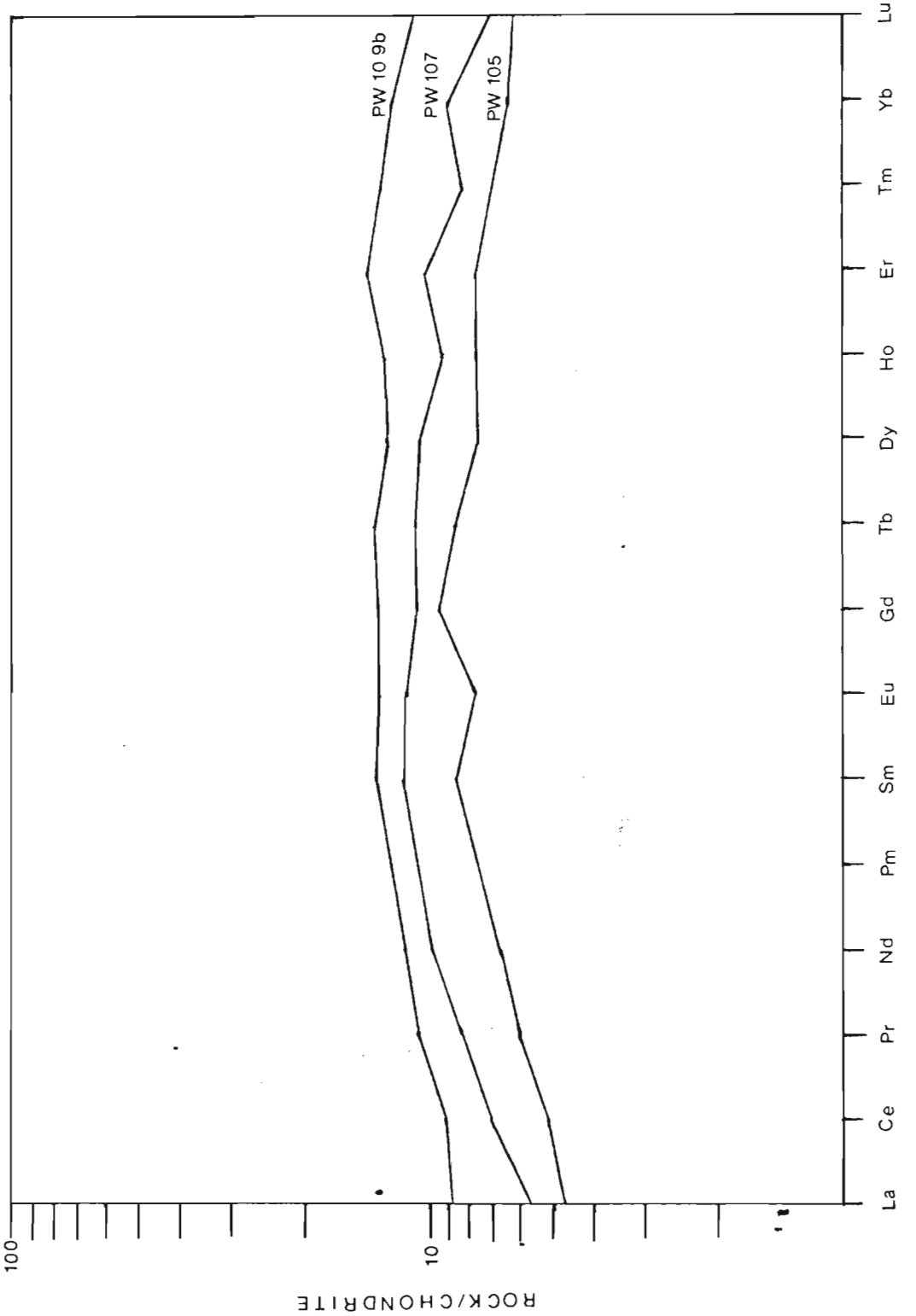
PW 10 9b
PW 107
PW 105
La
Ce
Pr
Nd
Pm
Sm
Eu
Gd
Tb
Dy
Ho
Er
Tm
Yb
Lu
100
10
ROCK/CHONDRITE

Figure 4.20

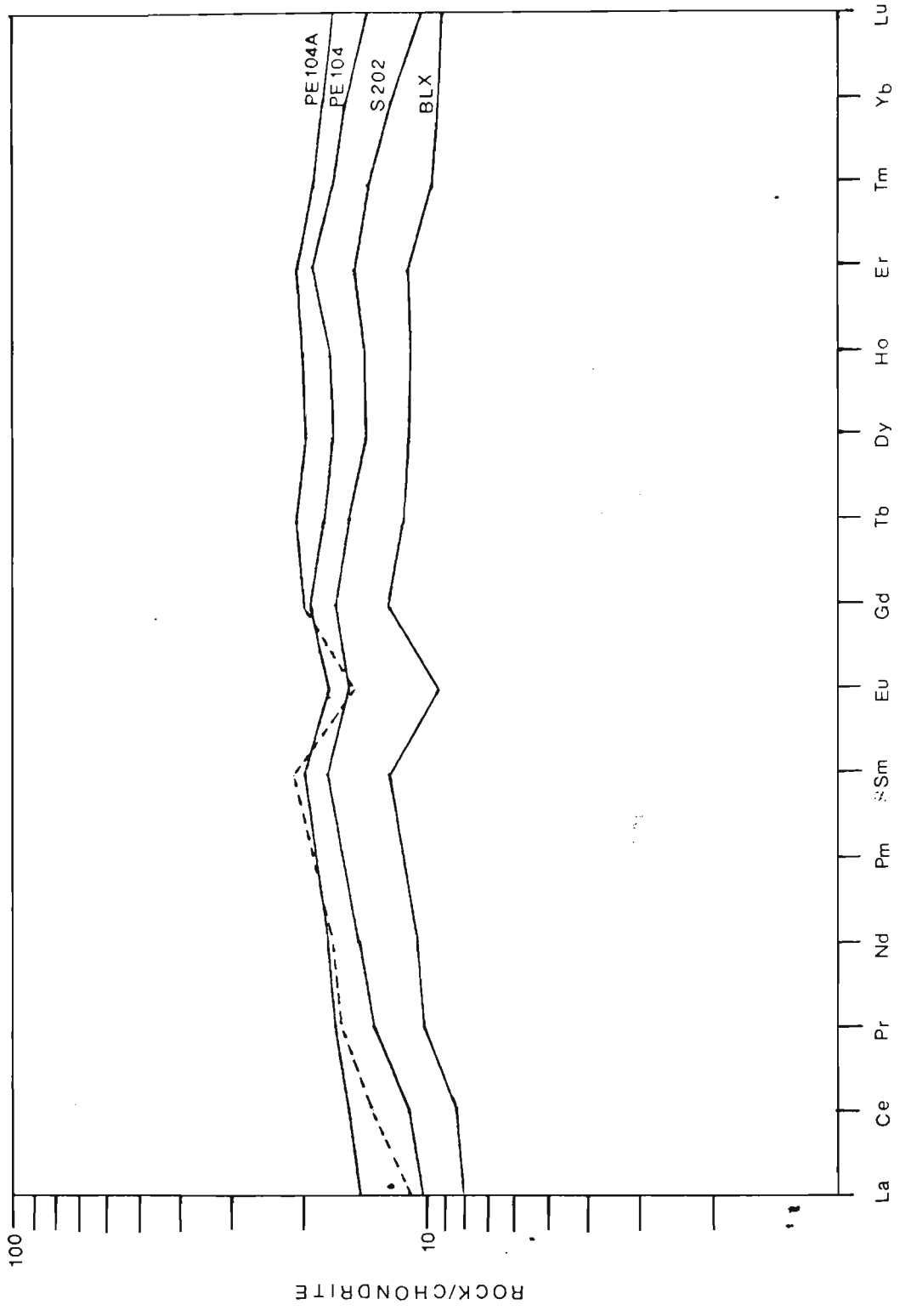
PE104A
PE104
S202
BLX
La
Ce
Pr
Nd
Pm
Sm
Eu
Gd
Tb
Dy
Ho
Er
Tm
Yb
Lu
100
10
ROCK/CHONDRITE

Figure 4.21

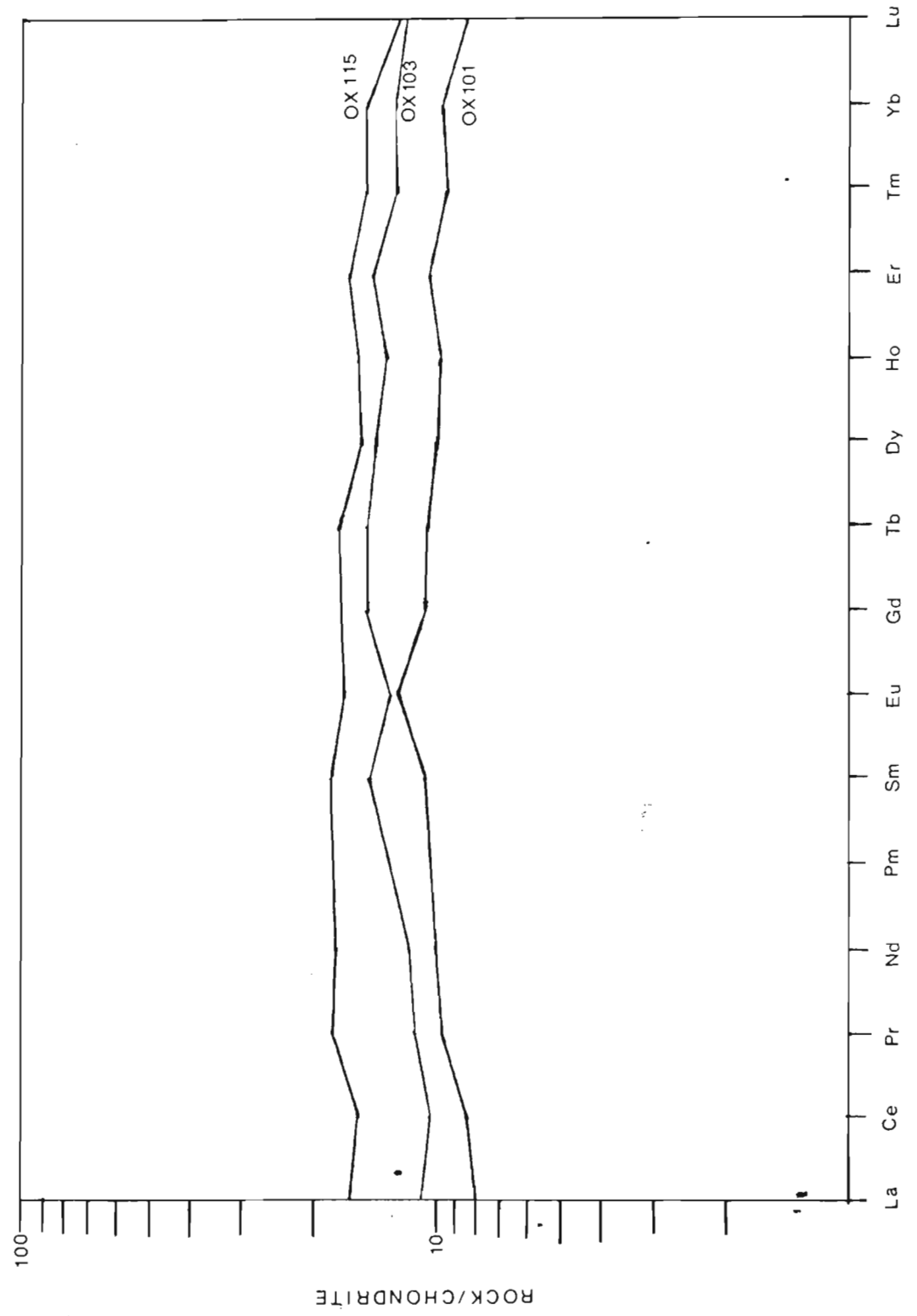
OX 115
OX 103
OX 101
100
10
ROCK/CHONDRITE
La
Ce
Pr
Nd
Pm
Sm
Eu
Gd
Tb
Dy
Ho
Er
Tm
Yb
Lu

Figure 4.22

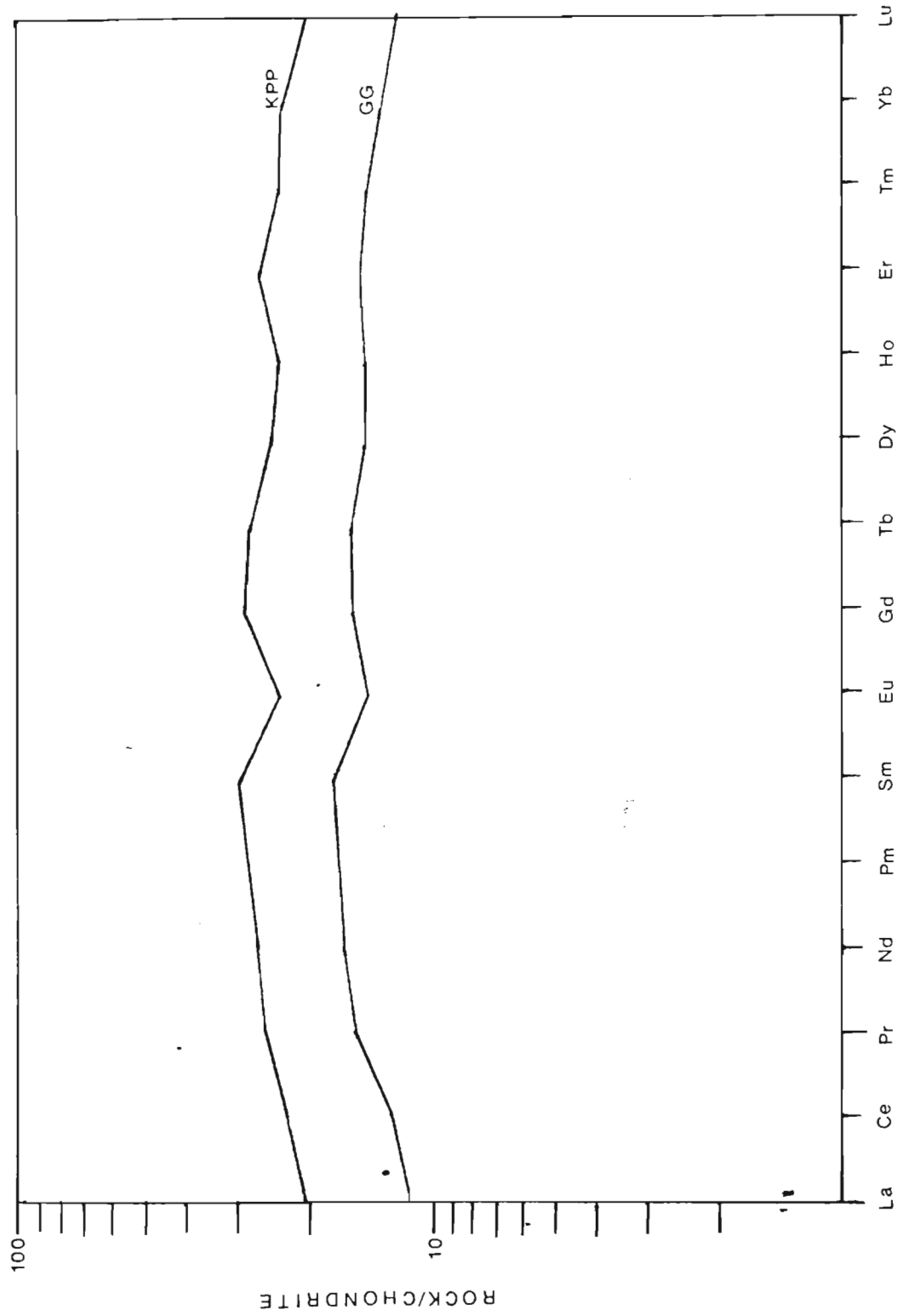
100
10
ROCK/CHONDRITE
KPP
GG
La
Ce
Pr
Nd
Pm
Sm
Eu
Gd
Tb
Dy
Ho
Er
Tm
Yb
Lu

Figure 4.23

LREE segment with [La/Sm] N = 0.65 and a relatively flat heavy rare earth element (HREE) profile with [Sm/Yb] N = 1.2 (Figure 4.20-4.23).

In contrast, Group II samples are characterised by LREE enrichment with a [La/Sm] N = 1.6 and a relatively higher fractionated HREE segment with [Sm/Yb] N = 1.9 (Figure 4.24). These two samples were collected in the northern volcanic belt with one of the sample exhibiting a gabbroic texture while the other possesses a schistose appearance.

As for the relative abundances of the REE, most range from 6 to 20 X chondrite. Besides this, they also show negative Eu anomalies (Eu/Eu* = 0.81 to 0.85), with the exception of samples OX101 which shows a positive anomaly and samples PW107 and 109b where there are negligible Eu anomalies. The negative Eu anomalies seen in most samples suggest that the oxidizing condition of the melt is low, implying that during the melt evolution, oxygen fugacity is likely to be low (Henderson, 1984). This is consistent with the interpretation based on major and trace element chemistry (Section 4.3). The presence of negative Eu anomalies also suggests that Ca-rich plagioclase was removed from the melt. Approximately 20% plagioclase fractionation is required to produce a negative Eu anomaly (Schilling, 1971; Sun and Nesbitt, 1977; Basaltic Volcanism Study Project, 1981).

Plagioclase involvement in the evolution of the melt would also facilitate, to a limited extent, in the explanation of the depleted nature of the LREE since this mineral phase has a preference for La over Sm. This would in effect cause a decrease in the La/Sm ratio. Sun and Nesbitt (1978) suggest that the presence of clinopyroxene in the fractionating assemblage would counteract the LREE depletion, producing a relatively flat REE profile. The ratio required to produce this flat profile was suggested to be 4 plagioclase to 1 clinopyroxene. An alternative explanation for the depleted nature of the observed LREE pattern is that the source from which these rocks were derived could have experienced

earlier melting events, thereby depleting the LREE. Similar inferences have been made by Sun and Nesbitt (1978), based on comparative studies, concluded that a depleted source similar to the present normal mantle was available prior to 2.7 Ga. Depletion of LREE in the source material would in effect give rise to a depleted LREE profile in any subsequent melt.

The unfractionated nature of the HREE in Group 1 samples, with [Sm/Yb] N = 1.2, and the presence of negative Eu anomalies, suggests that neither garnet nor plagioclase is a residual component of the source region. Note also that the involvement of garnet fractionating out in the melt is not supported by the recorded increase in Mn, since fractionation of garnet would cause a depletion of Mn, Sc and a relatively well defined, gradual, depletion in Al_2O_3.

The presence of plagioclase as a residual phase would result in a negative Eu anomaly. This implies that the melt separation is not likely to have occurred at relatively shallow depth, i.e., between 8.6 to 10 kbar in the mantle. This pressure regime corresponds to the stability of plagioclase (Schilling, 1975).

The presence of clinopyroxene in the residual phase leads to a melt enriched in LREE and rocks subsequently derived from this melt will possess LREE enrichment. The LREE depletion observed (Figure 4.20-4.23), suggests that clinopyroxene is not a residual phase in the source material.

The role of olivine in REE fractionation is considered to be minor since its REE Kd values are much less than 1 (Henderson, 1984). The presence of other mineral phases in the residual phases such as amphibole and phlogopite is difficult to evaluate due to the mobility of K, Rb, Ba and Sr. However, the presence of amphibole in the residual solid is not likely since the presence of amphibole will result in a depletion of middle rare earth elements (MREE) and cause a positive Eu anomaly in the melt.

The Group II profile is illustrated by Figure 4.24. These two samples display a highly fractionated profile characterised by LREE enrichment

FIGURE 4.24: Chondrite normalised rare earth patterns for Group II basalts designated as calc-alkaline basalt by Ti/100-Zr-Y(3) diagram.

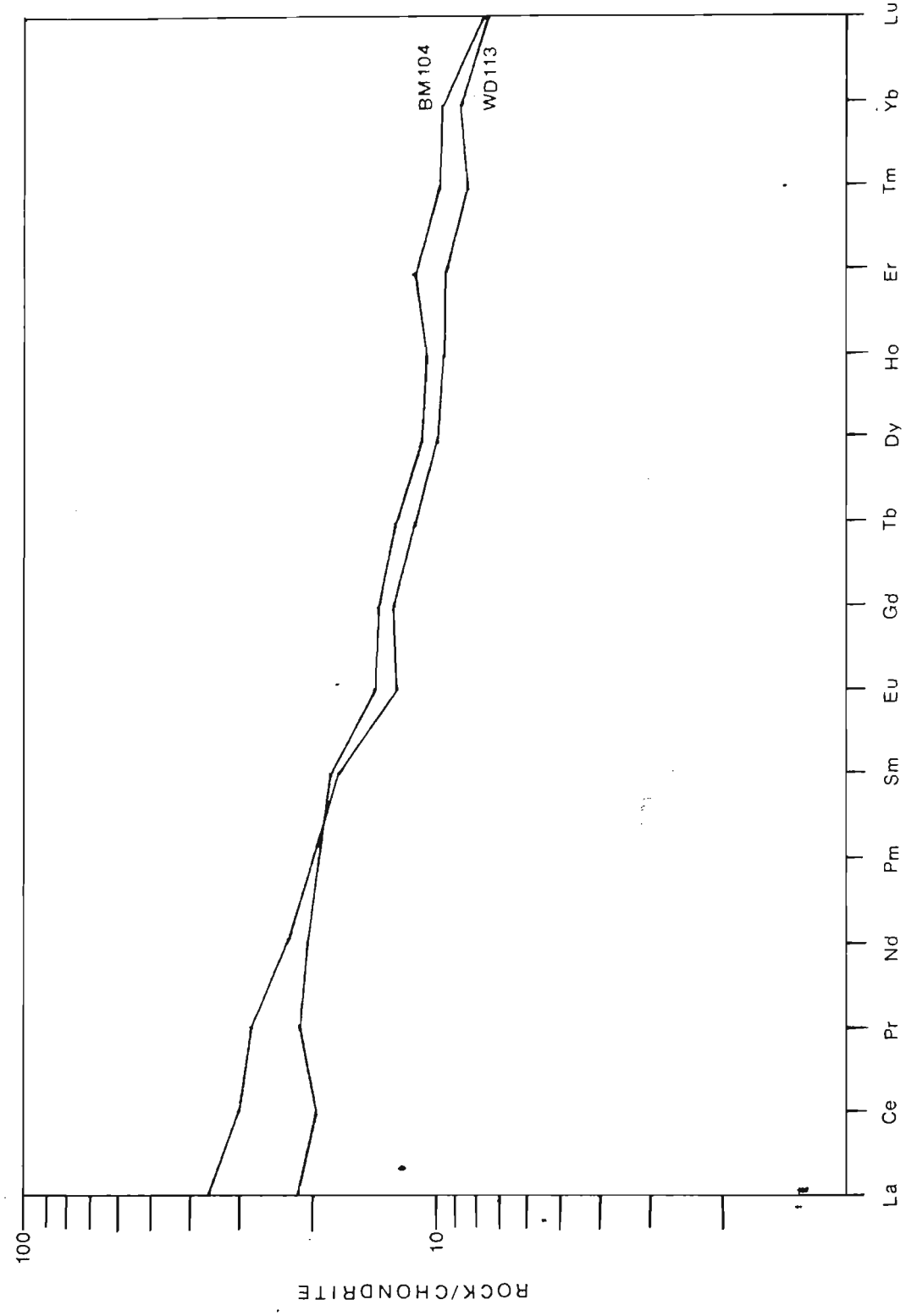
BM104
WD113
La
Ce
Pr
Nd
Pm
Sm
Eu
Gd
Tb
Dy
Ho
Er
Tm
Yb
Lu
100
10
ROCK/CHONDRITE

Figure 4.24

(20-40 X chondrites) with [La/Sm] N > 1 and a HREE depletion (10 X chondrites) pattern with [Sm/Yb] N close to 2. The LREE enriched profile observed could be a reflection of either i) degree of partial melting; ii) the presence of garnet or amphibole in the residual phases or iii) a result of contamination (Hawkesworth, 1982). This will be elucidated further in Chapter 7.

4.8 EFFECTS OF ALTERATION ON ELEMENTS: INTRODUCTION

Some elements such as Ti, Y and Zr have been shown to be useful in evaluating the probable nature of the tectonic settings while others like Ni, Cr and Mg have been shown to be invaluable in the interpretation of the magmatic history of volcanic rocks (Jakes and White 1972; Pearce and Cann, 1973; Pearce and Norry, 1979; Pearce et al., 1981; Floyd and Winchester, 1975). However, before embarking on the application of chemical classification and interpretation of the whole rock chemistry, the effects of secondary processes such as weathering and metamorphism on solidified magmas should be investigated. These post eruptive processes have the ability to mobilise elements and hence their respective concentration within the rocks (Alderton et al., 1980, and Henderson, 1984). This would eventually bring about with it uncertainty in the original chemistry and erroneous interpretation.

Pearce and Cann (1971; 1973) and Humphris and Thompson (1978) have documented the relative immobility of the trace elements Ti, P, Zr, Y, and Nb during greenschist facies metamorphism. Storey and Meneilly (1985) have defended the applicability of immobility of these elements to as high as the amphibolite facies. However, Murphy and Hynes, (1986) suggested that a CO_2 rich fluid introduced during metamorphism, has the ability to complex with various high field strength (HFS) elements (Y, Zr and Ti) and subsequently cause their mobilility.

In contrast, large ion lithophile elements (LILE) like Ba, K, Sr and Rb have been shown to be enriched in altered basalt (Hart 1971 and Hart et al. 1974). Henderson (1984) and Vallance (1974) interpreted the mobility of these elements to be affected not simply by metamorphic grade but also by the nature of the accompanying fluid phase.

The above discussion suggests that there is no single factor, but a series of interacting factors which dictates the mobility of the elements. In this study, all the elements analysed are examined for potential mobility by i) molecular proportion ratio diagrams such as those proposed by Pearce, (1968; 1969) and Beswick and Soucie (1978); ii) factor analysis and iii) element (s) versus CO_2 plots (after Murphy and Hynes 1986). Each of these analyses has its own merits and are briefly discussed in the following sections.

4.9 MOLECULAR PROPORTION RATIO DIAGRAMS

This method, first proposed by Pearce (1968), evaluates the effects of allochemical metamorphism on the mobility of individual elements. The method involves the application of discriminant analysis to altered and unaltered samples (Pearce 1968;1969; Beswick and Soucie, 1978). The procedure plots the ratio of the element of interest to an immobile element or oxide. An immobile element will display a single well defined trend while a mobile element will exhibit a scattered distribution. The application of this method to a suite of volcanic rocks requires that the primary compositional variation of the rocks is minor and that Al_2O_3 is indeed immobile.

Representative results of this application are shown in Figure 4.25 to 4.30. Elements K_2O, Na_2O, Sr, Cu, and Co are shown here to be mobile. Mobility of these elements are shown by the displacement of data along the y-axis while the variations along the x-axis are a manifestation of the fractionation trend. Elements CaO and Sc are depicted to be moderately

FIGURE 4.25 to 4.30 : Representatives of molecular ratio plots of samples. Al_2O_3 is used as a constant divisor, Fe_2O_3t along the x-axis is used as fractionating index.

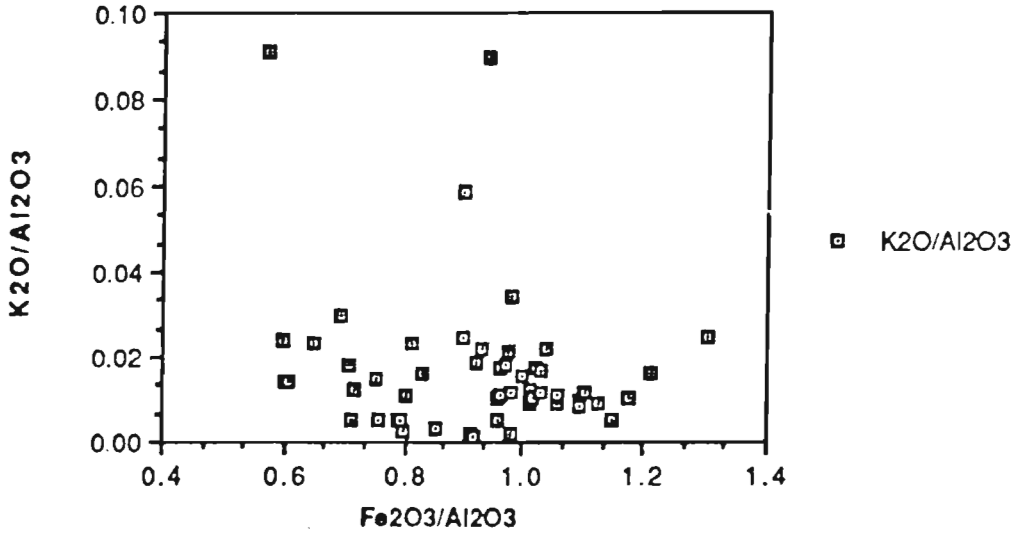

Figure 4.25

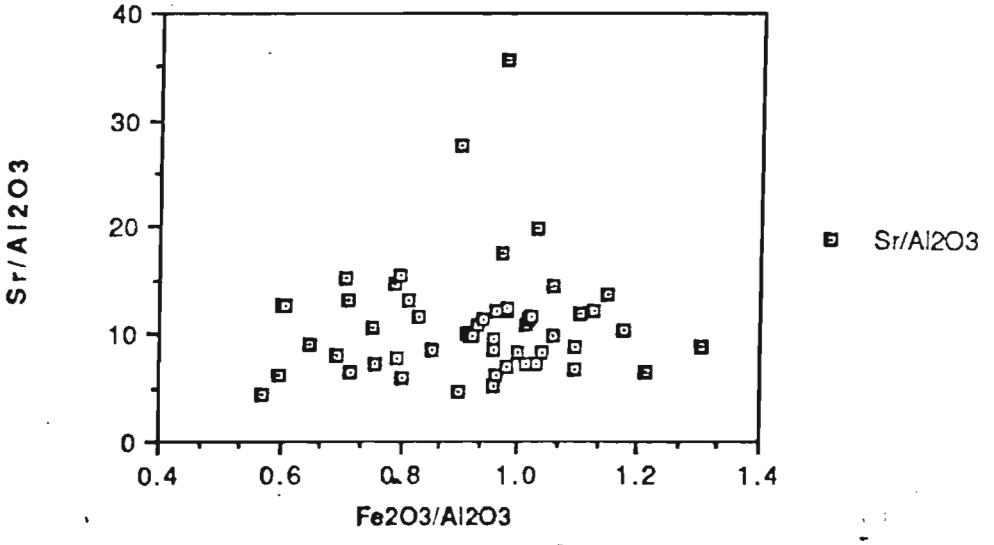

Figure 4.26

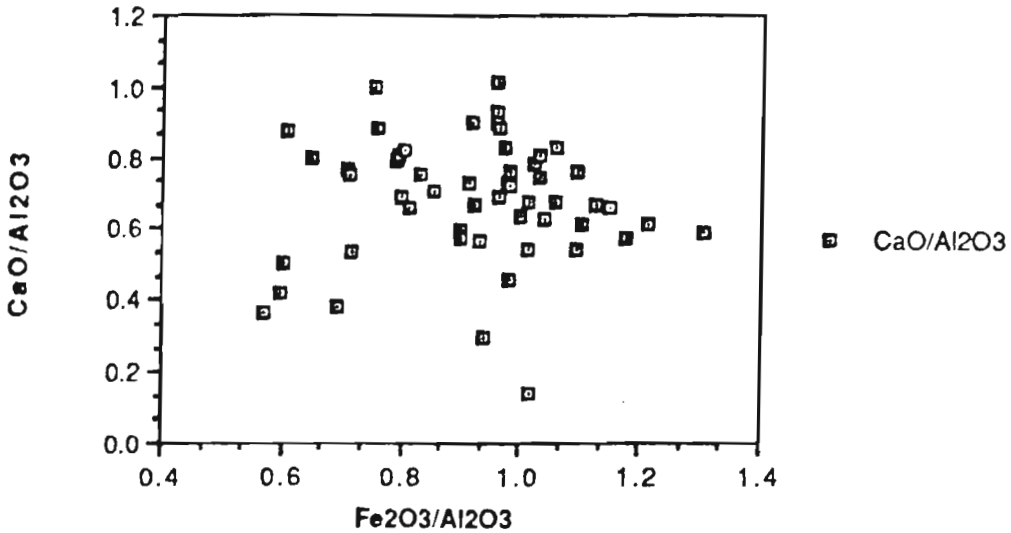

Figure 4.27

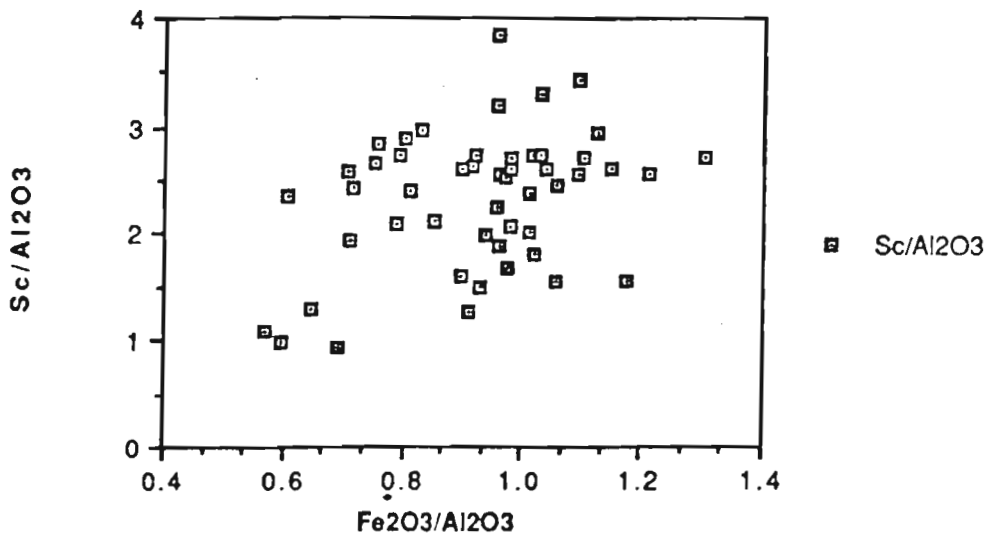

Figure 4.28

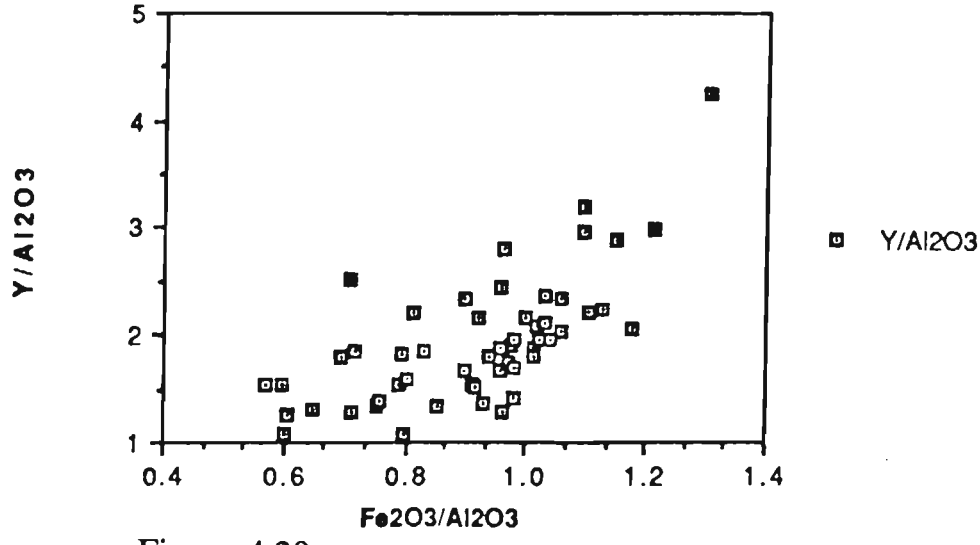

Figure 4.29

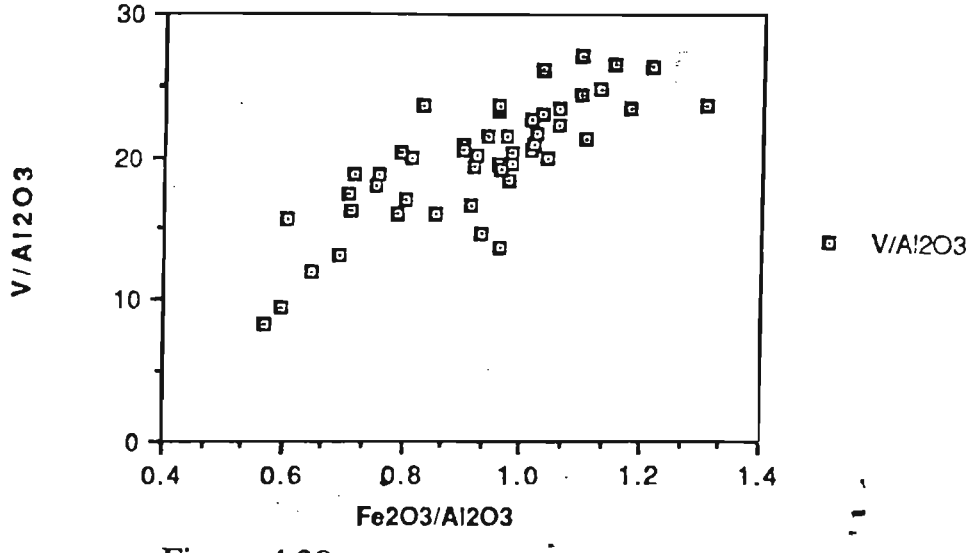

Figure 4.30

mobile while TiO_2, P_2O_5, Mn, Cr, Ni, V, Zr, Y and Zn are shown to be relatively immobile during the alteration processes.

4.10 FACTOR ANALYSIS

Factor analysis, a method rarely used in high temperature geochemistry, is employed here in an attempt to elucidate the inter-relationship of chemical elements (variables) that exist in the bulk rock chemistry. This method can be viewed as a means of evaluating the variation trends documented earlier in the variation diagrams (Figure 4.1-4.17).

Factor analysis essentially involves four major steps: i) computation of correlation coefficients for the variables. ii) The arrangement of correlation coefficients in a matrix. iii) Determining the factor (or axis) that accounts for the pattern of correlation values observed in the correlation matrix. iv) Rotation of factors (axes) to remove ambiguous loadings (coefficient), Comrey (1973) .

The number of factors extracted here is based on the Kaiser criterion, that is, factors with an eigenvalue greater than 1 are considered a factor, while those with an eigenvalue of less than 1 are discarded. An eigenvalue can be defined as a measurement of the magnitude of the data variation along a factor and it can be derived by adding the sum of the square loadings observed under each factor. The eventual factors obtained by this final procedure are often assigned to a specific causal connotation or geologic phenomenon such as alteration. However, Temple (1978) has suggested that erroneous interpretation could arise from the desire to assign causal connotation to the factors obtained. If there exists a cause for the observed correlation coefficient (factor), the lack of or absence of a correlation coefficient must also have a cause. As a result, the validity of the interpretation must be confirmed by other evidence. Other cautionary measures include the size of the sample and the possible existence of a

curvilinear relationship between the variables, since factor analysis is based on the assumption that correlations between the variables are linear.

Factor analysis was performed on both the major and trace elements using the SPSS package run on the Burroughs 7900, at Brock University. The major and trace elements were run independantly to avoid the possibility of obscuring factors. Table 2a and 2b show the eigenvalues and the percentage contribution of each factor. The cut off point for a significant loading is taken at an arbitary number of .30000. For the major elements, the first 5 factors account for 80% of the data variation. The first factor, which accounts for 26% of the variation is interpreted to reflect a primary magmatic process, involving the removal of Ca and Mg due to fractionation of clinopyroxene. The high positive loading for the elements such as K and Na further supports this interpretation. Factor 2 also reflects magmatic differentiation. The positive loadings for the elements Ti, total Fe, Mn and P reflects the accumulation of these elements in the residual melt. Factors 3 and 5 can be assigned to carbonitization and sulphidisation processes, respectively. In contrast, factor 4 posesses some problems in assigning a causal effect rather than providing some insight. The author is not aware of any processes that could fit the observed loadings.

It should be pointed out that the loading for the variables Al_2O_3 and Na_2O be interpreted with some caution. Their low communalities, that is the sum of square of the loadings for these variables over the 5 factors, suggest that approximately 40% of the variance is unaccounted for by the 5 factors. In conjunction with the 5 factors, this could not account for the total observed variance suggesting that the inter-relationship between the variables is much more complex. Table 2b essentially provides a similar interpretation, with factor 1 and 2 being assigned to magmatic processes, while ambiguity exist in interpreting factor 3. The communality values for Ni, Sr and Cu suggest caution in interpreting these variables.

Table 2a. Varimax rotated factor analysis on major element chemistry of BGB basalts.

Variables.	Factor 1	Factor 2	Factor 3	Factor 4	Factor 5	Communality.
SiO2	.36747	-.26981	-.12645	.85804	-.08603	.96745
TiO2	.12432	.82160	-.12645	.32944	.20718	.85823
Al2O3	.38487	-.05672	-.47055	-.52274	-.03622	.64734
Fe2O3	.02222	.80830	-.28977	-.24844	.21674	.84651
MnO	-.15427	.77784	.32858	-.04640	-.12549	.75470
MgO	-.41933	-.31974	-.09633	-.68947	-.05216	.76544
CaO	-.86783	-.11780	.00176	-.12054	.07726	.78751
Na2O	.73691	.08789	-.18850	.15598	-.05958	.61418
K2O	.77798	-.19614	.00169	.11420	.08484	.66396
P2O5	.23244	.43386	-.18656	.38725	-.51915	.69655
CO2	-.05944	.01659	.96465	.13843	-.00681	.95356
S	.02284	.23635	-.10946	.05479	.87694	.84039
LOI	-.03967	-.10677	.95092	-.16145	-.06729	.94783

Factor	Eigenvalue	Pct. of Var.	Diagnosis.
1	3.36021	25.8	Magmatic differentiation.
2	2.44579	18.8	Magmatic differentiation.
3	2.31839	17.8	Carbonitization.
4	1.14581	8.8	?
5	1.07345	8.3	Sulphidisation.

Table 2b. Varimax rotated factor analysis on trace element chemistry of BGB basalts.

Variables	Factor 1	Factor 2	Factor 3	Communality.
Co	.79697	-.14345	.19096	.69220
Cr	.00580	-.18970	.85941	.77461
Cu	.47506	-.59144	-.03368	.57661
Ni	.19268	-.41219	.62487	.59748
Zn	.80671	.22308	.15337	.72407
Sr	-.08324	.12277	.66324	.46188
Y	.37712	.83112	-.21041	.87725
Zr	.07904	.91090	-.06071	.83968
V	.90786	.19495	-.06674	.86668
Sc	.77631	-.07449	-.29189	.69340

Factor	Eigenvalue	Pct. of Var.	Diagnosis.
1	3.19057	31.9	Magmatic differentiation.
2	2.50728	25.1	Magmatic differentiation.
3	1.40602	14.1	?

From factor analysis, it appears that some consistency in interpretation has been achieved, compared with the results of section 4.3. Complications in assigning causal effects to some factors also arises from the observed loadings, suggesting that the inter-relationship or underlying structure between the variables is more complex than it appears to be.

4.11 CO_2 VERSUS HFS DIAGRAMS

Contary to the wide interpretation that HFS are immobile (Pearce et al. 1981; Reid et al. 1987), Murphy and Hynes (1986) have documented the mobility of these elements under the influence of high CO_2. Since some of the HFS elements are used in determining the possible paleotectonic setting of the BGB lithologies, their potential mobility are evaluated by plotting these elements against CO_2 concentration. Figure 4.31 to Figure 4.34 suggest that the CO_2 concentration in the rocks has no influence on the concentration of these elements, implying that for the BGB samples, these elements are immobile.

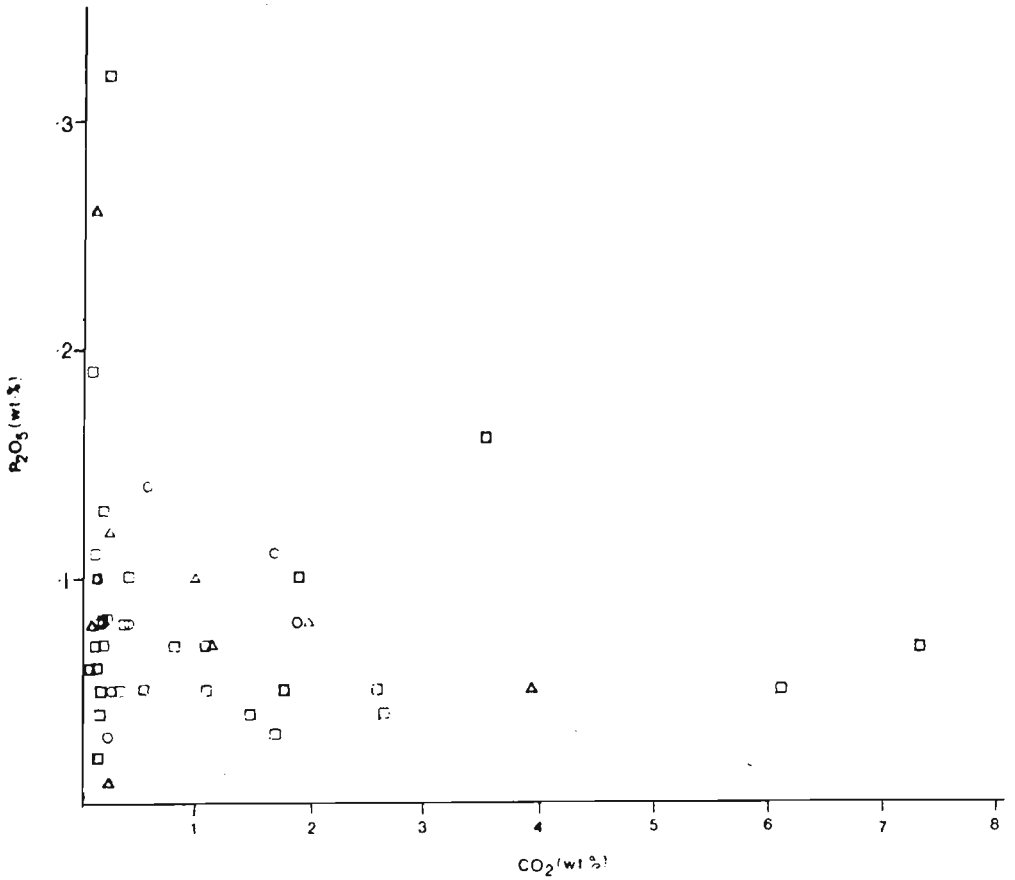

Figure 4.31: Plot of P_2O_5 versus CO_2 for volcanic rocks of the BGB.

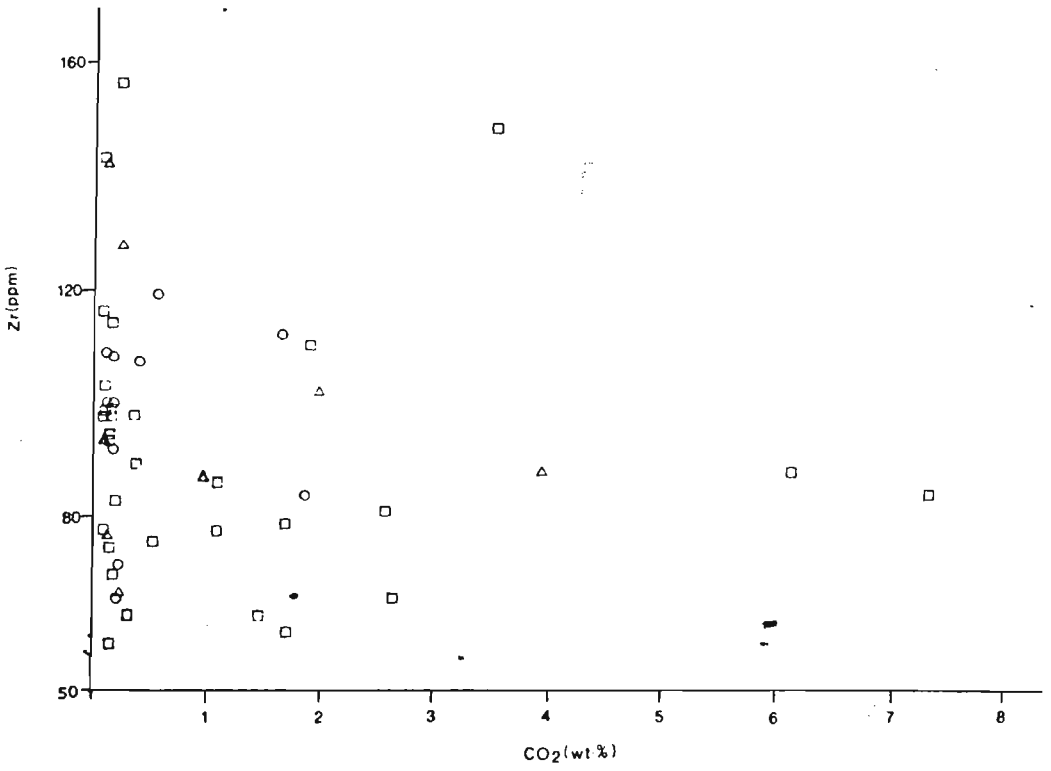

Figure 4.32: Plot Zr versus CO_2 for volcanic rocks of the BGB.

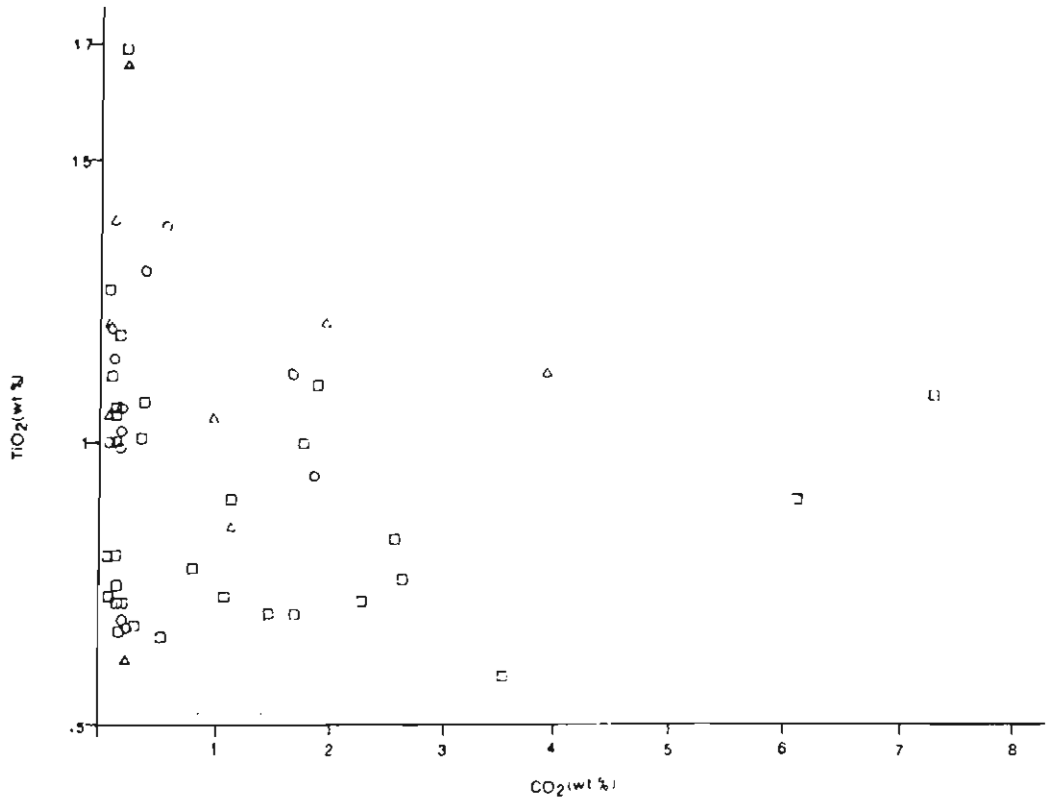

Figure 4.33: Plot of $Ti0_2$ versus CO_2 for volcanic rocks of the BGB.

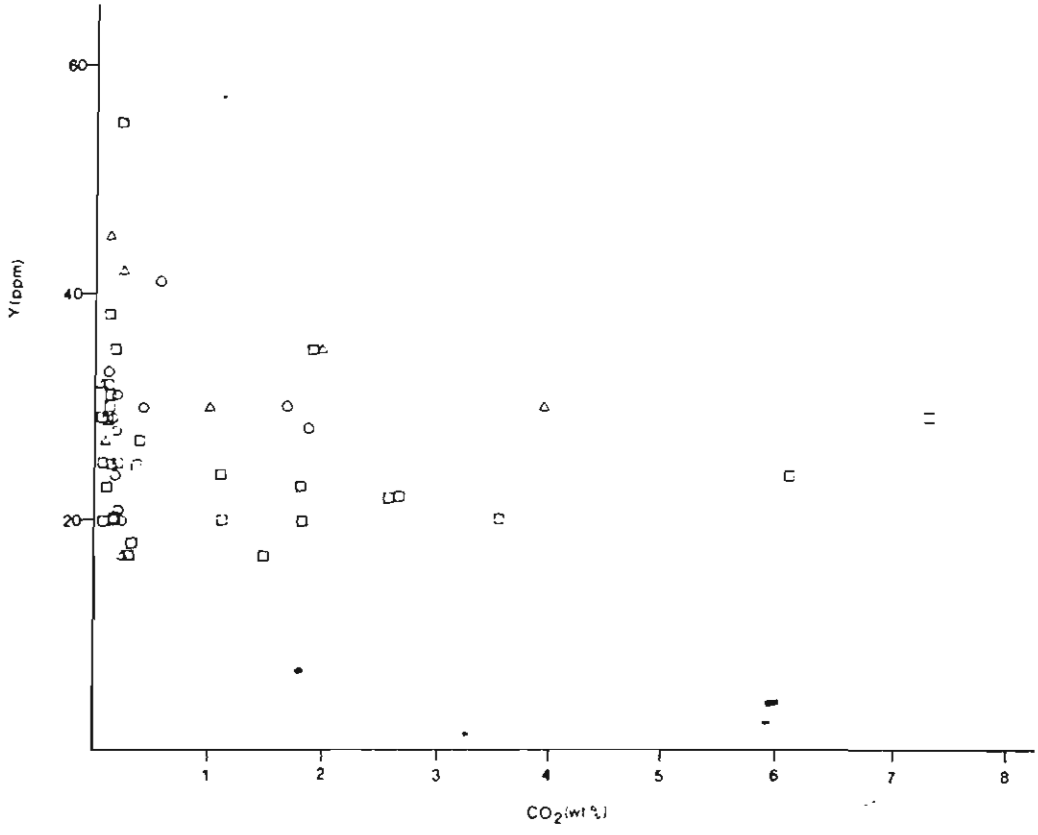

Figure 4.34: Plot of Y versus CO_2 for the volcanic rocks of the BGB.

CHAPTER 5

PALAEOTECTONIC SETTING FOR THE BGB BASALTS

5.1 INTRODUCTION

Different tectonic settings support distinct magma generating processes. These processes are indicated by the behaviour of the incompatible elements, such as Ti, Zr and Y, used in discriminant diagrams. The fundamental principle involved in the reconstruction of palaeotectonic setting of ancient volcanic rocks using geochemical data has been the comparison of major and trace element characteristics of the unknown volcanic setting with those of recent, known tectonic settings (Pearce and Cann, 1971; 1973; Pearce et al. 1975).

In this chapter, discriminant analysis is employed to identify the palaeotectonic setting of the volcanic component of the BGB. The validity of applying discriminant diagrams, constructed using data collected from Phanerozoic volcanic rocks, on rocks of Archaean age is questionable (Arculus, 1987). It has been suggested that the mantle has continuously evolved through geologic time (Rogers, 1978) and therefore, any resulting mantle derived melts should exhibit this variation. Pharaoh and Pearce (1984) pointed out that greater than 80% of Rb and 50% of Ba have been extracted from the primordial mantle. This is further compounded by secondary processes which inevitably give rise to repartitioning of trace and major elements. The assumption has to be made that for a specific tectonic setting, the distribution of elements in the Archaean volcanic rocks is similar to those of the present.

Despite some of the problems mentioned above, it has been shown that the applications of immobile elements in discriminating tectonic setting for the Archaean volcanic rocks is viable (Floyd and Winchester, 1976; Smith and Smith, 1976; Pearce and Norry, 1979), providing that other independent information, such as structural and sedimentological data are

used in conjunction with geochemical results. Furthermore, the ratio of Ti/Y, Zr/Y, Zr/Nb, Ti/Zr and TiO_2/Al_2O_3 for low-magnesium basalt (MgO < or = to 10%) have remained the same since the Archaean (Sun and Nesbitt, 1978). The similarity in element ratios does not suggest that the actual abundances of these elements have remained constant. Whilst the magmatic processes since the Archaean are not greatly different from the present (Sun and Nesbitt, 1977;1978) the feasibility and applicability of discriminant diagrams to differentiate the tectonic environment within Archaean rocks is valid.

5.2 DISCRIMINANT DIAGRAMS AND THE BGB VOLCANIC ROCKS

To alleviate some of these difficulties discussed above, the effects of allochemical metamorphism on the mobility of individual elements has been examined in chapter 4. It has been shown that elements such as K and Sr are relatively mobile, while Ti, Zr and Y are relatively immobile.

In Chapter 4, the BGB volcanic rocks were classified as having a tholeiitic composition. This classification does not indicate the possible types of tectonic settings (volcanic arcs, ocean floor, ocean island or intracontinental) in which these rocks formed. Further discrimination is required to identify the tectonic setting. By using established discriminant diagrams some of these possible settings can be ruled out.

On the Ti/100-Zr-Y(3) diagram of Pearce and Cann (1973); Figure 5.1, approximately 75% of the BGB data falls within the oceanic floor basalt (OFB) field with the remaining 25% within the calc-alkaline (CAB) field. The applicability of this diagram to Archaean rocks have been substantiated by the constant inter-element ratios for Ti, Zr and Y with time (Sun and Nesbitt, 1978). The results for the BGB rocks (Figure 5.1) are interpreted to be real. The tight clustering displayed by the data further attests to the immobility of the elements involved.

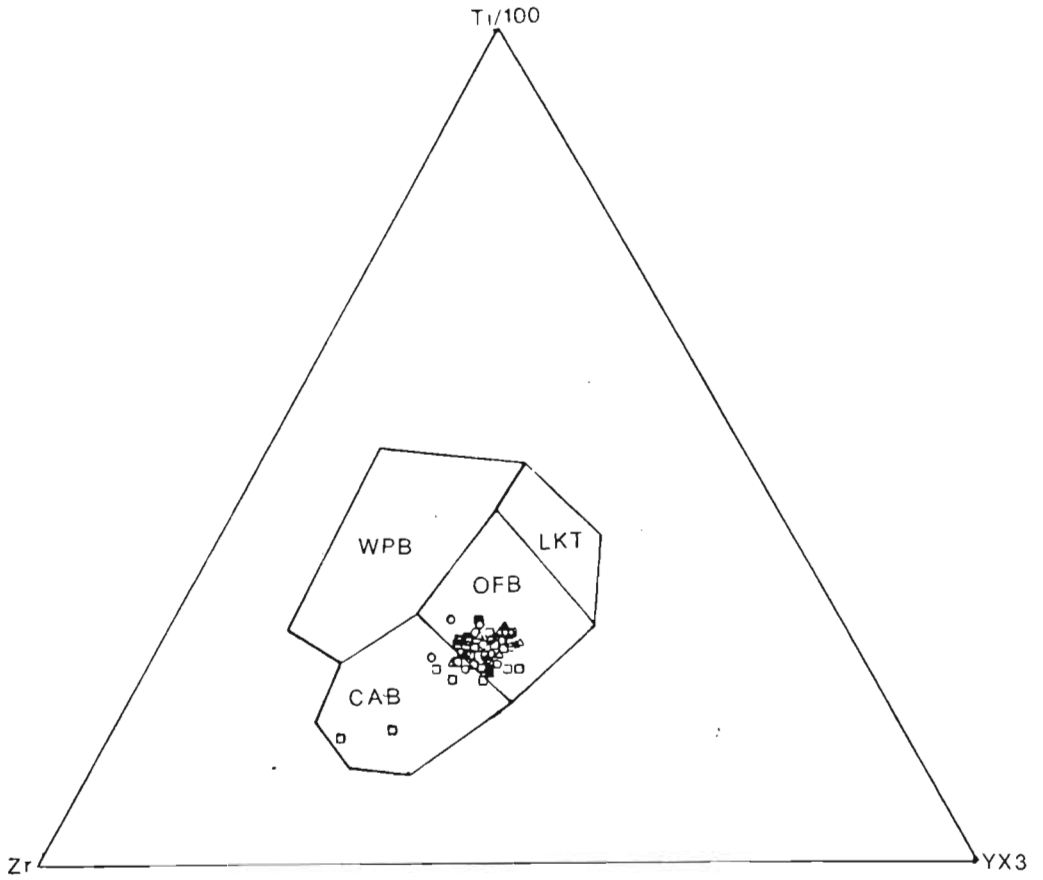

Figure 5.1: Plot of volcanic rocks on Ti/100-Zr-3Y discriminant diagram of Pearce and Cann (1973). WPB: within plate basalt; LKT: low potassium tholeiite; CAB: calc-alkaline basalt; OFB: ocean floor basalt. Symbols as in Figure 4.18.

Pearce et al. (1975), proposed the TiO_2-K_2O-P_2O_5 diagram based on the principle that P_2O_5 and TiO_2 are resistant to alteration with each oxide having a diagnostic concentration in oceanic and continental environments. P_2O_5 is generally concentrated in continental environments while the concentration of TiO_2 is higher in the oceanic environment. The BGB results when plotted on this diagram exhibit a strong tendency to be drawn towards the K_2O apex with the ratio of TiO_2/P_2O_5 remaining relatively constant (Figure 5.2). This suggests the mobility of K_2O as was documented in chapter 4. Regardless of K_2O mobility, the majority of the data falls within the OFB field.

On Figure 5.1 and 5.2, the BGB data falls within the OFB field. However, on plot of Ti/100-Zr-Sr/2 (Figure 5.3), the reverse situation is observed, where samples lie within CAB field. This contradictory result can be explained by Sr mobility for the BGB volcanic rocks. Sr mobility, that is, enrichment has occurred causing the data to be displaced towards the Sr apex, placing the majority of the samples in the non-oceanic field (Smith and Smith 1976). It should be pointed out that some of the samples in Figures 5.1 and 5.2, which plot within the island arc or non-oceanic field are relatively unaltered, suggesting that their composition reflects their original chemistry.

5.3 SPIDERGRAMS

Documented settings in which tholeiitic basalts can be produced include island arcs, marginal back arc basins and mid-oceanic ridges. To obtain a better perspective of types of tectonic settings to which the BGB volcanic rocks belong, spidergrams are employed. These diagrams are derived from normalising the geochemical data of the sample of interest to that of known tectonic setting. Figures 5.4 to 5.6 illustrate the use of such diagrams. BGB samples with the highest (H), intermediate (I) and lowest

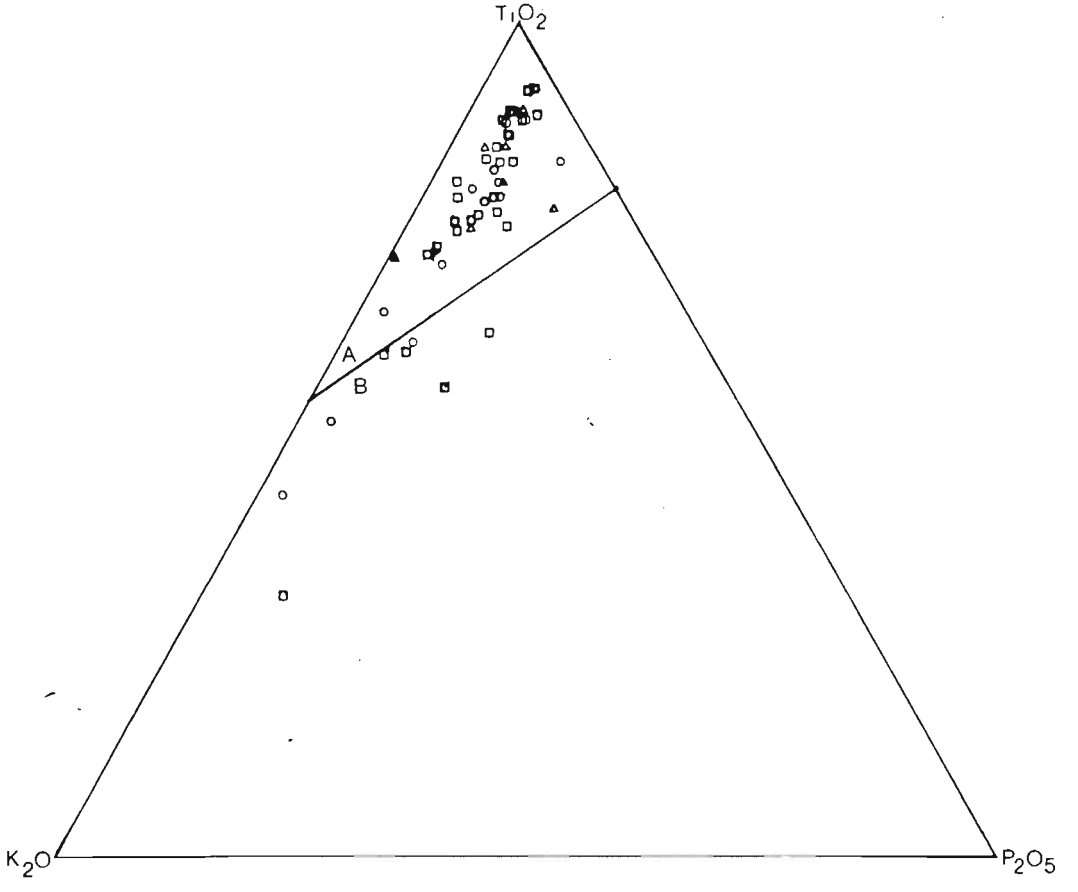

Figure 5.2: Plot of volcanic rocks on TiO_2-K_2O-P_2O_5 discriminant diagram of Pearce et al. (1975). Symbols as in Figure 4.18. Field A: ocean floor basalt; Field B: non-oceanic basalt.

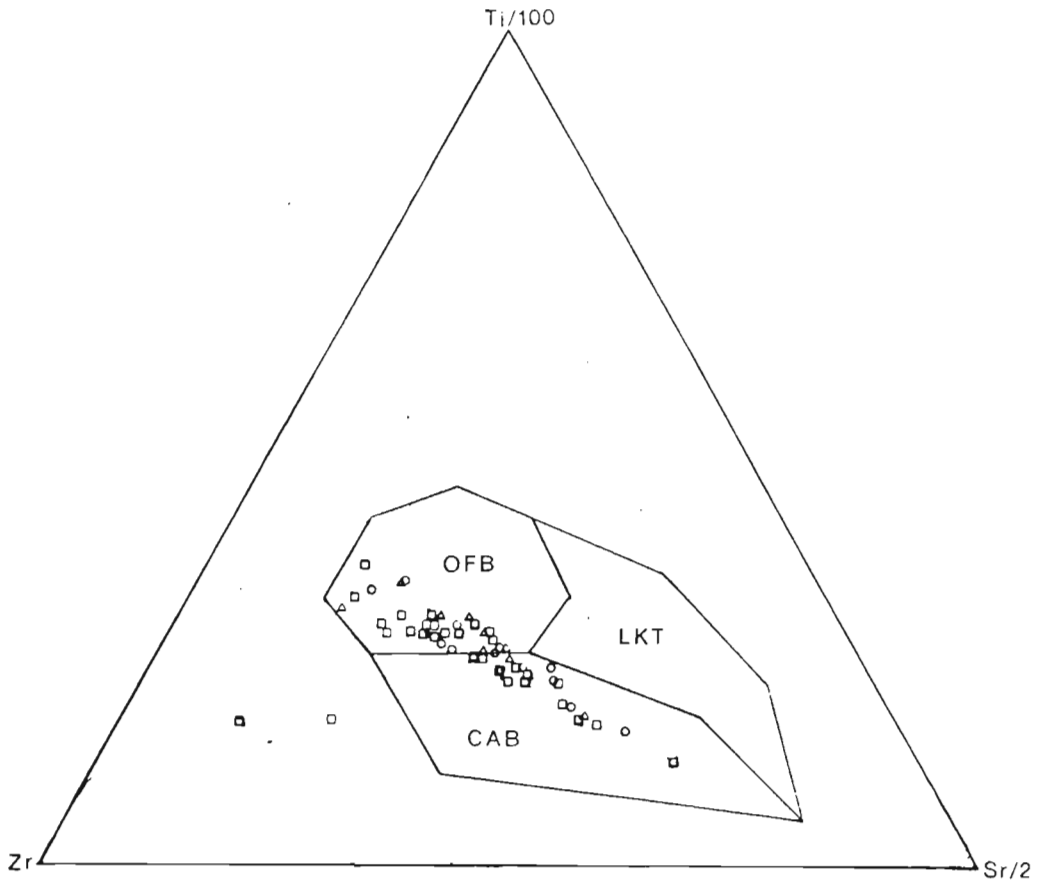

Figure 5.3: Plot of volcanic rocks on Ti/100-Zr-Sr/2 discriminant diagram of Pearce and Cann (1973). OFB, LKT and CAB as in Figure 5.1. Symbols as in Figure 4.18.

Figure 5.4, 5.5 and 5.6: Samples normalised to mid-oceanic ridge basalts (MORB), island arc tholeiite (IAT) and marginal back arc basin basalts (MBB). I,L, and H represents samples with intermediate, low and high Mg # respectively. Normalising values for MORB are from Condie (1976); IAT from Jakes and White (1972) and MBB from Saunders et al. (1981).

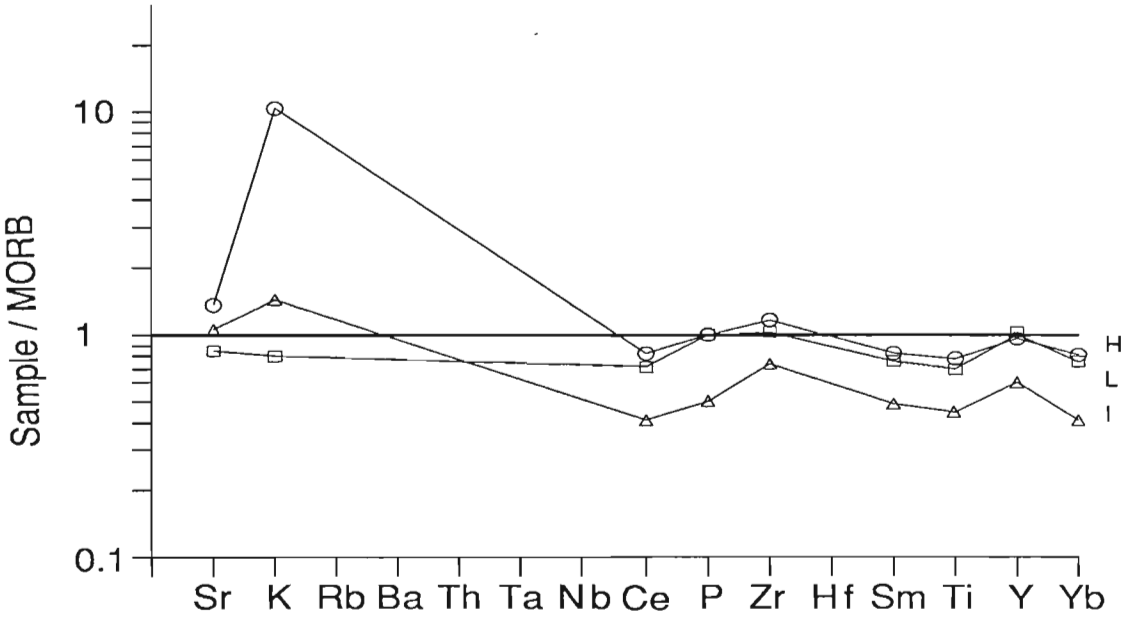

Figure 5.4 : (after Pearce et al. 1981)

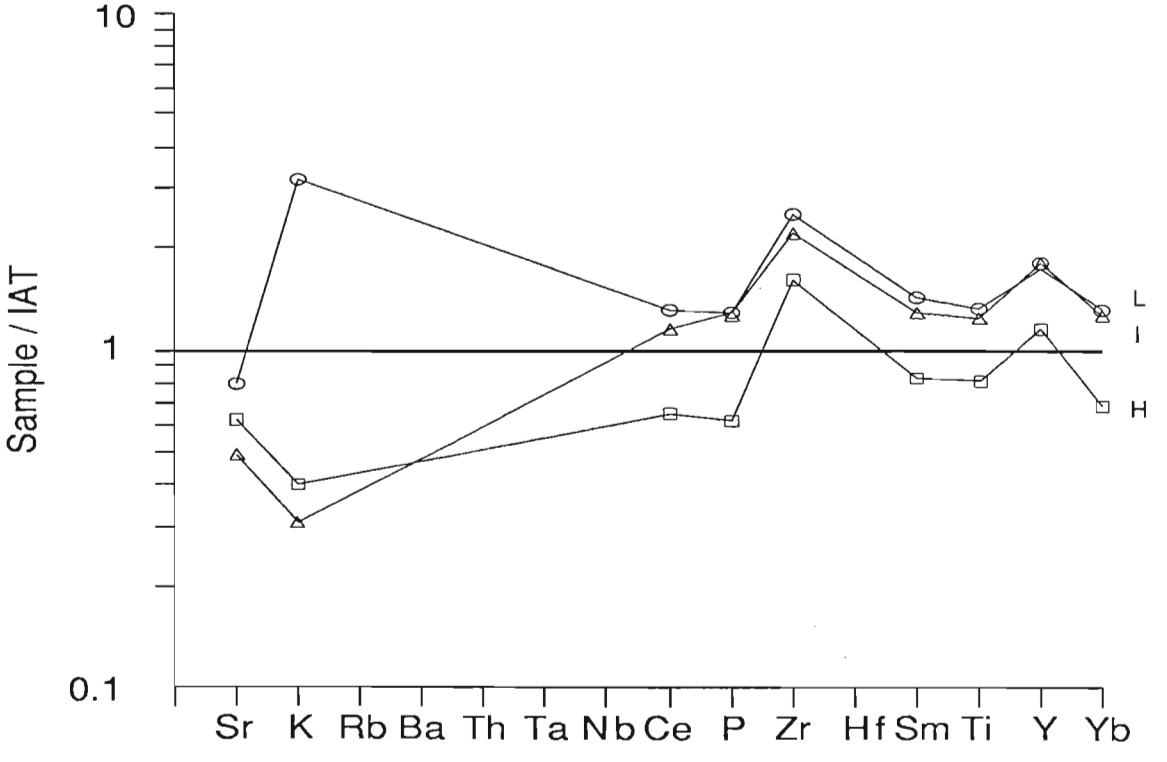

Figure 5.5

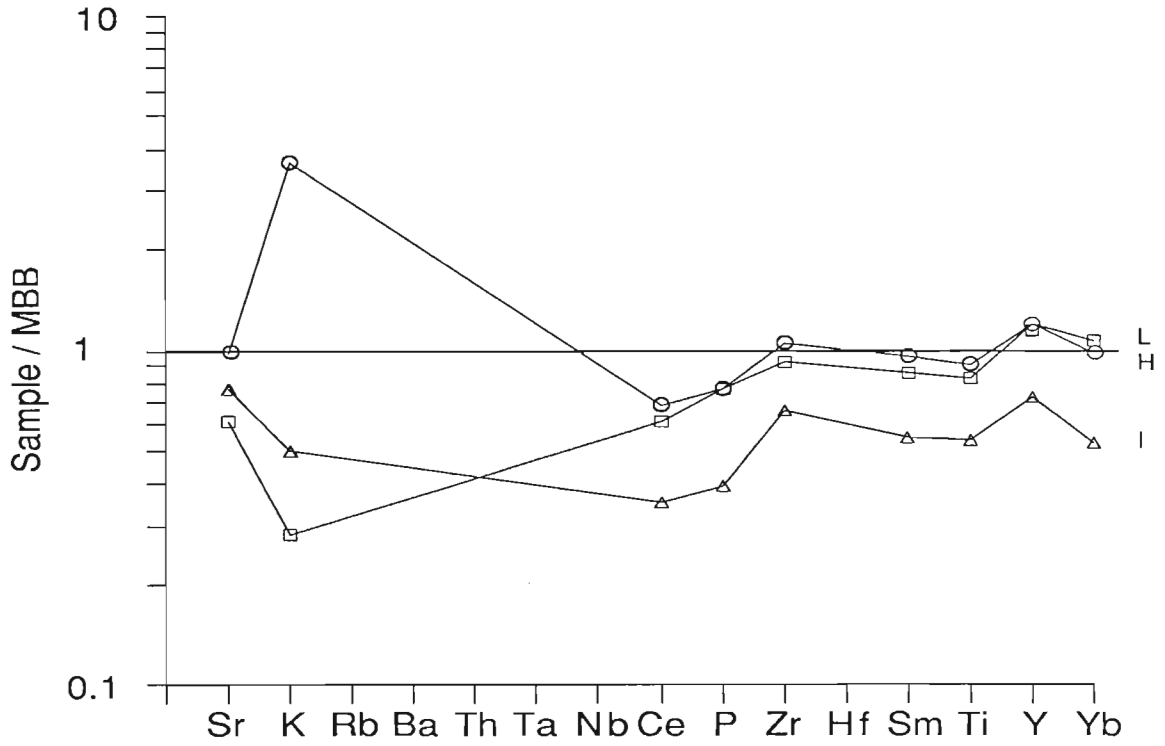

Figure 5.6

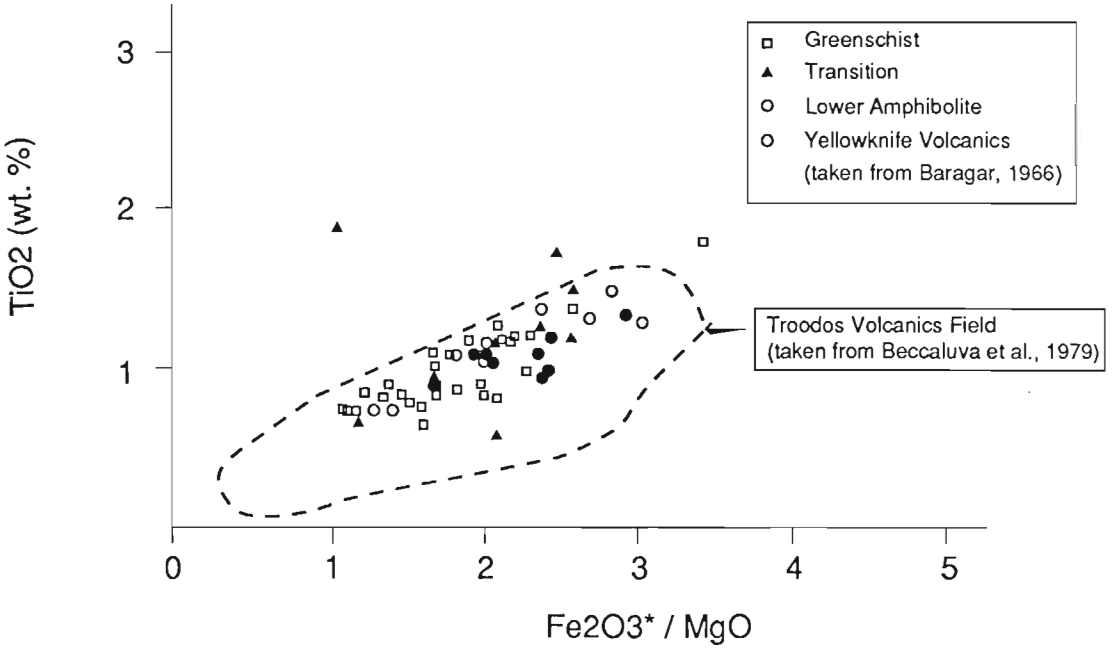

Figure 5.7: Plot of TiO2-(FeO*/MgO) diagram after Beccaluva et al. (1979).

(L) Mg numbers , are normalised to an average mid-oceanic ridge basalt (MORB), island-arc tholeiite (IAT) and marginal back-arc basin tholeiitic basalts (MBB). The BGB data for incompatible immobile elements (Ti, Zr, Y, P) appears to have a better correlation to MORB, (Figure 5.4), than with either IAT or MBB (Figure 5.5 and 5.6 respectively). The source for ocean floor basalts is suggested to contain higher concentration of HFS elements and maintain a lower oxygen fugacity than those of island arcs (Jakes and White, 1972). Support for a mid oceanic ridge affinity to the BGB basalts can be seen in the relatively low oxygen fugacity necessary to account for the negative Eu anomaly and the enrichment of Ti, V, and total Fe during melt evolution (Chapter 4).

5.4 GEOCHEMICAL COMPARISON OF BGB WITH ANCIENT AND RECENT OPHIOLITE

The data from Beardmore-Geraldton volcanic rocks are plotted on a TiO_2 vs Fe_2O_3t/MgO diagram, together with representatives of Archaean oceanic crust, the Yellwoknife volcanics (Helmstaedt et al., 1986) and Phanerozoic oceanic crust, the Troodos Complex (Malpas et al. 1984), Figure 5.7. The majority of the BGB compositional data is observed to overlap the data representing the Yellowknife volcanics and Troodos complexes. This may suggest a comparable tectonic setting to that proposed for these modern and ancient representatives of ocean floor material. One should note that the Troodos Complex is grouped into an upper and lower pillowed flow sequence. The upper flow is considered to be of island arc affinity, while the lower flow is suggested to be of oceanic affinity (Pearce, 1975). The chemistry of the Troodos flow employed here is that of the lower flow.

5.5 DISCUSSION

Discriminant analysis on the palaeotectonic setting of the BGB are summarised in Table 3. These results suggest that the majority of the BGB volcanic rocks originated in an ocean ridge environment, and the BGB as a whole, represents remnants of oceanic crust. An ocean ridge environment for the BGB basalts is further supported by the predominance of tholeiitic basalts within the 3 belts and the apparent lack of calc-alkaline material, Figure 4.18 and 4.19. It is appropriate to point out here that the OTT to the north of the BGB displays a calc-alkaline affinity (Kresz and Zayachkivsky, 1986) and was previously interpreted by Thurston (1980), and Amukun (1980) to represent an island arc complex.

One should note that even though the spidergrams documented above appear to suggest a mid-oceanic ridge environment for the BGB, this does not rule out the possibility of a marginal back-arc basin environment. Marginal back-arc basins can be recognised in their early stages of development by having a chemistry that reflects a subducted component, i.e., one enriched in LILE, LREE and depleted in Nb and Ta (Tarney et al., 1981). As the the back-arc spreading continues, the oceanic floor basalts (sensu lato) produced in this environment will lose these chemical characteristics as the back-arc spreading ridge migrates further away from the subduction zone. As a result, these basalts will possess many similarities, both petrographically and geochemically, to those generated in a mid-oceanic ridge environment. Tarney et al. (1981) have suggested variable sedimentary characteristics for the environments which flank both sides of the arc. This high variability in sedimentary components and similarities in the chemical characteristics of the basalts combined with the lack of data on Ta and Nb data for the BGB samples makes the distinction between MORB and MBB settings difficult.

Mixed chemical characteristics are found in the BGB. Miyashiro (1973), has also documented such characteristics in the Troodos massif and the

Table 3: A summary of the interpretation derived from discriminant diagra

DISCRI. DIAGRAM	NOTES
Ti/100-Zr-Y X 3	75% IN OFB FIELD 25% IN CAB FIELD
TiO2-K2O-P2O5	75% IN OFB FIELD 25% IN NON-OFB FIELD
Ti/100-Zr-Sr/2	25% IN OFB FIELD 75% IN CAB FIELD
TiO2 vs FeOt/MgO	OVERLAP WITH YELLOWKNIFE AND TROODOS VOLCANIC
SAMPLES NORMALISED TO MORB, IAT AND MBB.	BEST RESULT OBTAINED WITH MORB

Kurile Arc . These mixed geochemical characteristics could be interpreted to result from the mechanical mixing of island arc basalt with ocean floor basalt during a subduction event. However, field evidence is not forthcoming on this suggestion. Another possible explanation for the mixed geochemical characteristics could be attributed to post accretionary intrusion similar to that described by Echeverria (1980), Jakes and Miyake (1984) and Lash (1986). This latter explanation may be a probable solution if one considers the fact that subparallel mafic intrusions are observed in the adjacent sedimentary belts (Mackasey, 1975 and 1976) and the proximity of known CAB rocks to the north.

CHAPTER 6

OVERALL TECTONIC HISTORY

6.1 RARE EARTH DATA

The majority of the REE patterns for the BGB basalts are relatively flat, Figure 4.20-4.23, (Section 4.6). The unfractionated nature of the REE patterns imply that no crustal contaminants are involved in the formation of most of the Group I volcanics of the BGB, suggesting the absence of a sialic basement to these volcanics and further enhancing the oceanic affinity of the BGB volcanics. In contrast, Group II BGB basalts, Figure 4.24, (designated as CAB by Ti/100-Zr-YX3 discriminant diagram) exhibit a LREE enrichment. The minor calc-alkaline component within the BGB was interpreted earlier to represent post accretionary intrusive material. CAB has been shown to carry with it the inherited, contaminated nature of the source region (O' Nions et al., 1977; Mysen, 1979). Tarney et al. (1982) have documented that CAB produced further from the trench axis tend to have a higher degree of LREE enrichment than those originating nearer the trench axis, with [Ce/Yb] N ratios of 2 to greater than 6. This change could be a reflection of the changing nature of the source, variation in the degree of melting or a higher contribution by one of the components involved in the genesis of CAB, such as the crust. Higher overall abundances of REE, away from the trench axis, towards the continental margin has also been documented by Boettcher (1972), suggesting the greater involvement of crustal material. From the observed REE profiles for the BGB CAB [low (Ce/Yb) N = 2 to 3 and low total REE contents], it appears that either the CAB originated in close spatial proximity to the trench axis, or that the contribution of components enriched in incompatible elements (the crust or the hydrated mantle wedge) is relative less than that observed in modern settings. This may suggest that underplating instead of subduction

has limited the involvement of the various components involved in the genesis of the calc-alkaline magma.

6.2 DISCRIMINATION USING STRUCTURAL AND STRATIGRAPHIC DATA

Geochemical discrimination in itself should not be considered independantly in defining the palaeotectonic setting of a suite of ancient or modern volcanic rocks. Other geological displines (stratigraphy, structural geology and sedimentology) should be considered. For the BGB published structural and stratigraphic data is available to lend support to or refute the geochemical interpretation.

Compilation of structural data from the Wabigoon, Quetico and Wawa subprovinces by Williams (1986; 1987) has led to the erection of a tectonic model, indicating arc-arc accretion. This model is similar to that of Langford and Morin (1976) where northward merging island arcs, represented by the Wawa, Wabigoon and Uchi subprovince, were proposed for the development of the Superior Province. In the model, proposed by Williams (1986; 1987), the BGB was suggested to represent an imbricated metavolcanic-metasedimentary prism which is juxtaposed against volcanic centers situated to the north of the Paint Lake Deformation Zone (Figure 2.1). The imbricated sequence was recognised on the basis of detailed lithostratigraphic mapping and structural field data. Individual layered sediment-volcanic tectonic units are separated by layer parallel shear zones interpreted to be thrust faults. Such tectonic features are considered to be common in convergent plate margins (Karig and Sharman, 1975) and resemble the imbricate structures seen in the Southern Uplands of Scotland, (McKerrow and Leggett, 1977) and on Signy Island, Antarctic Peninsula, (Storey and Meneilly, 1985).

Sedimentological studies carried out on the sedimentary component of BGB, by Devaney and Fralick (1985), suggests that this material represents

a laterally continuous prograding sedimentary clastic wedge, produced in a fluvial-marine environment. These conclusions were based on the recognition of primary sedimentary structures, (swale cross-stratification, rythmites, cross-stratified sandstone) and the variation in the proportion of the various lithofacies within the 3 sedimentary belts. Devaney and Williams (in prep.) further suggest that the presently observed alternating sedimentary and volcanic belts was once a continuous sedimentary-volcanic basin that has been broken up and repeated by thrust imbrication. These sedimentological and structural interpretations coupled with field evidence suggest a mafic volcanic basement to the sedimentary material (Mackasey, 1975) and the presence of pillow lavas at the top of each volcanic sequence, further supports the oceanic origin of the BGB volcanic rocks.

6.3 IS BGB REPRESENTATIVE OF AN OPHIOLITE SEQUENCE?

From the preceding documentation, it appears, that geochemical interpretation of the palaeotectonic setting of the BGB, using the various discriminant diagrams is in agreement with complimentary studies carried out by other workers. However, if these volcanic rocks within the BGB do indeed represent remnants of oceanic crust, the recorded stratigraphy does not resemble an idealized obducted oceanic crust (ophiolite). Typical ophiolites, such as those seen in the Troodos Complex (Gass, 1980), are characterised by chemical sediments, pillow lavas, sheeted diabase dykes, gabbros and peridotite, in descending stratigraphic order. The individual volcanic belts of BGB are characterised by clastic sediments, pillow lavas and massive, fine to coarse-grained flows, in descending order. A similar stratigraphic sequence was also documented in the Makimine Formation of the Shimanto accretionary complex of Japan (Needham and Mackenzie, 1988). The lack of the typical ophiolitic sequence, that is, the absence of

sheeted dykes and ultramafic rocks, in the BGB volcanic sequence could be attributed to the high heat flow and high rate of magma supply during the formation of the oceanic crust (Tarney et al., 1976). It has been suggested by Gass (1980), that the sheeted dyke complex is formed when the seafloor spreading is slow, and the cooling time is sufficient for a chilled margin to form between dykes. High heat flow and an increased rate of magma supply would presumably deter formation of the sheeted dykes, forming medium-grained, structureless flows instead.

Lewis (1983), attributes the absence of sheeted dykes in some ophiolites, to the depth at which the magma chamber is located within the crust. A shallow magma chamber would tend to result in the production of shorter dykes.

Another possible explanation for the absence of sheeted dykes can be found in the rifting model proposed by Gibson et al. (1986). These authors envisage that dykes were produced sequentially above a magma chamber and subsequently rotated and transposed into a zone of decollement, resulting in dykes becoming sheared out along this zone. Unfortunately, field evidence for such zones of rotation and decollement are lacking in the study area, however, the volcanic rocks in the study area are invariably sheared at their base. The nature of the exposed rocks therefore render this explanation for the absence of sheeted dykes equivocal.

The absence of ultramafic rocks in the BGB volcanics suggests that only the top portion of the oceanic crust was accreted and incorporated into the imbricated prism during underplating. Such incomplete sequences are known to occur in obducted ocean crust (Condie, 1983) and have been documented in Papua New Guinea (Lewis, 1983). The thickness of the volcanic belts seen in Beardmore-Geraldton area is variable along their length and less than the average thickness of most obducted oceanic crust (the former is <5 km and the latter is approximately 8 km, Condie, 1983). In addition, the <5 km thickness of the volcanic units in the BGB includes

post-imbrication intrusion of mafic dikes. Accretion of an incomplete sequence of oceanic crust into the BGB imbricate structure is therefore another possible explanation for this less-than-ideal ophiolite stratigraphy.

If the above geochemical interpretation of the tectonic setting for the BGB is valid, a probable tectonic setting would be similar to that shown in Figure 6.1 This tectonic setting is also in agreement with the lithostratigraphic and structural studies carried out by other workers for the same study area.

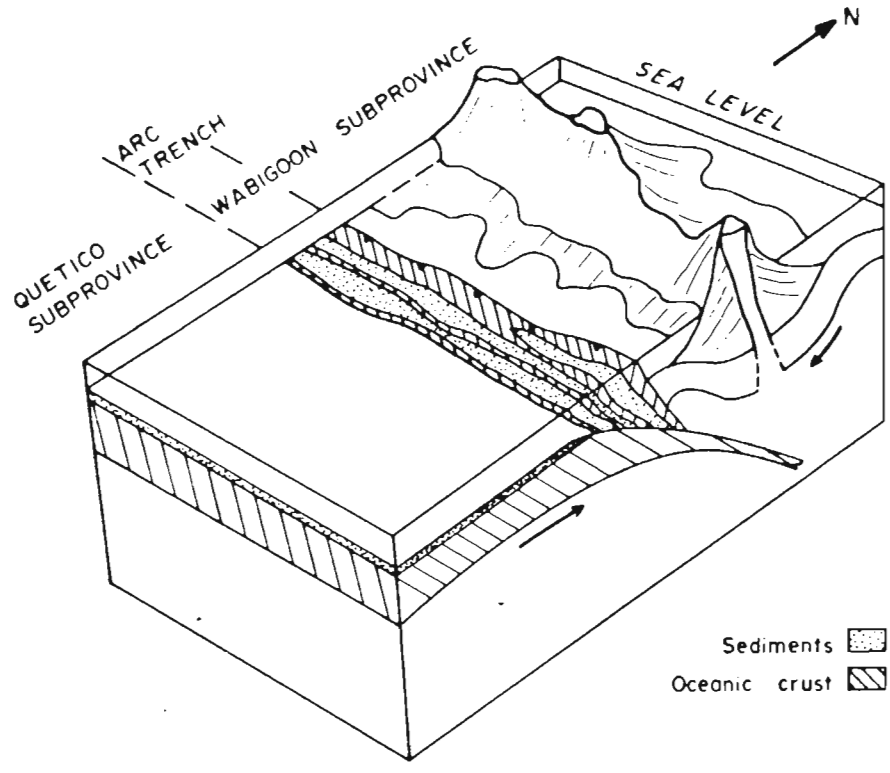

Figure 6.1: A schematic diagram showing the hypothetical plate tectonic configuration between the Wabigoon metavolcanic subprovince and the Quetico metasedimentary subprovince. The convergent plate suture zone is defined by the present linear Beardmore-Geraldton Belt.

CHAPTER 7

PETROGENETIC MODELLING

7.1 BASICS OF PARTIAL MELTING

The equation (7.1) employed to model the melting process is that of Shaw (1970), where the liquid phase remains in equilibrium with the residual solid phases until removal.

7.1] $C_L / C_O = 1 / D_O + F (1 - P)$

where: F is the fraction of melting,

C_O is the initial trace element concentration of the solid/source and

C_L is the trace element concentration of the liquid.

D_O is the bulk distribution coefficient for the starting mineral assemblage and is defined by :-

7.2] $D_O = Xo^a K^{a/L} + Xo^b K^{b/L} + \ldots\ldots Xo^n K^{n/L}$

where: Xo^a is the initial weight fraction of the phase "a" and

$K^{a/L}$ is the solid - liquid distribution coefficient for phase "a".

P is given by :-

7.3] $P = p^a K^{a/L} + p^b K^{b/L} + \ldots\ldots p^n K^{n/L}$

where: $p^a, p^b \ldots\ldots p^n$ are the fractions of liquid contributed by each of the phases observed in the source during melting.

This simplistic theoretical model assumes that the trace elements involved in the modelling are dilute and abide by Henry's law, where the activity of a solute component (ai) is considered to be proportional to its mole fraction (xi), given by the expression:-

7.4] $ai = kh\ xi,$

where; kh is the Henry's law constant, its value being derived from experimental work.

The use of Henry's law also assumes equlibrium conditions. Another assumption is that partition coefficient values remain constant throughout the course of melting. The applicability of equilibrium partial melting to

natural process has been examined by Hart and Allegre (1980) and Haskin (1984). Taking kinetic arguments into consideration, these workers conclude that equilibrium melting is a more likely process than non-equlibrium melting.

Crystal fractionation modelling was employed in the second part of the petrogenetic study to test for a genetic link between samples from the suite. The modelling was carried out using the Rayleigh equation (7.5) for equilibrium fractional crystallisation, given by the expression:-

7.5] $C_L / C_i = F^{(Ds-1)}$

where: F is the fraction of liquid remaining,

C_i is the concentration of the original melt,

C_L is the concentration in the differentiated liquid and

Ds is the bulk distribution coefficient given by:-

$$Ds = W^aK^{a/L} + W^bK^{b/L} + ... W^nK^{n/L}$$

where: K is the solid-liquid partition coefficient and

W^a represents the weight fraction of a in the crystallising phases.

This method of crystal fractionation modelling assumes that the mineral phases involved maintain constant proportions throughout crystallisation and the distribution coefficient for an individual element remains constant. Though this model is simplistic compared to actual geological situations, it is used here as a means to evaluate the possible relationships that exist within the rock suite.

In this chapter, an attempt is made to model the least evolved basalt reported in the study area (Group I basalts), sample PW105, by equlibrium batch partial melting. Similar treatment is also employed for the Group II basalts. Primary magma with REE abundance similar to that of sample PW105 is then differentiated by fractional crystallisation in an attempt to explain the evolution of the more evolved basalts within the Group I rock suite. This treatment is in accordance to the concept developed by Bowen (1928); O'Hara and Yoder (1967) and Green and Ringwood (1967), that is,

evolved basalts are an end product of polybaric crystal fractionation, as reviewed by Wyllie (1980). Samples PW107 and PW109B were chosen for this part of the modelling because they are in close spatial lithostratigraphic position with each other.

7.2 SOURCE COMPOSITION

The concentrations of the REE recorded in a sample is a reflection of i) the source concentration of these elements; ii) the extent through which chemical fractionation occurs during melt separation and iii) the degree of chemical fractionation that has occurred during magma ascent. There is insufficent data and/or a lack of a general consensus on the exact composition of the Archaean mantle, therefore the source composition is speculative. The REE pattern for the BGB Group I basalts are similar to those reported for modern day mid-oceanic ridge basalts (Basaltic Volcanism Project, 1981). This suggests that the late Archaean mantle may have had a similar REE composition to that of the Cenozoic mantle.

The nature of the upper mantle, from which most basaltic materials are believed to have originated, can be deduced from geophysics, mantle xenoliths within basaltic flows and from obducted oceanic crust. In the latter, a continuum of rock types ranging from dunite to lherzolite is possible. In order to deduce a probable source for the BGB basalts, material of upper mantle composition is needed. It is considered here, from the discussion in Chapter 5, that the BGB basalts modelled are of oceanic affinity. In this study, a spinel lherzolite (R717) from Ronda, Spain was used as a source. The source employed in this study was also documented by Frey et al. (1985) to be a possible source for the mid-oceanic ridge basalts (MORB). Kushiro (1972), based on major element chemistry, has shown that partial melting of spinel lherzolite, at temperatures between 1340-1460^{o}C and at pressure of 10 kbar (30 km), yield tholeiitic basalts similar to those of mid-oceanic ridges. Similar

pressure and temperature results were also suggested in the Basaltic Volcanism Study Project (1981) and by Takahashi and Kushiro (1983). It should be noted that these pressure and temperature values are for modern oceanic basalts. In the Archaean, the depth of partial melting may be shallower (Abbott and Hoffman, 1984).

The spinel lherzolite used here is slightly serpentinised (<10%), however, the chemistry was considered to be essentially similar to those of the unaltered samples (Frey et al. 1985). The spinel lherzolite is recalculated on a spinel free basis. Such treatment was considered by Schilling (1971) to have little influence on the conclusion derived from the modelling, since the abundance of spinel is often less than a few percent. The recalculated mineralogical modal abundance of this peridotite is 54% olivine, 32% orthopyroxene and 14% clinopyroxene. The REE composition of the source is given by Frey et al. (1985). The elements Sm, Gd, and Er were not reported by these authors and interpolated values are used.

7.3 THOLEIITIC BASALT (Group I)

Results of batch melting for a representative sample is shown in Figure 7.1. The modelled melt gives a REE profile that is complementary to the least evolved BGB basalts and is, at best, a first approximation since most melts undergo some form of crystal fractionation during the course of magma ascent. The result shown is obtained for 20% non-modal melting of the spinel lherzolite source (R717). At this degree of melting, all the clinopyroxene has been used up leaving behind a harzburgite residue consisting of 66.25% olivine and 33.75% orthopyroxene. The disappearance of clinopyroxene at 20% partial melting is in agreement with observation based on experimental work on natural peridotite Green (1972) and Wyllie (1979). The percentage of partial melting is in agreement with that documented by Schilling (1975) for the genesis of tholeiitic oceanic basalts by melting of a lherzolite source. The conclusions to be drawn here are: i)

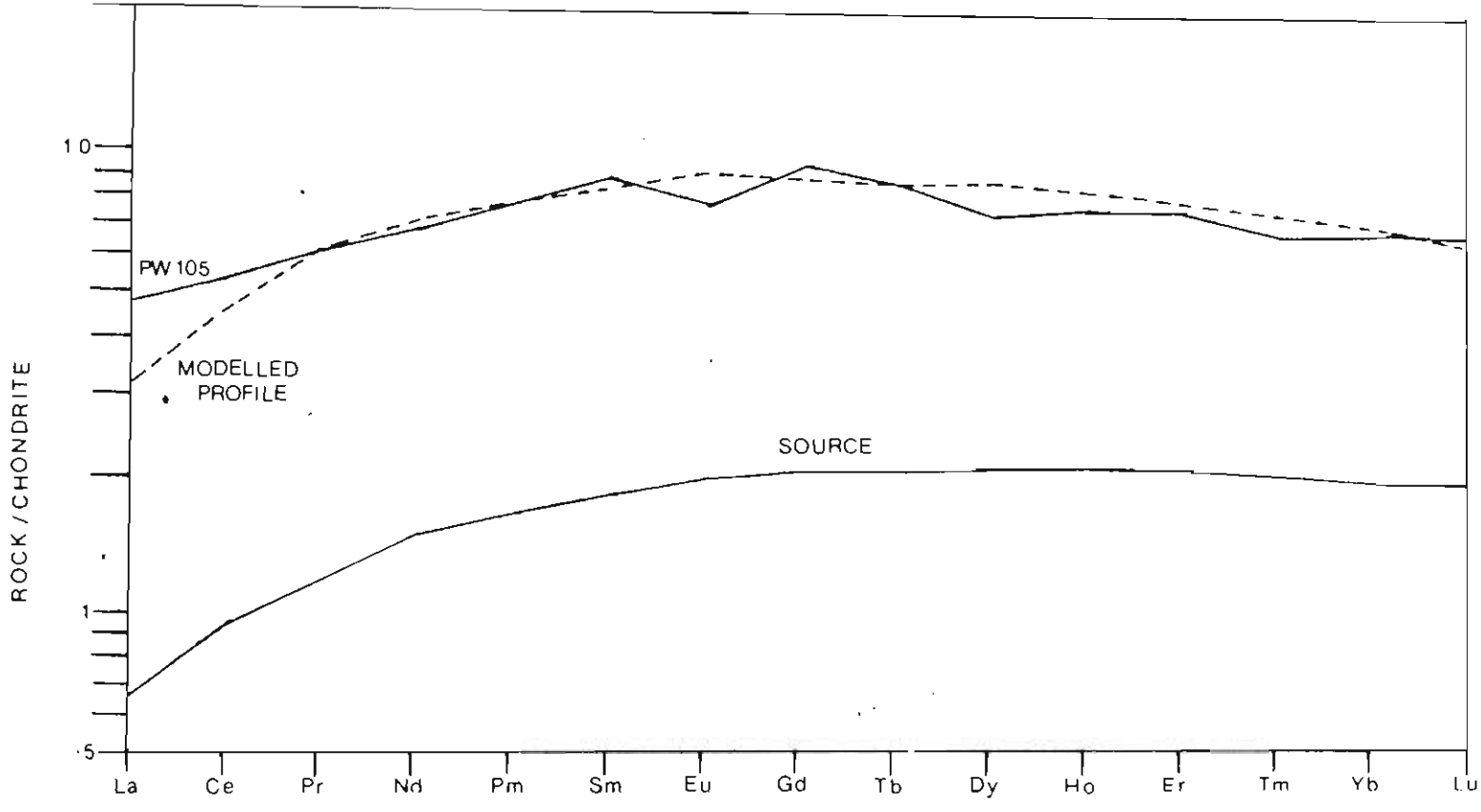

Figure 7.1: Chondrite-normalised rare-earth plot depicting rare-earth content of tholeiitic basalts predicted by equilibrium non-modal partial melting equation of Shaw(1970). Partition coefficients for all basaltic liquids are from Arth (1977). Mineral percentages of the source (spinel lherzolite), recalculated on spinel free basis are 54% olivine, 32% orthopyroxene and 14% clinopyroxene. After 20% melting, all clinopyroxene has disappeared, leaving a residue of 66.25% olivine and 33.75% orthopyroxene. Profile being modelled is that of the least evolved basalt (PW105) in the study.

the source to the BGB basalts was depleted in incompatible elements (LREE) and, ii) the source for the BGB basalts is similar to that which give rise to ocean floor basalts, as shown by Frey et al. (1985).

The depleted nature of the source for ocean floor basalts has been postulated by Gast (1968), Schilling (1971; 1975) and the Basaltic Volcanism Study Project (1981) and the availability of a depleted mantle in the late Archaean has been suggested by Sun and Nesbitt (1978). The depletion of incompatible elements of the source could be achieved through prior, previous low degrees of melting of a source with a 2X chondritic, unfractionated REE distribution; assuming that the primitive source has a flat chondrite profile. Such early melting could have occurred during initial rifting of oceanic plate.

7.4 CRYSTAL FRACTIONATION

Results of crystal fractionation modelling are shown in Figure 7.2. The modelling results suggest that samples, PW105 and PW107, can be related to each other by 40% fractionation of 0.1% olivine, 82.1% clinopyroxene and 17.8% plagioclase. Similar proportions of clinopyroxene and plagioclase have been documented by Arndt and Jenner (1986) for the Kambalda basalts, Western Australia. This extracted modal proportion of mineral phases is in accordance with the least square mixing modelling for the major elements (Table 4). One should point out that this modelling is a first approximation since least square modelling makes use of LILE and trace elements which are usually documented to be mobile. The attempt to model sample PW109B using the same treatment has proven unsuccessful. This failure is attributed to the possibility that PW109B samples a separate flow, that may have been brought together by tectonic juxtaposition. The 3 samples examined are separated from each other by covered intervals and do not necessarily sample a single flow. The model

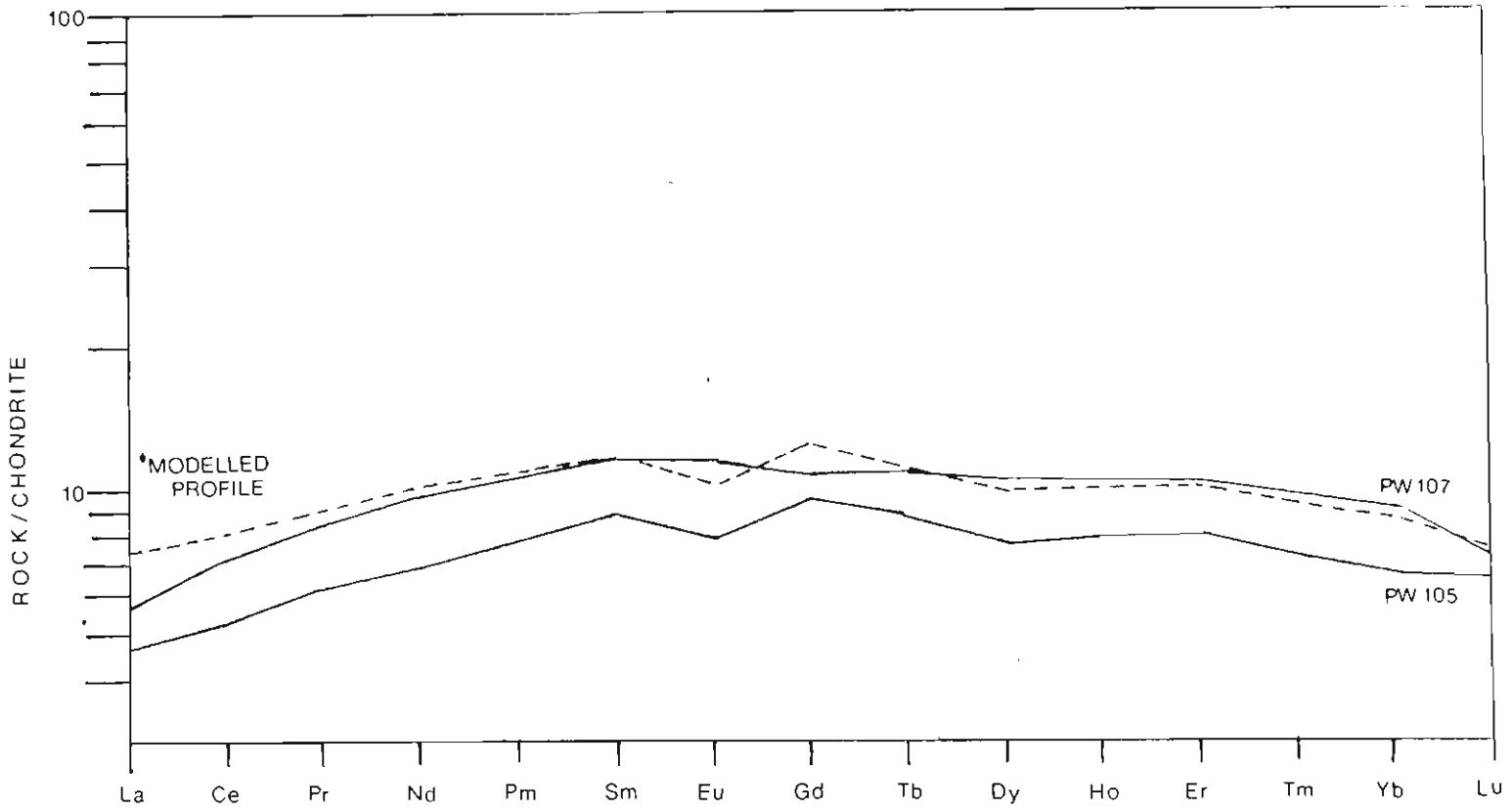

Figure 7.2: Chondrite normalised profile illustrating rare-earth element content of evolved tholeiites predicted by a model for 40% fractional crystallisation of the least evolved basalt (PW105). Equation used was that of Rayleigh for crystallisation of phases in constant proportions with constant Kd values.

Table 4: Fractional crystallisation model: Results of least-squares petrographic calculation.

	PW107	Plag.	Ol.	Cpx.	Obs.	PW 105 Cal.	Diff.
SiO2	53.46	51.40	40.50	52.80	50.46	53.12	-1.06
TiO2	00.88	00.61	00.00	00.61	00.70	00.76	-0.06
Al2O3	14.01	29.50	00.00	2.61	14.03	11.79	1.12
FeO	10.46	00.45	10.70	5.42	9.47	8.49	0.98
MnO	00.22	00.00	00.15	0.18	0.20	0.19	0.00
MgO	6.94	00.25	49.10	16.90	9.41	9.28	0.13
CaO	10.48	13.90	00.47	20.30	14.03	13.36	0.68
Na2O	3.23	4.38	00.00	00.27	1.43	2.48	-1.05
K2O	00.23	00.01	00.00	00.00	00.21	00.15	0.05
P2O5	00.07	00.00	00.00	00.00	00.05	00.05	0.00
SOLUTION:		17.8%	.1%	82.1%			

Hypothetical phenocryst phases composition is from Frey et al. 1974.

employed here suggests that some of these basaltic rocks can be related to each other by fractionation of major rock forming mineral phases.

7.5 CALC-ALKALINE BASALTS (Group II)

Calc-alkaline basalts (CAB) are usually found in island arcs and continental margin settings (Miyashiro, 1973; Best, 1982). Petrogenetic models proposed for the genesis of CAB are variable and include i) fractional crystallisation of basaltic magma involving garnet and amphibole (Hawkesworth and O'Nions, 1977); ii) contamination of basaltic magma by sialic crust (Tilley, 1950); iii) mixing of melts contributed by the hydrated mantle wedge, sediments and subducted slab (Fyfe, 1982; Ellam et al. 1988); iv) magma mixing between melts derived from the mantle wedge and the subducted slab (Green and Ringwood 1968; Jakes and White 1972). Current knowledge based on experimental work and geochemical results, including isotopic data, show that all of the above models can be evoked to explain the chemistry of the CAB (Boettcher, 1973; Condie, 1982). Isotopic data (Sr, Nd and Pb) have been used as evidence for contamination (Hawkesworth 1982; Ellam et al. 1988). Current trends appear to favour the derivation of modern CAB melts by the mixing of three components, that is, the melt derived from metasomatised mantle wedge, the crustal component introduced during the course of melt ascent, and the melt derived from the subducted slab, including the subducted sediment. The number of components involved and their contribution, however, could be constrained by the type of tectonic setting. For example, in immature ocean island arcs, both crustal and sediment contribution are limited as compared to continental margin.

From the above discussion and from the hypothesis postulated in Chapter 5, that the, CAB represent post accretionary intrusions emplaced an along existing fault system in the wedge complex, an attempt is made here to model the origin of the BGB CAB by partial melting of the

subducted slab. It is assumed that the geothermal gradient in the Archaean is higher than present to cause the subducted slab to melt (Ghomshei et al., 1988) and that underplating (<130 km) rather than subduction is the likely mechanism for plate consumption (Burke et al., 1976). The higher geothermal gradient in the Archaean also implies the downgoing plate is slightly warmer, buoyant and younger than present day subducting plate material, a prerequisite derived from geophysical modelling (Sacks, 1983). Note that the lack of basalt-eclogite transformation in the Archaean due to high thermal gradient also supports an underplating mechanism rather than a subduction mechanism. If the latter assumption is indeed valid, it also places a limit on the contribution of the mantle wedge in the formation of the ancient CAB. Other assumptions made include the limited contribution by crustal contamination and sediment contribution. The latter assumption is not likely to be valid since sedimentary packages are found in association with the volcanic rocks in the study area and is suggested by Ce anomaly, Figure 4.24. However, these assumptions are necessary to test the validity of the hypothesis proposed in Chapter 5. Furthermore, the role of crustal and sediment contribution are difficult to assess and quantify due to the mobility of elements which indicate crustal involvement (e.g Sr, Ba and Rb) and to the absence of isotopic data for Pb, Sr, and Nd.

Figure 7.3 depicts the results of REE modelling using equation 7.1 (Shaw's (1970) batch equilibrium melting). The source composition used, sample OX101 is interpreted to represent typical subducted material, assuming that the REE remain immobile during the course of phase transformation (Green et al. 1972 and Jahn et al. 1987). During the course of underplating, the oceanic slab is transformed to amphibolite facies consisting of equal proportion of plagioclase and amphibole. Ten per cent non modal melting of this amphibolitized slab yields a complementary REE pattern to that for the observed CAB in the study area. The introduction of

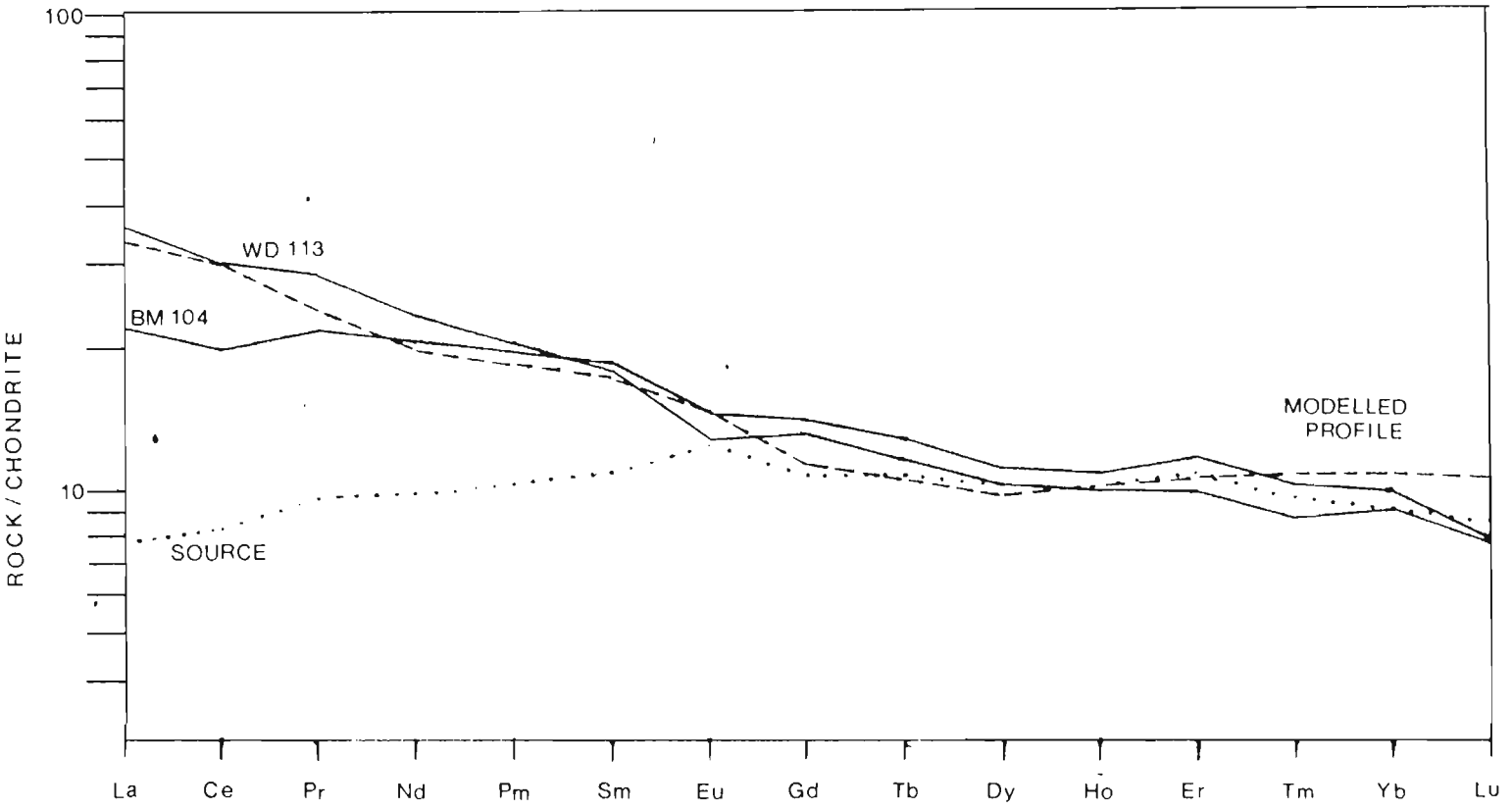

Figure 7.3: Chondrite normalised rare-earth plot showing rare-earth content of calc-alkaline basalt predicted by non-modal partial melting equation of Shaw (1970). Mineral percentage of the source is 50% amphibole and 50% plagioclase. Sample being modelled after is that of Group II basalts designated as calc-alkaline by Ti/100-Zr-Y(3) diagram.

garnet (at greater depth) in the source mineral assemblage has also been tested. The REE pattern produced from this parent yields a highly fractionated HREE pattern which does not fit the profile of the observed samples. This lack of garnet involvement is consistent with the situation hypothesized by Abbott and Hoffman (1984) and Ghomshei et al. (1988) where underplating (<100 km) is likely to prevail in the Archaean. The feasibility of deriving an intermediate melt by partial melting of an amphibolitised, subducted slab has been documented by Wyllie (1983) based on experimental constraint, but this requires the subducting plate to be warmer than modern day analogues. Similar degree of partial melting of amphibolite mineralogies has also been suggested as a process capable of explaining the major and trace element composition of some of Archaean volcanics of intermediate composition (Condie and Harrison, 1976). The conclusion to be drawn is that the CAB observed in the BGB can be modelled by partial melting of an amphibolitized underplated oceanic slab at 1000-1045 ^{o} C represented by the BGB MORB type samples (Abbott and Hoffman 1984).

CHAPTER 8
SUMMARY

8.1 THE DEVELOPMENTAL HISTORY OF BGB

From the above study, the evolution of the Beardmore-Geraldton Belt is as follows:

i) Partial melting of a depleted mantle peridotite to yield parental magma subsequently emplaced in an oceanic ridge setting.

ii) Translocation of oceanic crust to the consuming plate margin where fragments of the oceanic crust are accreted and imbricated with the sediments that flank the arc margin.

iii) Decoupling of oceanic crust at the consuming plate margin leads to underplating of part of the overlying crust, which eventually results in the transformation of oceanic rocks to amphibolitized rocks.

iv) Subsequent partial melting of the amphibolitized rocks to give rise to the formation of calc-alkaline magma which migrates upwards into the overlying accreted material along pre-existing parallel to subparallel fault zones.

v) The imbricated complex, consisting of both volcanics and sediments, is exhumed and eroded to the present exposure level. The exact timing of the metamorphic events affecting the BGB could not be ascertained in this study, however, Card (1986) has suggested that the major deformation, metamorphism and plutonism in the Wabigoon subprovine occurred between 2.7 to 2.66 Ga, as indicated by U-Pb zircon dating.

8.2 FURTHER WORK

The following work is suggested in order to better understand the developmental history of the BGB volcanic rocks:

i) Geochronological work to establish the relationship between the fine-grained flows and coarse-grained gabbroic rocks.

ii) Microprobe analysis of mineral phases, especially the amphiboles, to establish the pressure and temperature of metamorphism that the rock have been subjected to.

iii) Further refinement on the petrogenetic modelling. This can be achieved through isotopic work on Sr, Pb, Nd. Rocks derived from a common source should possess identical isotopic ratios (eg. $^{87}Sr/^{86}Sr$). Sr isotopes used in conjunction with Nd isotopes should provide further insight to the source(s) for Group I and Group II basalts documented in the study area.

iv) More field work to acquire a better distribution of samples from the 3 volcanic belts.

8.3 CLOSING REMARKS

It should be noted that the above proposed scenerio may change through time as our understanding on Archaean geology develops. The gathering of knowledge on Archaean geology is often marred by not only field geology, but also on the lack petrological experiments under conditions postulated for Archaean settings. In addition to this, the geochemical aspects of the Archaean rocks are complicated by post emplacement affects such as metamorphism. Insufficient outrcrops and inaccessibility also tend to hinder the progress in data base acquisition.

REFERENCES

REFERENCES

ABBOTT, D.H. and HOFFMAN, S.E., 1984. Archaean plate tectonic revisited1: Heat flow, spreading rate and the age of subducting oceanic lithosphere and their effects on the origin and evolution of continents. Tectonics, v3, (4), pp.429-448

ALDERTON, D.M., PEARCE, J.A. and POTTS, P.J., 1980. Rare earth elements mobility during granite alteration: Evidence from southwest England. Earth Planetary Science Letters, v49, pp.149-165

AMUKUN, S.E., 1980. Geology of the Conglomerate Lake area, District of Thunder Bay. Ontario Geological Survey Report 197, 101p

ANDERSON, A.T. and GREENLAND, L.P., 1969. Posphorous fractionation diagram as a quantitative indicator of crystallisation differentiation of basaltic liquids. Geochimica et Cosmochimica Acta, v33, pp.493-505

ANGLIN, C.D. and FRANKLIN, J.M., 1985. Gold mineralisation in the Beardmore-Geraldton area of northwestern Ontario: Structural considerations and the role of iron formations; in current research, Part A. Geological Survey of Canada, Paper 85-1A, pp.193-201

APTED, M.J. and LIOU, J.G., 1983. Phase relations among greenschist, epidote-amphibolite, and amphibolite in a basaltic system. American Journal of Science, v283-A, pp.328-354

ARCULUS, R.J., 1987. The significance of source versus process in the tectonic controls of magma genesis. Journal of Volcanology and Geothermal Research, v32, pp.1-12

ARNDT, N.T. and JENNER, G.A., 1986. Crustally contaminated komatiites and basalts from Kambalda, Western Australia. Chemical Geology, v56, pp.229-255

ARTH, J., 1976. Behaviour of trace elements during magmatic processes- a summary of theoretical models and their applications. Journal Research U.S. Geological Survey, v4, pp.41-47

AYRES, L.D., 1969. Early Precambrian stratigraphy of part of the Lake Superior provincial park, Ontario, Canada, and its implications for the origin of the Superior province; Unpublished Ph.D. Thesis, University of Princeton, 399p.

BARAGAR, W.R.A., 1966. Geochemistry of the Yellowknife volcanic rocks, Canadian Journal of Earth Sciences, v3, p9-30.

BARRETT, T.J. and FRALICK, P.W., 1985. Sediment redeposition in Archaean iron formation: Examples from the Beardmore-Geraldton greenstone belt, Ontario. Journal of Sedimentary Petrology, v55, pp.205-212.

BASALTIC VOLCANISM STUDY PROJECT, 1981. Basaltic volcanism on the terrestrial planets. Pergamon Press, Inc., New York,1286p.

BATEMAN, R., 1984. On the role of diapirism in the segregation, ascent and final emplacement of granitoid magmas. Tectonophysics, v110, pp.211-231

BEACH, A., 1980. Retrogressive metamorphic process in shear zones with special reference to the Lewisian complex. Journal of Structural Geology, v2, pp.257-263

BECCALUVA, L., PICCARDO, G.B. AND SERRI, G., 1979. Petrology of northern Apennine ophiolites and comparison with other Tethyan ophiolites. Ofioliti, v4, pp.43-66

BEST, M.G., 1982. Igneous and metamorphic petrology. W.H. Freeman and Company, 630p

BESWICK, A.E. and SOUCIE, G., 1978. A correction procedure for metasomatism in an Archean greenstone belt. Precambrian Research, v.6, pp.235-248

BICKLE, M.J., 1978. Heat loss from the Earth: Constraint on the Archean tectonics from the relationships between geothermal gradients and the rate of plate production. Earth and Planetary Science Letters, v40, pp301-315

BICKLE, M.J., BETTENAY, L.F., BOULTER, C.A., GROVES, D.I. and MORANT, P., 1980. Horizontal tectonic interaction of an Archean gneiss belt and greenstones, Pilbara block, Western Australia. Geology, v8, pp.525-529

BLACKBURN, C.E., 1980. Towards a mobilist tectonic model for part of the Archean of Northwestern Ontario. Geoscience Canada, pp.64-72

BOETTCHER, A.L., 1972. The origin of andesites. Tectonophysics, v17, pp. 223-240

BOWEN, N.L., 1928. The evolution of the igneous rocks, Princeton University Press, Princeton, 332p.

BRODIE, K.H. and RUTTER, E.H., 1985. Deformation and metamorphism of basic rocks. In: A.B. Thompson and D.C. Rubie (Eds), Metamorphic

Reactions-Kinetics, Textures and Deformation. Springer-Verlag, New York, pp. 138-180

BRUCE, E.L., 1936. The eastern part of the Sturgeon River area; Ontario Department of Mines, v45, part 2, pp.1-59

BUCK, S., 1986. Structural studies and gabbro mylonitisation within the Barton Bay deformation zone, Geraldton, Ontario; Unpublished M.Sc. Thesis, Brock University, Ontario, 172p

BUCK, S. AND WILLIAMS, H.R., 1984. Structural studies in the Geraldton area; pp208-212. In: Summary of Fieldwork, 1984, Ontario Geological Survey, edited by J. Wood, O.L. White, R.B. Barlow, and A.C. Colvine, Ontario Geological Survey, Miscellaneous Paper 119, 309p.

BURKE, K., DEWEY, J.F. and KIDD, W.S.F., 1976. Dominance of horizontal movements, arc and microcontinental collisions during the later permobile regime. In: B.F. Windley (Ed), The Early History of the Earth. John Wiley and Sons, New York, pp.113-130

CARD, K.D., 1986. Tectonic setting and evolution of late Archaean greenstone belts of Superior province, Canada. In: Workshop on the tectonic evolution of greenstone belt, compiled by: Lunar and Planetary Institute, Lunar Planetary Institute Contribution 584, supplement, Houston, Texas, pp15-19

CARTER, M.W., 1983. McComber and Vincent Townships, District of Thunder Bay; p32-36 In: Wood, J., White, O.L., Barlow, R.B., and Colvine, A.C. editors: Summary of fieldwork, 1983, by the Ontario Geological Survey; Onatario Geological Survey Miscellaneous Paper116, 313p.

COISH, R.A. and ROGERS, N.W., 1987. Geochemistry of the Boil Mountain ophiolite complex, northwest Maine, and tectonic implications. Contribution to Mineralogy and Petrology, v97, pp.51-65

COMREY, 1973. A first course in factor analysis. Academy Press, New York. 316p.

CONDIE, K.C., 1976. Plate tectonics and crustal evolution. Pergamon Press, Table 7.3.

CONDIE, K.C., 1980. Geochemical and isotopic constraints on the origin and source of Archaean granites. In: J.E. Glover and D.I. Groves (Eds.), Archaean Geology. Special Publication Geological Society of Australia, no.7, pp.469-479

CONDIE, K. C., 1981. Origin and evolution of Archean granite-greenstone terranes. In: Archean Greenstones Belts. Elsevier, Amsterdam, pp313-425

CONDIE, K.C., 1982. Archaean Andesites. In: Andesites, R.S. Thorpe (Ed.), John Wiley and Sons, New York, pp.575-590

CONDIE, K.C., 1983. Plate Tectonics and Crustal Evolution, 2nd Edition, Pergamon Press, 310p.

CONDIE, K.C. and BARAGAR, W.R.A., 1974. Rare earth element distribution in volcanic rocks from Archean greenstone belts. Contribution to Mineralogy and Petrology, v45, pp.237-246

CONDIE, K.C. and HARRISON, N.M., 1976. Geochemistry of the Archaean Bulawayan Group midland greenstone belt, Rhodesia. Precambrian Research, v3, pp.253-271.

COOPER, A.F., 1972. Metamorphism of metabasic rocks. Journal of Petrology, v13 , pp457-492

COOPER, A.F. and LOVERING, J.F., 1970. Greenschist amphiboles from Haast River, New Zealand. Contribution to Mineralogyand Petrology, v27, pp.11-24

COX, K.G., BELL, J.D. and PANKHURST, R.J., 1984. The Interpretation of Igneous Rocks. Publishers: George Allen and Unwin, 450p.

CRAIG, R.R. and VAUGHAN, D.J., 1981. Ore microscopy and ore petrography. John Wiley and Sons, New York. 406p.

DAVIS, J.C., 1986. Statistics and data analysis in geology, 2nd Edition. John Wiley and Sons, New York, 646p.

DAVIS, D.W., CORFU, F. and KROGH, T.E., 1986. High precision U-Pb geochronology and implications for the tectonic evolution of the Superior province. In: Workshop on the tectonic evolution of greenstone belt, compiled by Lunar and Planetary Institute, Lunar and Planetary Institute Contribution 584, supplement, Houston, Texas, pp.20-23

DEER, W.A. HOWIE, R.A. and ZUSSMAN, J., 1982. An introduction to the rock forming minerals. Longman, England, 528p.

DEVANEY, J.R., 1987. Sedimentology and stratigraphy of the northern and central metasedimentary belts in the Beardmore-Geraldton area of northern Ontario. Unpublished M.Sc. Thesis, Lakehead University, Ontario, 227p.

DEVANEY, J.R. and FRALICK, P.W., 1985. Regional sedimentology of the Namewaminikan Group, Northern Ontario: Archaean fluvial fans, braided rivers, deltas and an aquabasin; pp.125-132, In: Current Research, Part B, Geological Survey of Canada, Paper 85-1B.

DEVANEY, J.R. AND WILLIAMS, H.R. 1988. Evolution of an Archean subprovince boundary: A sedimentological and structural study of part of the Wabigoon-Quetico boundary in northern Ontario. (In preparation)

DICKINSON, W.R. and SEELY, D.R., 1979. Structure and stratigraphy of forearc region. The American Association of Petroleum Geologists Bulletin, v63, pp2-31

ECHEVERRIA, L.M., 1980. Oceanic basaltic magmas in accretionary prisms: The Franciscan intrusive gabbros. American Journal of Science, v.280, pp.697-724.

EHLERS, E.G. and BLATT, H., 1982. Petrology: Igneous, Sedimentary and Metamorphic. W.H. Freeman and Company. 732p.

ELLAM, R.M. and HAWKESWORTH, C.J., 1988. Elemental and isotopic variations in subduction related basalts: evidence for a three component model. Contribution to Mineralogy and Petrology, v98, pp.72-80

ENGLAND, P.C., and RICHARDSON, S.W., 1977. The influence of erosion upon the mineral facies of rocks from different metamorphic environments. Journal Geological Society of London, v134, pp.201-213

ERNST, W.G., 1971. Metamorphism zonation on presumably subducted lithospheric plates from Japan, California and the Alps. Contribution to Mineralogy and Petrology, v34, pp.43-59

ETHRIDGE, F.G. and WESTCOTT, W.A., 1984. Tectonic setting, recognition and hydrocarbon reservoir potential of fan-delta deposits. In: Koster, E.H. and Steel, R.J. (Eds.). The sedimentology of gravels and conglomerates. Canadian Society of Petroleum Geologists, Memoir10.

ETHERIDGE, M.A., WALL, V.J. and VERNON, R.H., 1983. The role of the fluid phase during regional metamorphism and deformation. Journal of Metamorphic Geology, v1, pp.205-226

EXLEY, R.A., 1980. Microprobe studies of REE rich accessory minerals: implications for Skye Granite petrogenesis and REE mobility in hydrothermal systems. Earth and Planetary Science Letters, v48, pp.97-110

FAWCETT, J.J. and YODER, H.S., 1966. Phase relations of chlorites in the system $MgO-Al_2O_3-SiO_2-H_2O$. American Mineralogist, v.51, pp.353-383

FLOYD, P.A. and WINCHESTER, J.A., 1975. Magma type and tectonic setting discrimination using immobile elements. Earth Planetary Science Letters, v27, pp.211-218

FLOYD, P.A. and WINCHESTER, J.A., 1976. Geochemical magma type discrimination: Application to altered and metamorphosed basic igneous rocks. Earth Planetary Science Letters, v28, pp.459-469

FRALICK, P.W. and BARRETT, T.J., 1983. The sedimentology of banded iron formation in the Beardmore-Geraldton area: A preliminary appraisal; in Summary of field work, 1983, Ontario Geological Survey, Miscellaneous Paper 116, pp.201-203

FREY, F.A., BRYAN, W.B. and THOMPSON, G., 1974. Atlantic ocean floor: Geochemistry and petrology of basalts from Legs 2 and 3 of the deep-sea drilling project. Journal of Geophysical Research, v79, pp.5507-5526

FREY, F.A., SUEN, C.J. and STOCKMAN, H.W., 1985. The Ronda high temperature peridotite: geochemistry and petrogenesis. Geochemica et Cosmochemica Acta, v49, pp.2469-2491

FURNES, H., THON, A., NORDAS, J. and GARMANN, L.B., 1982. Geochemistry of Caledonian metabasalts from some Norwegian ophiolite fragments. Contribution to Mineralogy and Petrology, v79, pp.295-307

FYFE, W.S., 1978. The evolution of the Earth's crust: modern plate tectonics to ancient hot spot tectonics. Chemical Geology, v23, pp.89-144

FYFE, W.S., 1982. Andesite-product of geosphere mixing. In: Andesite, R.S. Thorpe (Ed.), John Wiley and Sons, New York, pp.663-667

GASS, I.G. ,1972. Proposal cocerning the variation of volcanic products and processes within the oceanic environment. Philosophical Transaction of the Royal Society of London, A.271, pp.131-140

GASS, I.G., 1980. The Troodos Massif: its role in the unravelling of the ophiolite problem and its significance in the understanding of constructive plate margin process. In: Panayiotou, A. (Ed.) Ophiolites, Proceeding International Ophiolite Symposium Cyprus, pp.23-35

GAST, P.W., 1968. Trace element fractionation and the origin of tholeiitic and alkaline magma types. Geochimica et Cosmochimica Acta, v32, pp.1057-1086

GELINAS, L., BROOKS, C. and TRZCIENSKI, W.E. Jr., 1976. Archean variolites quenched immiscible liquids. Canadian Journal of Earth Sciences, v13, pp.210-230

GHOMSHEI, M.M., ARKANI-HAMED, J., STRANGWAY, D.W. and RUSSELL, R.D., 1988. Underplating and hydrous fusion of the overlying lithosphere: A possible source of Archaean komatiites. (In preparation).

GIBSON, I.L., ROBERTS, R.G. and GIBBS, A.D., 1986. An extensional fault model for the early development of greenstone belts with reference to a portion of the Abitibi belt, Ontario, Canada. Earth and Planetary Science Letters, v79, pp.159-167

GILL, J., 1981. Orogenic andesites and plate tectonics. Springer-Verlag, New York. 390p.

GOODWIN, A.M. and SMITH, I.E.M., 1980. Chemical discontinuities in Archean metavolcanic terrains and the development of Archean crust. Precambrian Research, v10, pp.301-311

GORMAN, B.E., PEARCE, T.H. and BIRKETT, T.C., 1978. On the structure of Archean greenstone belts. Precambrian Research, v6, pp.23-41

GRAHAM, C.M., 1974. Metabasite amphiboles of the Scottish Dalradian. Contribution to Mineralogy and Petrology, v47, pp.165-185

GRAPES, R.H., 1975. Actinolite-Hornblende pairs in metamorphosed gabbros, Hidaka Mountains, Hokkaido. Contribution to Mineralogy and Petrology, v49, pp.125-140

GRAPES, R.H. and GRAHAM, C.M., 1978. The actinolite-hornblende series in metabasites and the so-called miscibility gap: A review. Lithos, v11, pp.85-97

GREEN, D.H., 1971. Experimental melting studies on a model upper mantle composition at high pressure under water saturated and water undersaturated conditions. Earth Planetary Science Letters, v19, pp.37-53

GREEN, D.H., 1972. Magmatic activity as the major process in the chemical evolution of the earth's crust and mantle. Tectonophysics, v13, pp.47-71

GREEN, D.H., 1975. Genesis of Archaean peridotitic magmas and constraints on Archaean geothermal gradients and tectonics. Geology, v3, pp.15-18

GREEN, D.H. and RINGWOOD, A.E., 1967. The genesis of basaltic magmas. Contribution to Mineralogy and Petrology, v18, pp.103-190

GREEN, D.H. and RINGWOOD, A.E., 1968. Genesis of calc-alkaline igneous rock suite. Contribution to Mineralogy and Petrology, v18, pp.105-162

GREEN, T.H., BRUNFELT, A.O. and HEIER, K.S., 1972. Rare earth element distribution and K/Rb ratios in granulites, mangerites and anorthosites, Lofoten-Vesteraalen, Norway. Geochemica et Cosmochemica Acta, v36, pp.241-257

HANSON, G.N., 1980. Rare earth elements in petrogenetic studies of igneous systems. Annual Review on Earth Planetary Science, pp371-406

HARGRAVES, R.B., 1976. Precambrian geologic history. Science, v193, pp363-371

HARTE, B. and GRAHAM, C.M., 1975. The graphical analysis of greenschist to amphibolite facies mineral assemblages in metabasites. Journal of Petrology, v16, pp347-370

HART, S.R., 1971. K, Rb, Cs, Sr and Ba contents and Sr isotope ratio of ocean floor basalts. Philosophical Transaction of the Royal Society of London, A268, p573

HART, S.R., ERLANK, A.J. and KABLE, E.J.D., 1974. Sea-floor basalt alteration: some chemical and Sr isotopic effects. Contribution to Mineralogy and Petrology, pp.219-230.

HART, S.R. and ALLEGRE, C.J., 1980. Trace-element constraints on magma genesis. In: Hargraves (Ed.), Physics of Magmatic Processes, Princeton University Press, pp121-159

HART, S.R., BROOKS, C. KROGH, T.E., DAVIS, G.L. and NAVA, D., 1970. Ancient and modern volcanic rocks: A trace element model. Earth and Planetary Science Letters, v10, pp.17-28

HASKIN, L.A., 1984. Petrogenetic modelling-use of rare earth elements. In: P. Henderson (Ed.), Rare Earth Element Geochemistry, Elsevier, New York, pp.115-148

HASKIN, L.A., HASKIN, M.A. and FREY, F.A., 1968. Relative and absolute terrestrial abundances of the rare earths. In: Origin and distribution of elements, L.H. Ahrens (Ed.), Oxford, Pergamon, pp.881-912.

HAWKESWORTH, C.J., 1982. Isotope characteristics of magmas erupted along destructive plate margins. In: Andesite, R.S. Thorpe (Ed.). John Wiley and Sons, New York, pp.549-571

HAWKESWORTH, C.J. and O'NIONS, R.K., 1977. The petrogenesis of some Archaean volcanic rocks from southern Africa. Journal of Petrology, v18, pp.487-520

HELLMAN, P.L., SMITH, R.E., and HENDERSON, P., 1977. REE investigation of Cliefden outcrop, New South Wales, Australia. Contribution to Mineralogy and Petrology, v65, pp.155-164

HELLMAN, P.L., SMITH, R.E. AND HENDERSON, P., 1979. The mobility of the rare earth elements: Evidence and implications from selected terrains affected by burial metamorphism. Contribution to Mineralogy and Petrology, v71, pp.23-44

HELMSTAEDT, H., PADGHAM, W.A. and BROPHY, J.A., 1986. Multiple dikes in Lower Kam Group, Yellowknife greenstone belt: Evidence for Archean sea-floor spreading?. Geology, v14, pp.562-566

HENDERSON, P., 1984. General geochemical properties and abundances of the rare earth elements. In: P. Henderson (Ed.), Rare Earth Element Geochemistry, Elsevier, New York, pp.1-29

HIETANEN, A., 1974. Amphibole pairs, epidote minerals, chlorite and plagioclase in metamorphic rocks, Northern Sierra Nevada, California. American Mineralogist, v59, pp.22-40

HOBBS, B.E., MEANS, W.D. and WILLIAMS, P.F., 1976. An outline of structural geology. John Wiley and Sons, New york, 571p.

HOLDAWAY, M.J., 1972. Thermal stability of Al-Fe Epidote as a function of fO_2 and Fe content. Contribution to Mineralogy and Petrology, v.37, pp.307-340.

HORWOOD, H.C. AND PYE, E.G., 1951. Geology of Ashmore Township; Ontario Department of Mines Annual Report, v.LX, part V, 105p.

HUMPHRIS, S.E., 1984. The mobility of the rare earth elements in the crust. In: P. Henderson (Ed.), Rare Earth Element Geochemistry, Elsevier, New York, pp.317-340.

HUMPHRIS, S.E. and THOMPSON, G., 1978. Trace element mobility during hydrothermal alteration of oceanic basalts. Geochemica et Cosmochimca Acta, v1, pp.127-136

IRVINE, T.N. and BARAGAR, W.R.A., 1971. A guide to chemical classification of the common volcanic rocks. Canadian Journal of Earth Sciences. v8, pp.523-548

JAHN, B.M., SHIH, C. and MURTHY, V.R., 1974. Trace element geochemistry of Archean rocks. Geochimica et Cosmochimica Acta, v38, pp.611-627

JAHN, B.M., AUVRAY, B., CORNICHET, J., BAI, Y.L., SHEN, Q.H., and LIU, D.Y., 1987. 3.5 Ga old amphibolites from eastern Hebei Province, China: Field occurence, petrography, Sm-Nd, isochron age and REE geochemistry. Precambrian Research, v34, pp.311-346

JAKES, P. and GILL, J., 1970. Rare earth elements and the island arc tholeiitic series. Earth Planetary Science Letters, v9, pp.17-28

JAKES, P. and MIYAKE, Y., 1984. Magma in forearcs: implication for ophiolite generation. Tectonophysics, v106, pp.349-358

JAKES, P. and WHITE, A.J.R., 1972. Major and trace element abundances in volcanic rocks of orogenic areas. Geological Society of America Bulletin, v83, pp.29-40

JENSEN, L.S., 1976. A new cation plot for classifying subalkaline volcanic rocks. Ontario Division of Mines Geological Report 66

JOLLY, W.T., 1980. Development and degradation of Archean lavas, Abitibi area, Canada, in light of major element geochemistry. Journal of Petrology, v21, pp.323-363

JOLLY, W.T. and SMITH, R.E., 1972. Degradation and metamorphic differentiation of the Keweenawan tholeiitic lavas of northern Michigan, U.S.A. Journal of Petrology, v13, pp.273-309

KARIG, D. and SHARMAN, G.F., 1975. Subduction and accretion in trenches. Geological Society of America Bulletin, v86, pp.377-389

KEAYS, R.R. AND SCOTT, R.B., 1976. Precious metals in ocean ridge basalts: implications for basalts as source rocks for gold mineralization. Economic Geology, v.71, pp.705-720

KEHLENBECK, M.M., 1983. Structural studies in the Beardmore-Geraldton area. pp.201-203. In: Summary of Fieldwork 1983, Ontario Geological Survey. Edited by: J. Wood, O.L. White, R.B. Barlow, and A.C. Colvine, Ontario Geological Survey, Miscellaneous Paper 116, 313p.

KEHLENBECK, M.M., 1986. Folds and folding in the Beardmore-Geraldton Belt. Canadian Journal of Earth Sciences, v23, pp.158-171.

KEMP, A.E.S., OLIVER, G.H.J. and BALDWIN, J.R., 1985. Low grade metamorphism and accretion tectonics: Southern Uplands Terrain, Scotland. Sedimentology, v27, pp.401-417

KERRICH, R. and FRYER, B.J., 1979. Archaean precious-metal hydrothermal systems, Downe mine, Abitibi Greenstone belt II. REE and oxygen isotope relations. Canadian Journal of Earth Sciences, v16, pp.440-458

KERRICH, R., FYFE, W.S. and ALLISON, I., 1977. Iron reduction around gold quartz veins, Yellowknife district, northwestern Canada. Economic Geology, v72, pp.657-663

KRESZ, D.U. and ZAYACHIVSKY, B., 1986. Barbara, Meader and Pifher Townships, District of Thunder Bay, p90-94, In: Summary of Fieldwork and other activities 1986, by the Ontario Geological Survey, edited by Thurston, P.C., White, O.L., Barlow, R.B., Cherry, M.E. and Colvine, A.C., Ontario Geological Survey, Miscellaneous Paper 132, 435p.

KRISHNANMURTHY, P., 1978. Implications of phase equilibria and chemical parameters for the origin of Archaean ultramafic and mafic lavas. In: B.F. Windley and S.M. Naqvi (Eds.), Archaean Geochemistry, Elsevier, Amsterdam, pp.305-325

KRONER, A.I., 1981. Precambrian plate tectonics. In: A. Kroner (Ed.), Precambrian Plate Tectonics, Elsevier, Amsterdam, pp.57-90

KUNIYIOSHI, S. and LIOU, J.G., 1976. Contact metamorphism of the Karmutsen volcanics, Vancouver Island, British Columbia. Journal of Petrology, v.17, pp.73-99

KUSHIRO, I., 1972. Origin of some magmas in oceanic and circum-oceanic regions. Tectonophysics, v17, pp.211-222

LAIRD, H.C., 1937. The western part of the Sturgeon River area. Ontario Department of Mines, 45, part 2, (1936), pp60-117.

LIARD, J., 1982. Amphiboles in metamorphosed basaltic rocks: Greenschist facies to Amphibolite facies. In: Review in Mineralogy, v9B, Amphiboles; Reactions and experimental phase relations, pp.114-137

LANGFORD, G.B., 1929. Geology of the Beardmore-Nezah gold area, Thunder Bay District. Ontario Department of Mines 37, part 4 (1928), p83-108.

LANGFORD, F.F. and MORIN, J.A., 1976. The development of the Superior province of northwestern Ontario by merging island arcs. American Journal of Science, v276, pp.1023-1034

LASH, G.G., 1986. Sedimentology and geochemical evidence for Middle Ordovician near-trench volcanism in the Central Appalachian Orogen. Journal of Geology, v94, pp.91-107

LEGGETT, J.K., 1980. The sedimentological evolution of a Lower Palaeozoic accretionary fore-arc in Southern Uplands of Scotland. Sedimentology, v27, pp.401-417

LEWIS, B.T.R., 1983. The process of formation of oceanic crust. Science, v220, pp.151-157

LIOU, J.G., KUNIYOSHI, S. and ITO, K., 1974. Experimental studies of the phase relations between greenschist and amphibolite in a basaltic system. American Journal of Science, v274, pp.613-632

LUDDEN, J.N. and HUMPHRIS, S.E., 1978. Are REE mobile during alteration process? (abstract). Geological Society Bulletin, Abstracts with Program, 10, pp.447

LUDDEN, J.N. and THOMPSON, G., 1978. Behaviour of REE during submarine weathering of tholeiite basalt. Nature, v274, pp.147-149

LUDDEN, J.N. and THOMPSON, G., 1979. An evaluation of the behaviour of the rare earth elements during the weathering of sea-floor basalt. Earth and Planetary Science Letters, v43, pp.85-92

MACKASEY, W.O., 1975. Geology of Dorothea, Sandra and Irwin Townships, District of Thunder Bay. Ontario Division of Mines, Geological Report 122, 83p.

MACKASEY, W.O., 1976. The geology of Walters and Leduc Townships, District of Thunder Bay; Ontario Division of Mines, Geoscience Report 149, 60p.

MALPAS, J. and LANGDON, G., 1984. Petrology of the upper pillow lava suite, Troodos ophiolite, Cyprus. In: Ophiolites and Oceanic Lithosphere, I.G. Gass, S.J. Lippard and A.W. Shelton (Eds.). John Wiley and Sons, pp.155-168

MARTIN, H., 1986. Effect of steeper Archean geothermal gradient on geochemistry of subduction zone magmas. Geology, v14, pp.753-756

MARUYAMA, S., LIOU, J.G. and SUZUKI, K., 1983. Greenschist-amphibolite transition equilibria. Journal of Petrology, v24, pp.382-604

MASON, B. and MOORE, C.B., 1982. Principle of geochemistry. 4th Edition, John Wiley and Sons, New York, 344p

MASUDA, A., NAKAMURA, N. and TANAKA, N. 1973. Fine structures of mutually normalised RE patterns of Chondrite. Geochemica et Cosmochemica Acta, v37, pp. 239-248.

McINTIRE, W.L., 1963. Trace element partition coefficients - a review of theory and applications to geology. Geochemica et Cosmochemica Acta, v37, pp.1209-1264

McKERROW, W.S. and LEGGETT, J.K., 1977. Imbricate thrust model of the Southern Uplands of Scotland. Nature, v267, pp.237-239

MELSON, W. and THOMPSON, G., 1971. Petrology of a transform fault zone and adjacent ridge segments. Philosophical Transaction of the Royal Society of London, A. 268, pp.423-441

MENZIES, M., SEYFRIED, W.G., and BALANCHARD, D., 1979. Experimental evidence of REE immobility in greenstone. Nature, v282, pp.398-399

MOORBATH, S.M., 1975. Evolution of Precambrian crust from strontium isotopic evidence. Nature, v254, pp.395-398

MOORE, J.C., WATKINS, J.S., SHIPLEY, T.H., McMILLEN, K.J., BACHMAN, S.B. and LUNDBERG, N., 1982. Geology and tectonic evolution of a juvenile accretionary terrane along a truncated convergent margin: Synthesis of results from Leg 66 of the Deep Sea Drilling Project, southern Mexico. Geological Society of America Bulletin, v93, pp.847-861

MIYASHIRO, A., SHIDO, F. and EWING, M., 1970. Crystallisation and differentiation in abyssal tholeiites and gabbros from mid-oceanic ridges. Earth and Planetary Science Letters, v7, pp.361-365

MIYASHIRO, A., 1973a. Paired and unpaired metamorphic belts. Tectonophysics, v17, pp.241-254

MIYASHIRO, A., 1973b. The Troodos ophiolitic complex was probably formed in an island arc. Earth and Planetary Science Letters, v19, pp.218-224

MIYASHIRO, A., 1978. Metamorphism and metamorphic belts. John Wiley and Sons, New york, N.Y., 492p.

MURPHY, J.B. and HYNES, A.J., 1986. Contrasting secondary mobility of Ti, P, Zr, Nb and Y in two metabasaltic suites in the Appalachians. Canadian Journal of Earth Science, v23, pp.1138-1144

MYSEN, B.O. 1979. Trace-element partitioning between garnet peridotite minerals and water-rich vapor: experimental data from 5 to 30kbar. American Mineralogist, v64, pp.274-287

MYSEN, B.O. and FUJII, T., 1977. Experimental studies of water in crystalline peridotite and partitioning of some trace elements between water-rich vapor and crystals in the upper mantle. Extended Abstracts, Second International Kimberlite Conference, Santa Fe, New Mexico.

NAGASAWA, H., WAKITA, H., and ONUMA, N., 1969. Rare earths in peridotite nodules: an explanation of the genetic relationship between basalt and peridotite nodules. Earth Planetary Science Letters, v5, pp.377-381

NEEDHAM, D.T. and MACKENZIE, J.S., 1988. Structural evolution of the Shimanto Belt accretionary complex in the area of the Gokase River, Kyushu, SW Japan. Journal of Geological Society of London, v.145, pp.85-94

NESBITT, R.W. and SUN, S-S, 1976. Geochemistry of Archaean spinifex-textured peridotites and magnesian and low-magnesian tholeiites. Earth Planetary Science Letters, v31, pp.433-453

NESBITT, H.W., 1979. Mobility and fractionation of rare earth elements during weathering of a granodiorite. Nature, v279, no.5710, pp.206-210

O'HARA, M.J. and YODER Jr., H.S., 1967. Formation and fractionation of basic magmas at high pressues. Scotland Journal of Geology, pp.67-117

O'NIONS, R.K., HAMILTON, P.J., and EVENSEN, N.M., 1977. Variation in $^{143}Nd/^{144}Nd$ and $^{87}Sr/^{86}Sr$ ratios in oceanic basalts. Earth Planetary Science Letters, v34, pp.13-22.

PEARCE, J.A., 1975. Basalt geochemistry used to investigate past tectonic environment on Cyprus. Tectonophysics, v25, pp.41-67

PEARCE, J.A., ALABASTER, T. SHELTON, A.W. and SEARLE, M.P., 1981. The Onaman ophilolite as a Cretaceous arc-basin complex evidence and implications. Philosophical Transaction of the Royal Society of London, A. 300, pp.299-317

PEARCE, J.A. and CANN, J.R., 1971. Ophiolite origin investigated by discriminant analysis using Ti, Zr and Y. Earth Planetary Science Letters, v12, pp.339-349

PEARCE, J.A. and CANN, J.R., 1973. Tectonic setting of basic volcanic rocks determined using trace element analyses. Earth Planetary Science Letters, v19, pp.290-300

PEARCE, J.A., GORMAN, P.E. and BIRKETT, T.C., 1975. The TiO2-K2O-P2O5 diagram: A method of discriminating between oceanic and non-oceanic basalts. Earth Planetary Science Letters, v24, pp.419-426

PEARCE, J.A. and NORRY, M.J., 1979. Petrogenic implications of Ti, Zr, Y and Nb variations in volcanic rocks. Contribution to Mineralogy and Petrology, v69, pp.33-47

PEARCE, T.H., 1968. A contribution to the theory of variation diagrams. Contribution to Mineralogy and Petrology, v19, pp.142-157.

PEARCE, T.H., 1969. Chemical variations in the Palisade sill. Journal of Petrology, v11, pp15-32

PERCIVAL, J.A. and CARD, K.D., 1986. Greenstone belts: their boundaries, surrounding rock terrains and inter-relationships. In: Workshop on the tectonic evolution of greenstone belt, compiled by Lunar and Planetary Institute, Lunar and Planetary Institute Contribution 584, supplement, Houston, Texas, pp.15-19

PERFIT, M.R., 1977. Petrology and geochemistry of mafic rocks from Cayman Trench: Evidence for spreading. Geology, v5, pp.105-110

PHARAOH, T.C. and PEARCE, J.A., 1984. Geochemical evidence for the geotectonic setting of early Proterozoic metavolcanic sequences in Lapland. Precambrian Research, v25, pp.283-308

PYE, E.G., 1951. Geology of Errington Township, Little Long Lac area. Ontario Department of Mines Annual Report LX, part 6, 140p.

PYE, E.G., 1965. Geology and lithium deposits of Georgia Lake area. Ontario Department of Mines Geological Report 31, 113p.

PYE, E.G., 1968. Geology of the Lac Des Iles area, District of Thunder Bay. Ontario Department of Mines Geological Report 64, 47p

RAASE, P., 1974. Al and Ti contents of hornblende, indicators of pressure and temperature of regional metamorphism. Contribution to Mineralogy and Petrology, v45, pp.231-236

REILLY, B.A., 1988. Structural analysis of the Paint Lake Deformation Zone, Northern Ontario. Unpublished MSc Thesis, Brock University, 187p.

RINGWOOD, A.E., 1976. Phase transformations in descendingplates and impilcations for mantle dynamics. Tectonophysics, v32, pp.129-143

ROBINSON, A.M., 1986. A study of metamorphic textures in the Geraldton-Beardmore Belt; Unpublished B.Sc. Thesis Brock University, St. Catharines, Ontario, 58p.

ROEDDER, E., 1972. Composition of fluid inclusions. In M. Fleischer, (Ed.) Data of geochemistry, 6th Edition. U.S. Geological Survey Prof. paper 440-JJ.

ROGERS, J.J.W., 1978. Inferred composition of the early Archean crust and variation in crustal composition through time. In: B.F. Windley and S.M. NAQVI (Eds.), Archaean Geochemistry, Elsevier, Amsterdam, pp.25-39

RUST, B.R. and KOSTER, E.M., 1984. Coarse alluvial deposits. In: R.G.Walker (Ed.), Facies Models, 2nd Edition, Geoscience Canada, pp.53-71

SACKS, I.S., 1983. The subduction of young lithosphere, Journal of Geophysical Research, v88, pp.3355-3366

SAMPSON, G.A. and FAWCETT, J.J., 1977. Coexisting Amphiboles Canadian Mineralogist, v15, pp.283-296

SAUNDERS, A.D. and TARNEY, J., 1979. The geochemistry of basalts from a back-arc spreading centre in the East Scotia Sea. Geochemica et Cosmochimica Acta, v43, pp.555-572

SCHIFFMAN, P., and LIOU, J.G., 1980. Synthesis and stability relation of Mg-Al pumpellite, $Ca_4Al_5MgSi_6O_{21}(OH)_7$. Journal of Petrology, 21, pp.441-474

SCHILLING, J.G., 1971. Sea-floor evolution: rare earth evidence. Philosophical Transaction of the Royal Society of London, A268, pp.663-706

SCHILLING, J.G., 1975. Rare earth variations across normal ridge segments of the Reykjanes Ridge, 60^0-53^0 N, mid-Atlantic ridge, 29^0S and east Pacific Rise, 2^0-19^0S, and evidence on the composition of the underlying low velocity level. Journal Geophysical Research, v11, pp.1459-1473

SEIFERT, K.E., COLE, M.R.W. AND DALE, A. B., 1985. REE mobility due to alteration of Indian Ocean basalt. Canada Journal of Earth Science, v22, pp.1884-1887

SHAW, D.M., 1970. Trace element fractionation during anatexis. Geochemica et Cosmochemica Acta, v34, pp.237-243.

SMITH, R.E., 1968. Redistribution of major elements in the alteration of some basic lavas during burial metamorphism. Journal of Petrology, v9, pp.191-219

SMITH, R.E. and SMITH, S.E., 1976. Comments on the use of Ti, Zr, Y, Sr, K, P and Nb in classification of basaltic magmas. Earth Planetary Science Lettters, v32, pp.114-120

SPRY, A., 1983. Metamorphic textures, Pergamon Press, Sydney, Australia, 350p.

STOREY, B.C. and MENEILLY, A.W., 1985. Petrogenesis of metamorphic rocks within a subduction-accretion terrane, Signy Island, South Orkney Islands. Journal of Metamorphic Geology, v3, pp.21-42

STOTT, G.M., 1984a. Geraldton Sheet, Thunder Bay and Cochrane Districts; Ontario Geological Survey Map 241, Compilation Series-Preliminary Map, scale 1:126 720.

STOTT, G.M. 1984b. Lake Nipigon Sheet, Thunder Bay District; Ontario Geological Survey, Map 257, Compilation Series-Preliminary Map, scale1: 126 720.

SUN, S-S. and NESBITT, R.W., 1977. Chemical heterogeneity of the Archaean mantle, composition of the Earth and mantle evolution. Earth Planetary Science Letters, v35, pp.429-448

SUN, S-S. and NESBITT, R.W., 1978. Petrogenesis of Archaean ultrabasic and basic volcanics; Edvience from rare earth elements. Contribution to Mineralogy and Petrology, v65, pp.301-325

SUN, S-S. NESBITT, R.W and SHARASKIN, A.Y., 1979. Geochemical characteristics of mid-oceanic ridge basalts. Earth and Planetary Science Letters, v44, pp.119-138

TAGIRI, M., 1977. Fe-Mg partition and miscibility gap between coexisting calcic amphiboles from the southern Abukuma plateau, Japan. Contribution to Mineralogy and Petrology, v62, pp.270-281..

TAKAHASHI, E. and KUSHIRO, I., 1983. Melting of a dry peridotite at high pressures and basalt magma genesis. American Mineralogist, v68, pp.859-879

TANTON, T.L., 1935. Geology of the Sturgeon River area. Canadian Mining and Metallurgical Bulletin 280, pp.341-348

TARNEY, J, DALZIEL, I.W.D. and de WIT, M.J., 1976. Marginal basin 'Rocas Verdas' complex from S. Chile: A model for Archaean greenstone belt formation. In: B.F. Windley (Ed.), The Early History of the Earth. John Wiley and Sons, N.Y., pp.131-146

TARNEY, J., SAUNDERS, A.D., MERLEY, D.P., WOOD, D.A. and MARSH, N.G., 1981. Geochemical aspects of back-arc spreading in the Scotia Sea and western Pacific. Philosophical Transaction of the Royal Society of London. A 300, pp.263-285

TARNEY, J., WEAVER, S.D., SAUNDERS, A.D., PANKHURST, R.J. and BARKER, P.F., 1982. Volcanic evolution of the northern Antarctic Peninsula and the Scotia arc. In: Andesites, R.S. Thorpe (Ed.), John Wiley and Sons, pp.371-400

TEIL, H. and CHEMINEE, J.L., 1975. Application of correspondence factor analysis to the study of major and trace elements in the Erta Ale Chain (Afar, Ethiopia). Mathematical Geology, v7, pp.13-30

TEMPLE, J.T., 1978. The use of factor analysis in geology. Mathematical Geology, v10, pp.379-387

THURSTON, P.C., 1980. Geology of the northern Onaman Lake Area, District of Thunder Bay. Ontario Geological Survey Report 208, 81p.

TILLEY, C.E., 1950. Some aspect of magmatic evolution. Geological Society of London Quarterly Journal, pp.37-61.

TURNER, F.J. and VERHOOGEN, J., 1960. Igneous and Metamorphic Petrology. McGraw-Hill Book Company, New York. 694p.

TURNER, F.J., 1968. Metamorphic Petrology. McGraw-Hill Book Company, New York. 403p.

VALLANCE, T.G., 1974. Spilitic degradation of tholeiitic basalt. Journal of Petrology, v15, pp.79-96

VEBLEN, R.D. and RIBBE, P.H., (Eds.) 1982. Amphiboles: Petrology and Experimental Phase Relations, Reviews in Mineralogy, v9b, Mineralogy Society of America, 390p.

VERNON, R.H., 1976. Metamorphic processes. Murby, London, 247p.

VERNON, R.H., 1977. Relationships between microstructures and metamorphic assemblages. Tectonophysics, v39, pp.288-305

WEGENER, A., 1912. Die Entstehung der Kontinente, Petermann's Mitteilungen, pp.185-195

WILLIAMS, H.R., 1986. Structural studies in the Beardmore-Geraldton Belt, northern Ontario, pp138-146. In: Geoscience Research Grant Program, Summary of Research 1985-1986, edited by V.G. Milne, Ontario Geological Survey, Miscellaneous aper 130, 255p.

WILLIAMS, H.R., 1987. Structural studies in the Wabigoon and Quetico Subprovinces. Ontario Geological Survey, Final Report of Ontario Geoscience Research Fund Project No.242, 131p.

WINCHESTER, J.A. and FLOYD, P.A., 1976. Geochemical magma type discrimination: application to altered and metamorphosed basic igneous rocks. Earth Planetary Science Letters, v28, pp.459-469

WINDLEY, B.F., 1976. New tectonic models for the evolution of Archean continents and oceans. In: B.F. Windley (Ed.), The Early History of the Earth. John Wiley and Sons, New York, pp.105-112

WINDLEY, B.F., 1982. The Evolving Continents, 2 Eds. John Wiley and Sons, New York, 399p.

WINKLER, H.G.F., 1980. Petrogenesis of metamorphic rocks, 5th Edition: Springer-Verlag, New-York, 348p.

WISEMAN, J.D.H., 1934. The central and southwestern highland epidiorites: a study in progressive metamorphism. Geological Society of London, Quarterly, v90, pp.354-417

WOOD, D.A., 1978. Major and trace element variations in the Tertiary lavas of Eastern Iceland and their significance with respect to the Iceland geochemical anomaly. Journal of Petrology, v19, pp.393-436

WOOD, D.A., GIBSON, I.L. and THOMPSON, R.N., 1976. Elemental mobility during zeolite facies metamorphism of tertiary basalts of eastern Iceland. Contribution to Mineralogy and Petrology, v55, p241-253

WRIGHT, T.L. and DOHERTY, P.C., 1970. A linear programming and least squares computer method for solving petrologic mixing problems. Geological Society of America Bulletin, v81, pp.1995-2008

WRIGHT, T.L., 1974. Presentation and interpretation of chemical data for igneous rocks. Contribution to mineralogy and Petrology, v48, pp.233-248

WYLLIE, P.J., 1973. Experimental petrology and global tectonics, a preview. Tectonophysics, v17, pp.189-210

WYLLIE, P.J., 1980. Petrogenesis and the physics of the Earth. In: H.S. Yoder (Ed.), The Evolution of Igneous rocks; Princeton Press, 2nd Edition, 568p

WYLLIE, P.J., 1983. Experimental and thermal constraints on the deep-seated parentage of some granitoid magmas in subducting zones. In: M.P. Atherton and C.D. Gribble (Eds.), Migmatites, Melting and Metamorphism; Shiva Publishing Limited, 326p.

ZAYACHKIVSKY, B., 1985. Granitoids and rare earth pegmatite of the Georgia Lake area, northwestern Ontario. Unpublished MSc Thesis, Lakehead University, 234p.

APPENDIX I
GEOCHEMICAL ANALYSES

The major elements concentrations including the loss of ignition (LOI) are reported in weight per cent. Trace elements including rare earth data are given in parts per million (ppm).

SAMPLE #:	GG	GC101	KPP	PP101	BM104	S301	PE104	PE104A
SiO2	48.00	45.90	49.90	48.00	46.90	48.80	49.30	50.20
TiO2	1.06	00.66	1.69	1.06	00.80	1.05	1.38	1.39
Al2O3	14.30	15.80	12.90	13.80	13.10	13.80	13.70	14.10
Fe2O3	14.30	12.60	16.80	14.60	12.80	14.10	16.66	15.40
MnO	00.24	00.17	00.22	00.23	00.21	00.20	00.26	00.23
MgO	6.79	7.96	4.91	7.18	10.50	7.56	5.83	5.97
CaO	9.12	10.90	7.64	9.29	9.54	10.80	8.40	7.60
Na2O	3.19	1.82	2.75	3.02	2.59	1.42	2.15	3.00
K2O	00.22	00.04	00.32	00.15	00.28	00.24	00.22	00.14
P2O5	00.10	00.05	00.32	00.08	00.20	00.10	00.14	00.26
CO2	00.14	00.53	00.22	00.17	00.12	00.08	00.55	00.11
S	00.01	00.01	00.01	00.14	00.01	00.08	00.03	00.01
LOI	2.30	3.30	2.10	2.50	3.00	1.40	1.70	1.10
Total	99.60	99.20	99.50	99.90	99.90	99.40	99.70	99.40
Co	--	--	63	83	62	77	78	81
Cr	--	--	--	229	865	146	108	111
Cu	--	--	33	124	28	142	96	30
Ni	--	--	29	98	164	74	47	51
Sc	--	--	35	34	22	25	35	36
Sr	117	244	113	136	467	159	89	93
V	--	--	304	308	241	298	361	344
Y	31	17	55	28	25	27	41	45
Zn	--	--	94	120	111	139	145	132
Zr	95	76	156	92	98	93	119	142

SAMPLE #:	PE108A	PE113B	PW105	PW107	PW109B	CL104	CL112
SiO2	47.20	48.40	48.90	51.50	43.10	51.00	48.10
TiO2	00.94	1.01	00.68	00.85	1.04	1.12	00.67
Al2O3	14.40	14.20	13.60	13.50	16.00	13.60	15.80
Fe2O3	14.10	13.80	10.20	11.20	16.20	15.00	9.59
MnO	00.23	00.23	00.19	00.21	00.26	00.23	00.19
MgO	6.95	6.94	9.12	6.69	8.01	4.74	7.56
CaO	10.40	11.80	13.60	10.10	8.71	8.31	13.80
Na2O	2.07	1.61	1.39	3.11	2.58	1.86	1.57
K2O	00.17	00.26	00.20	00.22	00.14	00.16	00.22
P2O5	00.08	00.08	00.05	00.07	00.10	00.11	00.05
CO2	1.86	00.35	00.32	1.14	00.97	1.66	00.11
S	00.10	00.09	00.02	00.04	00.01	00.01	00.02
LOI	3.10	1.40	1.90	1.90	3.20	3.50	1.50
Total	99.60	99.70	99.80	99.30	99.30	99.60	99.50
Co	88	76	76	60	87	78	70
Cr	191	175	277	12	141	43	146
Cu	127	113	255	199	144	166	140
Ni	74	93	124	39	183	33	81
Sc	39	36	36	40	38	37	37
Sr	179	251	143	156	114	163	199
V	294	305	244	318	362	289	247
Y	28	25	18	25	30	30	20
Zn	185	112	70	68	153	109	67
Zr	84	97	63	77	87	112	72

SAMPLE #:	VM104	RC106	B104	WD113	WD117	0X101	OX103	OX113
SiO2	48.00	48.40	44.50	54.30	45.40	46.20	51.40	47.80
TiO2	00.73	00.72	00.73	00.73	1.07	00.67	1.15	00.80
Al2O3	15.50	14.40	16.20	16.20	15.00	15.40	16.20	14.10
Fe2O3	11.00	10.90	12.80	9.64	15.20	9.94	15.20	13.80
MnO	00.16	00.19	00.26	00.15	00.25	00.18	00.18	00.23
MgO	7.30	8.02	7.57	4.82	7.15	8.40	3.47	7.57
CaO	11.60	12.70	12.80	6.82	10.10	12.30	4.73	10.70
Na2O	1.47	1.74	1.43	4.95	2.37	2.10	3.97	1.36
K2O	00.08	00.07	00.08	00.39	00.18	00.36	1.45	00.48
P2O5	00.07	00.05	00.07	00.19	00.10	00.08	00.10	00.06
CO2	1.09	00.15	00.17	00.09	00.38	00.06	00.11	00.08
S	00.03	00.01	00.01	00.01	00.09	00.01	00.14	00.05
LOI	3.50	2.10	2.50	1.90	2.90	3.20	2.00	2.60
Total	99.40	99.30	98.90	100.0	99.70	98.80	99.80	99.50
Co	57	91	72	48	66	61	61	62
Cr	262	172	420	190	206	540	214	225
Cu	137	159	116	15	143	77	86	146
Ni	97	92	164	90	134	92	130	83
Sc	30	41	34	16	30	20	32	29
Sr	206	105	240	101	161	139	185	172
V	252	270	260	154	309	184	349	284
Y	20	20	25	25	27	20	29	20
Zn	75	70	106	77	150	66	60	101
Zr	78	58	83	143	89	70	100	78

SAMPLE#:	OX115	HWY101A	S201	SA101	BLX	GGd	GC101d	BLXd
SiO2	43.60	44.60	49.20	47.50	49.80	48.40	46.10	49.50
TiO2	1.27	00.78	1.20	1.02	00.99	1.03	00.62	00.94
Al2O3	15.50	14.90	14.10	17.20	14.40	14.40	15.90	14.30
Fe2O3	18.20	13.60	14.90	11.90	12.90	14.20	12.40	12.70
MnO	00.25	00.21	00.23	00.18	00.29	00.24	00.17	00.29
MgO	7.02	9.29	5.59	7.00	6.97	6.57	7.87	7.08
CaO	8.84	10.80	11.70	6.54	8.61	9.15	10.80	8.52
Na2O	1.83	1.20	1.97	3.84	2.94	2.99	1.93	3.17
K2O	00.16	00.03	00.13	00.51	00.85	00.22	00.05	00.83
P2O5	00.11	00.07	00.11	00.13	00.08	00.09	00.05	00.08
CO2	00.08	00.80	00.10	00.17	00.16	00.15	00.52	00.16
S	00.02	00.02	00.27	00.01	00.02	00.01	00.01	00.02
LOI	3.10	3.90	00.70	3.30	1.90	2.30	3.40	1.90
Total	99.90	99.40	99.80	99.10	99.70	99.60	99.30	99.30
Co	60	73	83	49	67	--	--	66
Cr	30	455	103	128	139	--	--	142
Cu	177	172	131	48	115	--	--	116
Ni	40	210	68	62	68	--	--	67
Sc	24	19	22	16	23	--	--	29
Sr	160	151	204	136	396	117	242	397
V	364	248	330	228	301	--	--	298
Y	32	23	33	31	24	31	16	23
Zn	146	106	121	86	95	--	--	94
Zr	116	74	109	100	108	94	75	107

SAMPLE#:	GGL	GGD	RM101	S202	PE108	PE114	PW109A	PW109
SiO2	49.90	45.20	52.20	48.70	45.70	46.00	49.30	45.10
TiO2	1.05	1.00	1.10	1.30	00.69	1.21	1.12	1.08
Al2O3	13.90	14.90	13.90	14.30	15.30	15.80	12.70	11.90
Fe2O3	12.80	15.50	9.80	14.70	14.20	12.80	13.10	11.40
MnO	00.20	00.24	00.20	00.22	00.21	00.28	00.28	00.39
MgO	7.35	8.54	5.18	6.25	10.00	6.63	4.96	5.22
CaO	9.29	9.33	10.60	10.60	8.63	10.40	10.20	11.10
Na2O	2.23	1.56	2.20	2.36	1.53	2.76	2.29	1.45
K2O	00.26	00.33	00.25	00.24	00.34	00.37	00.15	00.12
P2O5	00.07	00.06	00.10	00.08	00.03	00.08	00.05	00.07
CO2	00.12	00.13	1.90	00.40	00.20	1.98	3.93	7.33
S	00.05	00.01	00.02	00.25	00.02	00.19	00.01	00.01
LOI	2.30	3.20	4.00	1.00	3.10	3.00	5.70	11.20
Total	99.30	99.80	99.50	99.70	99.70	99.30	99.80	99.00
Co	82	73	94	55	75	73	69	49
Cr	172	190	118	84	136	128	78	144
Cu	95	57	5	164	157	125	118	82
Ni	161	162	57	47	215	89	58	48
Sc	38	39	36	39	23	38	42	38
Sr	137	122	211	284	164	209	91	61
V	280	298	241	328	224	316	332	282
Y	30	29	35	30	21	35	30	29
Zn	114	116	83	69	101	99	131	89
Zr	94	88	110	107	66	102	88	84

SAMPLE#:	PW110A	NL101	NL124	VM107	VM108	VM113	B116	OX105
SiO2	48.30	46.70	45.80	48.60	49.60	47.00	50.20	50.70
TiO2	1.21	1.00	1.66	00.76	00.70	00.75	00.90	1.12
Al2O3	14.30	13.80	14.60	11.70	12.50	15.10	14.20	12.80
Fe2O3	16.10	13.20	16.80	11.20	10.00	12.90	13.90	14.00
MnO	00.22	00.23	00.21	00.21	00.16	00.20	00.25	00.21
MgO	6.59	6.71	6.62	7.96	9.34	7.39	6.05	6.07
CaO	9.47	12.40	9.60	11.90	10.30	10.60	6.47	9.68
Na2O	2.34	1.78	1.30	2.23	2.50	1.69	3.36	3.16
K2O	00.13	00.07	00.08	00.06	00.14	00.05	00.03	00.11
P2O5	00.08	00.05	00.12	00.04	00.03	00.04	00.05	00.08
CO2	00.08	1.77	00.23	2.65	1.70	00.15	1.10	00.11
S	00.15	00.03	00.11	00.01	00.03	00.01	00.09	00.01
LOI	1.10	4.00	3.10	4.60	3.90	3.20	3.60	1.90
Total	99.80	99.90	99.80	99.30	99.20	98.90	99.00	99.80
Co	71	62	60	55	68	97	54	64
Cr	131	138	82	29	393	260	76	78
Cu	159	123	97	68	66	59	127	7
Ni	55	70	70	53	129	76	46	44
Sc	42	31	38	45	36	32	37	44
Sr	173	131	200	100	75	127	100	111
V	355	269	387	272	213	243	278	346
Y	32	23	42	22	20	20	24	38
Zn	153	89	170	81	68	50	98	81
Zr	98	79	128	66	60	75	86	103

SAMPLE#:	OX117	B107	J101	RC107	WD107	CL112	RL101	GGLd
SiO2	48.90	45.60	45.20	44.50	58.70	48.40	53.30	49.70
TiO2	1.00	00.83	00.90	00.70	00.59	00.62	1.19	1.01
Al2O3	13.90	14.40	13.10	13.30	12.90	15.90	12.50	13.80
Fe2O3	14.10	13.20	10.40	12.80	7.34	9.53	12.00	13.10
MnO	00.22	00.17	00.25	00.20	00.09	00.17	00.25	00.20
MgO	7.03	6.56	6.26	12.20	4.66	7.94	5.81	7.42
CaO	10.00	12.90	10.50	9.18	4.72	7.94	11.00	7.42
Na2O	1.89	00.42	1.73	1.25	1.98	1.80	00.84	2.32
K2O	00.14	00.02	00.07	00.15	1.17	00.23	00.22	00.26
P2O5	00.06	00.05	00.05	00.04	00.16	00.01	00.13	00.08
CO2	00.07	2.57	6.12	1.48	3.53	00.21	00.16	00.12
S	00.09	00.09	00.09	00.03	00.01	00.02	00.01	00.05
LOI	2.50	5.40	10.10	5.20	6.80	1.80	2.00	2.20
Total	99.70	99.50	98.60	99.50	99.10	99.80	99.20	99.30
Co	62	53	61	72	36	64	67	82
Cr	63	92	141	45	148	125	157	173
Cu	147	104	123	88	26	134	37	93
Ni	55	77	66	255	125	81	91	160
Sc	38	38	36	25	14	--	32	35
Sr	158	140	102	81	58	202	151	136
V	290	279	265	182	107	--	239	--
Y	29	22	24	17	20	17	35	29
Zn	108	87	86	99	74	62	90	115
Zr	98	81	88	63	148	67	114	92

SAMPLE#:	WD107d
SiO2	59.00
TiO2	00.58
Al2O3	12.90
Fe2O3	7.41
MnO	00.09
MgO	4.83
CaO	4.83
Na2O	1.83
K2O	1.18
P2O5	00.17
CO2	3.48
S	OO.01
LOI	6.70
Total	99.40
Co	36
Cr	147
Cu	27
Ni	124
Sc	15
Sr	58
V	108
Y	21
Zn	72
Zr	150

Rare earth analysis results of 14 selected samples.

	S2O2	OX101	OX115	GG	BLX	KPP	PE104
La	3.424	2.659	5.341	3.795	2.681	6.803	4.811
Ce	9.714	7.442	13.597	11.115	7.532	19.586	13.472
Pr	1.535	1.092	2.019	1.734	1.140	2.823	1.902
Nd	9.001	6.037	10.606	9.769	6.436	16.197	10.733
Sm	3.195	1.984	3.345	3.151	2.320	5.263	3.652
Eu	1.090	0.880	1.170	0.993	0.658	1.606	1.196
Gd	4.234	2.723	4.234	3.932	3.137	7.157	4.905
Tb	0.752	0.507	0.817	0.751	0.550	1.297	0.847
Dy	4.749	3.320	5.051	4.768	3.704	7.996	5.648
Ho	1.021	0.698	1.112	1.021	0.783	1.664	1.243
Er	3.110	2.121	3.307	3.197	2.279	5.301	3.900
Tm	0.437	0.287	0.451	0.430	0.299	0.719	0.532
Yb	2.585	1.960	3.005	2.663	1.973	4.640	3.252
Lu	0.367	0.291	0.428	0.416	0.290	0.684	0.506

	PW107	PW105	PW109B	OX103	PE104A	BM104	WD113
La	1.868	1.544	2.888	3.610	3.613	7.184	11.827
Ce	6.284	4.537	7.939	9.065	12.120	17.452	26.580
Pr	0.956	0.689	1.207	1.266	1.871	2.411	3.138
Nd	5.915	4.038	6.887	7.136	10.389	12.552	13.834
Sm	2.097	1.568	2.443	2.713	3.860	3.350	3.267
Eu	0.781	0.531	0.930	0.899	1.060	0.994	0.883
Gd	2.666	2.347	3.332	3.741	5.019	3.510	3.287
Tb	0.506	0.404	0.645	0.705	0.989	0.610	0.538
Dy	3.430	2.515	4.146	4.637	6.556	3.600	3.324
Ho	0.650	0.539	0.907	0.937	1.444	0.763	0.698
Er	2.055	1.555	2.823	2.929	4.298	2.337	1.991
Tm	0.251	0.215	0.397	0.381	0.583	0.302	0.260
Yb	1.818	1.318	2.485	2.598	3.785	1.957	1.857
Lu	0.245	0.212	0.374	0.411	0.603	0.271	0.266

NORMALISING VALUES:

La	Ce	Pr	Nd	Sm	Eu	Gd	Tb	Dy	Ho	Er	Tm	Yb	Lu
.330	.880	.112	.600	.181	.069	.249	.047	.325	.070	.200	.030	.200	.034

Dy value is derived from Leedy Chondrite divided by 1.2 (Masuda, A., Nakamura, N., Tanaka, T. 1973.

All other REE values are an average of nine chondrites derived from Haskin, L.A., Haskin, M.A., Frey, F.A. 1968.

APPENDIX II
SAMPLE LOCALITIES

SAMPLE LOCALITIES.

SAMPLE	ROCK CLASSIFICATION (AFM)	LATITUDE	LONGITUDE	TWSP.
BLX	THOLEIITIC	49.66934	87.56541	LEDUC
GG	THOLEIITIC	49.70760	86.94868	ASHMORE
GC	THOLEIITIC	49.71838	86.95561	ASHMORE
KPP	THOLEIITIC	49.70309	86.95146	ASHMORE
PP101	THOLEIITIC	49.67792	86.96812	ERRINGTON
BM104	THOLEIITIC	49.69588	87.07765	ERRINGTON
S301	THOLEIITIC	49.65509	87.27986	VIVIAN
PE104	THOLEIITIC	49.66551	87.40602	LEGAULT
PE104A	THOLEIITIC	49.66551	87.40602	LEGAULT
PE108A	THOLEIITIC	49.66643	87.40463	LEGAULT
PE113B	THOLEIITIC	49.66643	87.40463	LEGAULT
PW105	THOLEIITIC	49.66891	87.45871	LEGAULT
PW107	THOLEIITIC	49.66890	87.46425	LEGAULT
PW109B	THOLEIITIC	49.66623	87.45590	LEGAULT
CL104	THOLEIITIC	49.65393	87.59155	CLIST LAKE
CL112	THOLEIITIC	49.65453	87.64699	VINCENT
VM104	THOLEIITIC	49.64793	87.69676	VINCENT
RC106	THOLEIITIC	49.63062	87.86545	McCOMBER
B104	THOLEIITIC	49.59749	87.96036	BEARDMORE
WD113	CALC-ALKALINE	49.68501	87.80542	IRWIN
WD117	THOLEIITIC	49.68321	87.80678	IRWIN
OX101	THOLEIITIC	49.69714	87.58377	LEDUC
OX103	THOLEIITIC	49.69714	87.58377	LEDUC
OX113	THOLEIITIC	49.69983	87.58380	LEDUC
OX115	THOLEIITIC	49.69983	87.58380	LEDUC
HWY101A	THOLEIITIC	49.69203	87.69463	WALTERS
SA101	CALC-ALKALINE	49.67790	86.93486	ASHMORE
S201	THOLEIITIC	49.66043	87.30344	VIVIAN
GGL	THOLEIITIC	49.70670	86.94868	ASHMORE
GGD	THOLEIITIC	49.70670	86.94868	ASHMORE
RM101	THOLEIITIC	49.68602	87.02219	ERRINGTON
S202	THOLEIITIC	49.65900	87.30412	VIVIAN
PE108	THOLEIITIC	49.66803	87.40562	LEGAULT
PE114	THOLEIITIC	49.66946	87.40744	LEGAULT
PW109A	THOLEIITIC	49.66711	87.45868	LEGAULT
PW109	THOLEIITIC	49.66693	87.45868	LEGAULT
PW110A	THOLEIITIC	49.66623	87.45618	LEGAULT
NL101	THOLEIITIC	49.66217	87.64847	VINCENT
NL124	THOLEIITIC	49.64917	87.63930	VINCENT
VM107	THOLEIITIC	49.64975	87.69540	VINCENT
VM108	THOLEIITIC	49.65065	87.69542	VINCENT
VM113	THOLEIITIC	49.65784	87.69690	VINCENT
RL101	THOLEIITIC	49.62654	87.80695	McCOMBER
B116	THOLEIITIC	49.59424	87.96028	BEARDMORE
OX105	THOLEIITIC	49.69849	87.58379	LEDUC
OX117	THOLEIITIC	49.69966	87.58380	LEDUC
B107	THOLEIITIC	49.58736	87.96637	BEARDMORE
J101	THOLEIITIC	49.68027	87.53783	LEDUC
RC107	THOLEIITIC	49.61902	87.96701	McCOMBER

WD107	CALC-ALKALINE	49.68910	87.86302	IRWIN
CL112	THOLEIITIC	49.65608	87.59019	CLIST LAKE

See Figure 3.1 for mineral assemblage of each samples and their respective location in various traverses.

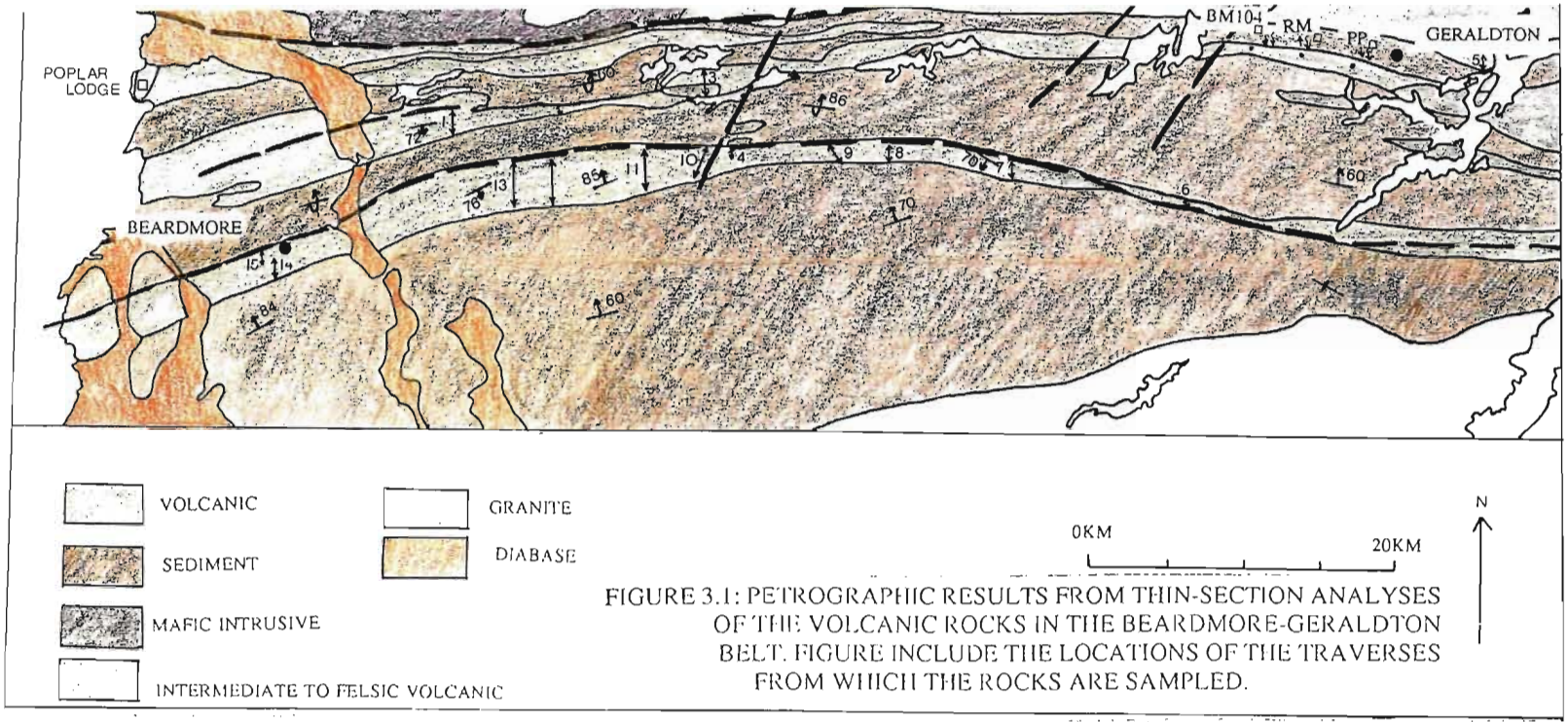

FIGURE 3.1: PETROGRAPHIC RESULTS FROM THIN-SECTION ANALYSES OF THE VOLCANIC ROCKS IN THE BEARDMORE-GERALDTON BELT. FIGURE INCLUDE THE LOCATIONS OF THE TRAVERSES FROM WHICH THE ROCKS ARE SAMPLED.

P103A □ AA↓↓
P103 □ ↓↓
P102 □ ↑↓
P101 □ ↓↑

BEARDMORE
117 □ ↑↓
116 □
115 □ ↑↑
114 □ ↑↑
113 □ ↑↓
112 □ ↑↑
111 □ ↑↑
110 □ ↑↑
109 □ ↑↑
108 □ ↑↑
107 □ ↑↑
106 □ ↓↑
105 □ ↑↑
104 □ ↓↓
103 □ ↑↑
102 □ ↑↑
101 □ ↑↓

GGL □ ↓↓
GGD □ ↓↓
KPP □ ↓↓

6 ST. CROIX
S401 ○ ↓↑
S402 ○ ↓↑
S201 ○ ↓↓
S301 △ ↓↓

49°30'N

7 GOLDFIELD RD.
S101 ○ ↓↑
S102 ○ ↓↑
S103 ○ ↓↓
S104 ○ B ↓↓
S105 ○ ↑↑

D TO PETROGRAPHIC ANALYSES:
GREENSCHIST FACIES
TRANSITION FACIES
LOWER AMPHIBOLITE
LOW CARBONATE CONTENT (<3%)
MODERATE CARBONATE CONTENT
HIGH CARBONATE CONTENT(>8%)
PRESENCE OF PREFERRED ORIENTATION
ABSENCE OF PREFERRED ORIENTATION
HIGH EPIDOTE CONTENT (> 20%)
PRESENCE OF BIOTITE
ABSENCE OF ACTINOLITE
PRESENCE OF RELICT TEXTURE

13 RALPH CREEK
RC116 □ B, AA↓↓
RC115 □ B↑↑
RC114 □ ↓↓
RC113 □ AA↑↑
RC112 □ ↑↓
RC111 □ AA↑↑
RC110 □ ↓↓
RC109 □ ↓↓
RC108 □ AA↑↑
RC107 □ E ↑↓
RC106 □ R → ↓
RC105 □ ↓↓
RC103 □ AA↑↓
RC102 □ → ↓
RC101 □ E → ↓

12 VINCENT MINE
VM119 □ (sed)↑↑
VM118 □ ↑↑
VM117 □ AA↑↑
VM116 △ ↓↓
VM115 □ AA↑↓
VM114 □ AA ↑↑
VM113 □ ↓↓
VM112 □ ↑↓
VM111 △ → ↓
VM110 △ → ↓
VM109 △ R → ↓
VM108 □ R ↓↓
VM107 □ R ↑↓
VM107A □ ↑↓
VM106A □ R ↓↓
VM106 □ R ↓↓
VM105 △ R ↑↓
VM105A △ ↑↓
VM104 □ R ↑↓
VM104S □ ↑↓
VM102 □ E ↑↓
VM101 □ ↑↓

11 NEZAH LAKE
NL101 □ ↑↓
NL104 □ AA↑↓
NL105 □ AA↑↓
NL106 □ AA↑↓
NL107 □ AA↑↑
NL108 ○ CUM.
NL109 □ AA↑↓
NL110 □ AA → ↓
NL111 □ AA↑↓
NL112 □ ↓↓
NL113 □ AA → ↓
NL114 □ AA↑↓
NL115 □ AA↑↓
NL116 □ B ↑↓
NL117 □ ↑↓
NL118 △ ↑↓
NL119 □ ↑↓
NL120 QFP
NL125 QFP
NL123 △ ↓↓
NL122 □ ↓↓
NL121 △ ↓↓

10 CLIST LAKE
CL116 □ ↓↓
CL115 □ ↓↓
CL114 □ → ↑
CL114B □ B AA ↓↓
CL113 ○ B ↓↓
CL112 △ ↓↓
CL111 □ ↓↓
CL110 □ AA ↑↑
CL109 △ ↑↓
CL108 □ ↑↑
CL101 □ ↓↑
CL102 △ → ↓
CL103 □ AA↑↓
CL104 □ ↓↑
CL104A □ AA ↓↓
CL105 ○ → ↓
CL106 □ ↓↓
CL107 □ E ↓↓

9 PATSY LAKE WEST
PW107 △ → ↓
PW106 △ ↑↓
PW105 □ ↓↓
PW108 △ ↑↓
PW109B △ ↑↓
PW109A △ ↑↓
PW109 □ → ↑
IRON ST.
PW109C ○ ↓↓
PW109D □ ↑↑
PW110A △ ↓↓
PW110B △ ↓↓
PW110D IRON ST.
PW110C ○ ↑↓
PW104 △ ↑↑
PW103 □ B → ↓
PW102 □ (sed) ↑↓
PW101 □ (sed) ↑↓

8 PATSY LAKE EAST
PE115 △ ↑↓
PE114 △ → ↑
PE113B □ B ↓↓
PE113A □ ↑↓
PE112C □ (sed) ↑↑
PE112B IRON ST.
PE112A ○ E ↓↓
PE111 ○ B ↑↑
PE110 □ (sed) ↑↓
PE108E △ R ↓↓
PE108D ○ B → ↓
PE108C IRON ST.
PE108B △ ↓↓
PE108A ○ → ↓
PE108 IRON ST.
PE107 ○ ↓↓
PE106 ○ → ↓
PE105 ○ → ↓
PE104A ○ → ↑
PE104 ○ → ↑
PE103 ○ ↓↑
PE102 ○ ↓↓
PE101 ○ → ↓

1 WINDIGOKAN LAKE
WD118 □
WD117 □
WD116 □
WD115 □
WD114 □
WD113 □
WD112 □
WD111 □ (sed)
WD110 □
WD109 □
WD108 □
WD107 □
WD106 □E
WD105 □
WD104 □
WD103 □
WD102 □
WD101 □

2 HWY. 801
HWY101A □
HWY101B □
HWY101C □(sed)

3 OXALINE LAKE
OX119 □ (sed)
OX118 □ (sed)
OX117 □
OX116 □
OX115 □
OX114 □ (sed)
OX113 □ R
OX112 □
OX111 □
OX110 □ R
OX109 □ R
OX108 □
OX107 □ R
OX106 □
OX105 □ R
OX104 □
OX103 △ R
OX102 □
OX101 □ R

4 BLACKWATER LAKE
BL101 □ AA
BL102 □ AA
BL103 □
BL104 △
BL105 ○

88°19′ 87°00′W 49°50′N

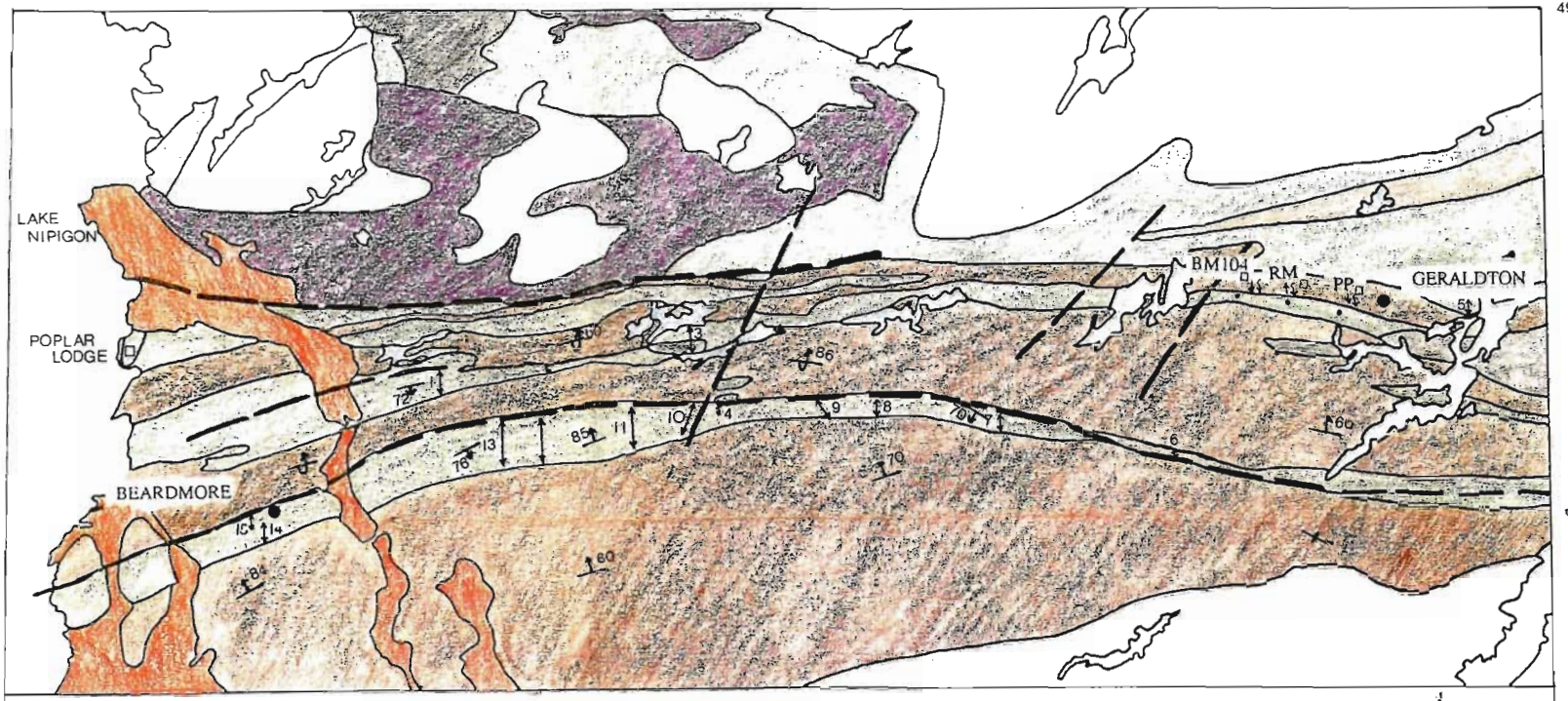

49°30′N

5 GC □
GG □
GGL □
GGD □
KPP □

6 ST. CROIX
S401 ○
S402 ○
S201 ○
S301 △

7 GOLDFIELD RD.
S101 ○
S102 ○
S103 ○

EARDMORE P
BP110 □
BP109 □
BP108 □
BP107 □
BP106 □
BP105 □ AA, B
BP104 IRON ST.
BP103A □ AA
BP103 □
BP102 □
BP101 □

14 BEARDMORE
B117 □
B116 □
B115 □
B114 □
B113 □
B112 □
B111 □
B110 □
B109 □
B108 □
B107 □
B106 □
B105 □
B104 □
B103 □
B102 □
B101 □